AGARD-AR-323

AGARD

ADVISORY GROUP FOR AEROSPACE RESEARCH & DEVELOPMENT
7 RUE ANCELLE 92200 NEUILLY SUR SEINE FRANCE

AGARD ADVISORY REPORT 323

Propulsion and Energetics Panel Working Group 22

on

Experimental and Analytical Methods for the Determination of Connected-Pipe Ramjet and Ducted Rocket Internal Performance

(Méthodes expérimentales et analytiques pour la détermination en conduite forcée des performances des statoréacteurs et des autolusées)

This Advisory Report was prepared
Propulsion and Energetics Panel o

NORTH ATLANTIC TREATY ORGANIZATION

Published July 1994

Distribution and Availability on Back Cover

AGARD
ADVISORY GROUP FOR AEROSPACE RESEARCH & DEVELOPMENT
7 RUE ANCELLE 92200 NEUILLY SUR SEINE FRANCE

AGARD ADVISORY REPORT 323

Propulsion and Energetics Panel Working Group 22

on

Experimental and Analytical Methods for the Determination of Connected-Pipe Ramjet and Ducted Rocket Internal Performance

(Méthodes expérimentales et analytiques
pour la détermination en conduite forcée
des performances des statoréacteurs et des statofusées)

This Advisory Report was prepared at the request of the
Propulsion and Energetics Panel of AGARD.

North Atlantic Treaty Organization
Organisation du Traité de l'Atlantique Nord

The Mission of AGARD

According to its Charter, the mission of AGARD is to bring together the leading personalities of the NATO nations in the fields of science and technology relating to aerospace for the following purposes:

- Recommending effective ways for the member nations to use their research and development capabilities for the common benefit of the NATO community;
- Providing scientific and technical advice and assistance to the Military Committee in the field of aerospace research and development (with particular regard to its military application);
- Continuously stimulating advances in the aerospace sciences relevant to strengthening the common defence posture;
- Improving the co-operation among member nations in aerospace research and development;
- Exchange of scientific and technical information;
- Providing assistance to member nations for the purpose of increasing their scientific and technical potential;
- Rendering scientific and technical assistance, as requested, to other NATO bodies and to member nations in connection with research and development problems in the aerospace field.

The highest authority within AGARD is the National Delegates Board consisting of officially appointed senior representatives from each member nation. The mission of AGARD is carried out through the Panels which are composed of experts appointed by the National Delegates, the Consultant and Exchange Programme and the Aerospace Applications Studies Programme. The results of AGARD work are reported to the member nations and the NATO Authorities through the AGARD series of publications of which this is one.

Participation in AGARD activities is by invitation only and is normally limited to citizens of the NATO nations.

Published July 1994

ISBN 92-835-0755-X

Printed by Specialised Printing Services Limited
40 Chigwell Lane, Loughton, Essex IG10 3TZ

Recent Publications of the Propulsion and Energetics Panel

CONFERENCE PROCEEDINGS (CP)

Smokeless Propellants
AGARD CP 391, January 1986

Interior Ballistics of Guns
AGARD CP 392, January 1986

Advanced Instrumentation for Aero Engine Components
AGARD CP 399, November 1986

Engine Response to Distorted Inflow Conditions
AGARD CP 400, March 1987

Transonic and Supersonic Phenomena in Turbomachines
AGARD CP 401, March 1987

Advanced Technology for Aero Engine Components
AGARD CP 421, September 1987

Combustion and Fuels in Gas Turbine Engines
AGARD CP 422, June 1988

Engine Condition Monitoring – Technology and Experience
AGARD CP 448, October 1988

Application of Advanced Material for Turbomachinery and Rocket Propulsion
AGARD CP 449, March 1989

Combustion Instabilities in Liquid-Fuelled Propulsion Systems
AGARD CP 450, April 1989

Aircraft Fire Safety
AGARD CP 467, October 1989

Unsteady Aerodynamic Phenomena in Turbomachines
AGARD CP 468, February 1990

Secondary Flows in Turbomachines
AGARD CP 469, February 1990

Hypersonic Combined Cycle Propulsion
AGARD CP 479, December 1990

Low Temperature Environment Operations of Turboengines (Design and User's Problems)
AGARD CP 480, May 1991

CFD Techniques for Propulsion Applications
AGARD CP 510, February 1992

Insensitive Munitions
AGARD CP 511, July 1992

Combat Aircraft Noise
AGARD CP 512, April 1992

Airbreathing Propulsion for Missiles and Projectiles
AGARD CP 526, September 1992

Heat Transfer and Cooling in Gas Turbines
AGARD CP 527, February 1993

Fuels and Combustion Technology for Advanced Aircraft Engines
AGARD CP 536, September 1993

Technology Requirements for Small Gas Turbines
AGARD CP 537, March 1994

ADVISORY REPORTS (AR)

Performance of Rocket Motors with Metallized Propellants *(Results of Working Group 17)*
AGARD AR 230, September 1986

Recommended Practices for Measurement of Gas Path Pressures and Temperatures for Performance Assessment of Aircraft Turbine Engines and Components *(Results of Working Group 19)*
AGARD AR 245, June 1990

The Uniform Engine Test Programme *(Results of Working Group 15)*
AGARD AR 248, February 1990

Test Cases for Computation of Internal Flows in Aero Engine Components *(Results of Working Group 18)*
AGARD AR 275, July 1990

Test Cases for Engine Life Assessment Technology *(Results of Working Group 20)*
AGARD AR 308, September 1992

Terminology and Assessment Methods of Solid Propellant Rocket Exhaust Signatures *(Results of Working Group 21)*
AGARD AR 287, February 1993

Guide to the Measurement of the Transient Performance of Aircraft Turbine Engines and Components *(Results of Working Group 23)*
AGARD AR 320, March 1994

Experimental and Analytical Methods for the Determination of Connected-Pipe Ramjet and Ducted Rocket Internal Performance *(Results of Working Group 22)*
AGARD AR 323, July 1994

LECTURE SERIES (LS)

Design Methods Used in Solid Rocket Motors
AGARD LS 150, April 1987
AGARD LS 150 (Revised), April 1988

Blading Design for Axial Turbomachines
AGARD LS 167, June 1989

Comparative Engine Performance Measurements
AGARD LS 169, May 1990

Combustion of Solid Propellants
AGARD LS 180, July 1991

Steady and Transient Performance Prediction of Gas Turbine Engines
AGARD LS 183, May 1992

Rocket Motor Plume Technology
AGARD LS 188, June 1993

Research and Development of Ram/Scramjets and Turboramjets in Russia
AGARD LS 194, December 1993

Turbomachinery Design Using CFD
AGARD LS 195, May 1994

AGARDOGRAPHS (AG)

Measurement Uncertainty within the Uniform Engine Test Programme
AGARD AG 307, May 1989

Hazard Studies for Solid Propellant Rocket Motors
AGARD AG 316, September1990

Advanced Methods for Cascade Testing
AGARD AG 328, August 1993

REPORTS (R)

Application of Modified Loss and Deviation Correlations to Transonic Axial Compressors
AGARD R 745, November 1987

Rotorcraft Drivetrain Life Safety and Reliability
AGARD R 775, June 1990

Abstract

Connected-pipe, subsonic combustion ramjet and ducted rocket performance determination procedures used by the NATO countries have been reviewed and evaluated.

A working document has been produced which provides recommended methods for reporting test results and delineates the parameters that are required to be measured.

Explanations and detailed numerical examples are presented covering the determination of both theoretical and experimental performances, the use of air heaters and uncertainty and error analyses.

Abrégé

Les méthodes de détérmination des performances des statoréacteurs et des statofusées au banc d'essais en conduite forcée, utilisées au sein de la communauté de l'OTAN, ont été examinées et évaluées.

Un document de travail a été élaboré afin de fournir des recommandations concernant la présentation des résultats d'essais et de préciser les paramètres indispensables à mesurer.

Des explications sont données et des exemples numériques détaillés sont présentés afin de déterminer les performances théoriques et expérimentales, incluant l'utilisation de foyers de préchauffage de l'air ainsi que l'emploi de procédures d'analyse des erreurs et des incertitudes.

Propulsion and Energet[illegible] Panel Working Group 22 M[illegible]bers

Chairman: Prof. David W. Netzer
Department of Aeronautics and [illegible]utics
Code AA/Nt
Naval Postgraduate School
Monterey, CA 93943–5000
United States

MEMBERS

Hans-L. Besser
Manager, Development
Deutsche Aerospace Bayern-Chemie
PO Box 1047
D-85501 Ottobrunn
Germany

Peter Boszko
Balistics and Mathematics Department
Department Manager
British Aerospace Defence Ltd
Royal Ordnance Rocket Motors Division
Summerfield, Kidderminster
Worcestershire DY11 7RZ
United Kingdom

Parker Buckley
WL/POPT
WPAFB, Ohio 45433-6563
United States

Philippe Cazin
ONERA
29 Avenue de la Division Leclerc
92322 Châtillon sous Bagneux
France

Alain Cochet
Direction de l'Energétique
ONERA
Fort de Palaiseau
91120 Palaiseau
France

[illegible]art Crispin
[illegible]sentalstrasse 10a
[illegible] München
[illegible]any

[illegible].O.G. Korting
[illegible], Rocket Propulsion Section
[illegible] Maurits Laboratorium TNO
[illegible]ox 45
[illegible]AA Rijswijk
[illegible]etherlands

Pro[illegible] Luigi De Luca
Poli[illegible]ecnico di Milano
Dipartimento di Energetica
Piazza Leonardo da Vinci 32
20133 Milano
Italy

William W. Muse
Manager, Analysis and Evaluation
Sverdrup Technology, Inc.
935 Avenue C
Arnold Air Force Base
Tullahoma, TN 37389-9800
United States

James A. Nabity
Code C2776
Naval Air Warfare Center
Weapons Division
China Lake, CA 93555
United States

Prof. Mario N.R. Nina
CTAMFUL
Instituto Superior Tecnico
Avenida Rovisco Pais
1096 Lisboa Codex
Portugal

John Oppelt
360 Northwest Dogwood St
No. D102
Issaquah, WA 98027
United States

Alberto Trovati
FIAT Avio
Combustion Department
112 Corso Ferrucci
10138 Torino
Italy

Claude Vigot
Direction de l'Energétique
ONERA
Fort de Palaiseau
91120 Palaiseau
France

Dr-Ing. Franz Vinnemeier
Manager, Aerodynamic Testing
BMW Rolls-Royce GmbH
Postfach 1246
61402 Oberursel
until July 1991
Deutsche Forschungsanstalt für Luft-
und Raumfahrt e.V.
Institut für Chemische Antriebe
und Verfahrenstechnik
Langer Grund
74239 Hardthausen
Germany

Anthony Whitehouse
Ballistics and Mathematics Department
Section Manager
British Aerospace Defence Ltd
Royal Ordnance Rocket Motors Division
Summerfield, Kidderminster
Worcestershire DY11 7RZ
United Kingdom

Wim B. de Wolf
National Aerospace Laboratory
PO Box 153
8300 AD Emmeloord
The Netherlands

PANEL EXECUTIVE
Dr P. Tonn (GE)

Tel: (1) 4738 5785
Telex: 610176F
Telefax: (1) 4738 5799

Mail from Europe:
AGARD–OTAN
Attn: PEP Executive
7, rue Ancelle
92200 Neuilly sur Seine
France

Mail from US and Canada:
AGARD–NATO
Attn: PEP Executive
PSC 116
APO New York 09777

Contents

List of Figures

List of Tables

Nomenclature, Acronymns and Definitions

Nomenclature

a	constant or speed of sound, m/s
$a^\star$	critical speed of sound ($M = 1$), m/s
A	geometric area, m^2
c	velocity, m/s
c_D	discharge coefficient
c_F	thrust coefficient
c_p	specific heat at constant pressure, $J/kg/K$
c_v	specific heat at constant volume, $J/kg/K$
c^*	characteristic velocity, m/s
e	internal energy, J/kg
$f()$	function
f/a	ratio of fuel-to-air mass flow rates
F	thrust or force, N
F_S	stream thrust, N
h	enthalpy, J/kg
i_{sp}	specific impulse, Ns/kg
i^*_{vac}	vacuum specific impulse at station 5, Ns/kg
n	pressure exponent
N	number of moles
m	mass, kg
$\dot{m}$	mass flow rate, kg/s
M	Mach number
$\mathcal{M}$	molecular mass, $kg/kmole$
p	static pressure, Pa
p_t	total or stagnation pressure, Pa
q	dynamic pressure, Pa
r_b	burning rate, m/s
R	gas constant ($\mathcal{R}/\mathcal{M}$), $kJ/kg/K$
$\mathcal{R}$	universal gas constant, $kJ/kmole/K$
s	entropy, $J/kg/K$
S_b	propellant burning surface area, m^2
t	time, s
t_b	burn time, s
T	static temperature, K
T_t	total or stagnation temperature, K
v	specific volume, m^3/kg
γ	ratio of specific heats
γ_f	frozen isentropic exponent
γ_p	process isentropic exponent
γ_s	local (shifting) equilibrium isentropic exponent
Δ	delta (difference)
Δh°_f	heat of formation, J/kg
η	efficiency parameter based on the ratio of experimental-to-theoretical values for a specific performance parameter
η_{c^*}	efficiency parameter based on the ratio of experimental-to-theoretical characteristic velocity ($c^\star$) where the experimental c^* can be determined from either measured thrust or pressure
$\eta_{i^*_{vac}}$	efficiency parameter based on the ratio of experimental-to-theoretical vacuum specific impulse ($i^\star_{vac}$)

$\eta_{\Delta T}$	efficiency parameter based on the ratio of experimental-to-theoretical temperature rise due to combustion
η_{ϕ}	efficiency parameter based on the ratio of theoretical equivalence ratio (ϕ_b) to the experimentally injected equivalence ratio (ϕ_{inj})
η_{ex}	efficiency parameter based on the ratio of the total injected fuel/propellant mass to the initial mass
ϱ	density, kg/m^3
ϕ	equivalence ratio $((f/a)/(f/a)_{stoich})$
ϕ_b	burned equivalence ratio necessary to theoretically produce the measured c^*_{exp}, assuming equilibrium combustion
ϕ_{inj}	injected equivalence ratio corresponding to the fuel mass flow rate in the experiment
φ_D	thrust nozzle expansion efficiency
χ	mole fraction of species

Subscripts

amb	ambient (local)
$A,\ B, \ldots$	multiple inlets or nozzle designations
b	base, burn
C	Carbon
eff	effective
exp	experimental
f	final, fuel or propellant grain, frozen
g	ducted rocket gas generator
$geom$	geometric
H	Hydrogen
H_2O	water
i	initial
id	ideal air
inj	injector
LC	load cell
$meas$	measured
O	Oxygen
O_2	make-up oxygen (i.e., vitiator oxidizer plus replenishment oxygen)
p	process
s	local or shifting equilibrium
$stoich$	stoichiometric
t	total
$tare$	tare
th	theoretical
ΔT	temperature rise
vac	vacuum
vf	vitiator fuel
vit	vitiator fuel, oxidizer and oxygen replenishment
vtd	vitiated air
$\infty, 0, 1 \ldots 6$	vehicle station identifications (see Fig. 3.1 – 3.3)
$4-5$, etc.	process representation between two stations (e.g. station 4 to station 5)
$\vert_{p,T,\ldots}$	constant p, T, ...

Superscripts

$\star$	secondary vehicle inlet designation (see Fig. 3.2) or $M = 1$ location
-	molar basis

Acronyms

AAAM	Advanced Air-to-Air Missile (U.S.)
ANS	Anti-Navire Supersonique, anti-ship supersonic missile (France)
ASMP	Air-Sol Moyenne Portée, air-to-surface medium range missile (France)

CARS	Coherent anti Stokes Raman spectroscopy
CFD	Computational fluid dynamics
DR	Ducted rocket
EFA	Experimental Feststau Antrieb, ducted rocket (Germany)
IR	Infrared
LFRJ	Liquid fuel ramjet
LIF	Laser induced fluorescence
MMH	Monomethylhydrazine
MPSR	Missile Probatoire Statofusée "*Rustique*", "*Rustique*" ducted rocket (France)
NASP	National Aero Space Plane (U.S.)
NG	Natural Gas
SA4	Surface-to-air missile type no. 4 (USSR)
SA6	Surface-to-air missile type no. 6 (USSR)
SFRJ	Solid fuel ramjet
SI	Système international d'unités (International system of units)
SLAT	Supersonic Low Altitude Target missile (U.S.)
UDMH	Unsymmetrical Dimethylhydrazine
VFDR	Variable Flow Ducted Rocket (U.S.)

Definitions

Heat of formation (Δh_f°) — Increment in enthalpy associated with the reaction of forming the given compound from its elements, with each substance in its thermodynamic standard state at 298.15K. (Also referred to as standard enthalpy of formation).

Make-up Oxygen — The sum of oxygen flow rates, vitiator oxidizer and replenishment oxygen, that must be added to maintain the "mole or mass fraction of oxygen in air" in the vitiated air stream supplied to the propulsion system.

Stream Thrust — $F_S = \dot{m}c + pA$

1 Introduction

Many NATO nations are now conducting research and development of ramjets for supersonic, extended range missiles and projectiles. In the context of this report the ramjet is taken to be a generic class of propulsion devices which comprise the liquid fuel ramjet, the solid fuel ramjet and the ducted rocket (sometimes referred to as the ramrocket). Accurate data are needed for trade-off studies (especially in the medium-range area where solid propellant motors can effectively compete) in which thrust-time characteristics are input into mission analysis codes. It is also necessary to standardize the techniques as much as possible so that performance data reported by one NATO nation (or facility) can be effectively and fairly compared to performance data reported by other organizations. Each facility may employ different types of air heaters, chemical equilibrium codes, instrumentation, calibration techniques and testing methods. Identical motors tested in different facilities can result in different reported thrust levels and combustion efficiencies. These differences become even more critical with the introduction of metallized fuels and with increased flight Mach number.

In recognition of these needs, the AGARD Propulsion and Energetics Panel established Working Group 22 to generate a working document which delineates the recommended methods for the determination of connected-pipe ramjet and ducted rocket performance. To accomplish this goal the Working Group collected, reviewed and evaluated the methods and techniques used in the NATO community.

The scope of this document restricts itself to experimental and analytical methods for the determination of connected-pipe, subsonic combustion ramjet (with solid and liquid fuels) and ducted rocket internal performance. In addition to an overview of ramjet and ducted rocket propulsion devices the following six major areas of interest are addressed:

1. Recommended methods for reporting test results, including the methodology for uncertainty analysis.
2. Explanation of the methods used for the prediction of theoretical thermodynamic and performance parameters (codes employed, values used, input data requirements, etc.).
3. Delineation of the parameters required to be measured.
4. Explanation of the calculation methods for experimental performance parameters.
5. Sample performance calculations for each of the propulsion devices and determination of the sensitivity of the various performance parameters to the measured variables. Also included is an example of uncertainty analysis.
6. Techniques for the utilization of air heaters and the effects of air heaters on theoretical and experimental performance.

2 Overview

After the end of the second world war, major research efforts were undertaken in several countries on supersonic, airbreathing propulsion. This led to numerous experimental missile and aircraft flight tests, for example the French *GRIFFON* aircraft, and to a few operational systems. Among the latter can be cited a first generation of airbreathing missiles, such as the American *BOMARC* and *TALOS*, the British *BLOODHOUND* and *SEA DART* (Fig. 2.1) and the Soviet *SA4*. In the seventies a second generation began to appear with new technologies, principally the ducted rocket and the integral booster. The Soviet *SA6*, a ducted rocket with an integral booster, showed the effectiveness of the new design in the field, in Middle East conflicts. In France, the *ASMP* missile, a liquid fuel ramjet, has been deployed by the aircraft of the strategic forces, since 1986 (Fig. 2.2).

Today, the ramjet is drawing attention again, throughout the world, for potential military (tactical and strategic) and civilian applications:

- **For missiles:**
  France and Germany are preparing the *ANS* supersonic antiship missile (Fig. 2.3). The USA is working on air-to-air advanced developments such as *VFDR* and *AAAM*, etc. There are also other cooperative efforts between several NATO countries.
- **For hypersonic or orbital aircrafts and space launchers:**
  Research on ramjet propulsion, with subsonic or supersonic combustion, is making a strong comeback in a number of countries, mainly in the USA and in Germany (Figs. 2.4 and 2.5), but the operational applications are expressed only in the long term.

2.1 Ramjet Configurations

The basic advantages of all ramjet configurations over conventional rocket propulsion systems are twofold. Firstly they have the potential to achieve an increased range and secondly having "power-on-to-target" and/or higher terminal velocity they offer increased effectiveness against manœuvring targets. Either or both of these advantages can be sufficient to justify the use of a ramjet over a conventional rocket motor in certain applications.

Among the various configurations which have been studied, a classification can be established according to the nature of the fuel, either liquid with its high performance, or solid with its operational simplicity and potentially lower cost.

2.1.1 Ramjets Using Liquid Fuel (LFRJ)

The liquid fuel ramjet can use classical kerosene, high density or slurry fuels. The liquid fuel ramjet (Fig. 2.6 and 2.7) dominates the operational applications, mainly because of its high throttleability and excellent performance.

2.1.2 Ramjets Using Solid Fuel (SFRJ)

It is possible to use special solid fuels in a solid fuel ramjet in order to obtain conditions of maintenance and storage similar to that of ordinary ammunitions or classical solid propellant rocket missiles (Fig. 2.8). The engine uses only one chamber, resulting in a very simple construction. The pure solid fuel, that is without oxidizer, covers the wall of the combustor. By ablation in the hot air flow, it is transformed into gases which burn in a combustion chamber. It is particularly well-suited for the high-acceleration environment of projectiles.

2.1.3 Ducted Rockets (DR)

The ducted rocket contains a solid propellant with only a small portion of oxidizer (fuel rich solid propellant). Just the quantity of oxidizer is used which is necessary to produce gases through pyrolyzing and/or burning reactions. The ducted rocket, like the solid fuel ramjet, has the maintenance and storage characteristics of a solid rocket motor. Like the liquid fuel ramjet, the ducted rocket may also have a throttling ability.

Two variants of the ducted rocket exist:

1. **Ducted rocket with separate gas generator (Figs. 2.9, 2.10 and 2.11)**
   The fuel is stored in a separate container, or gas generator, which works like a rocket. The gases produced, relatively low in temperature, can be injected into the combustion chamber through a control valve.

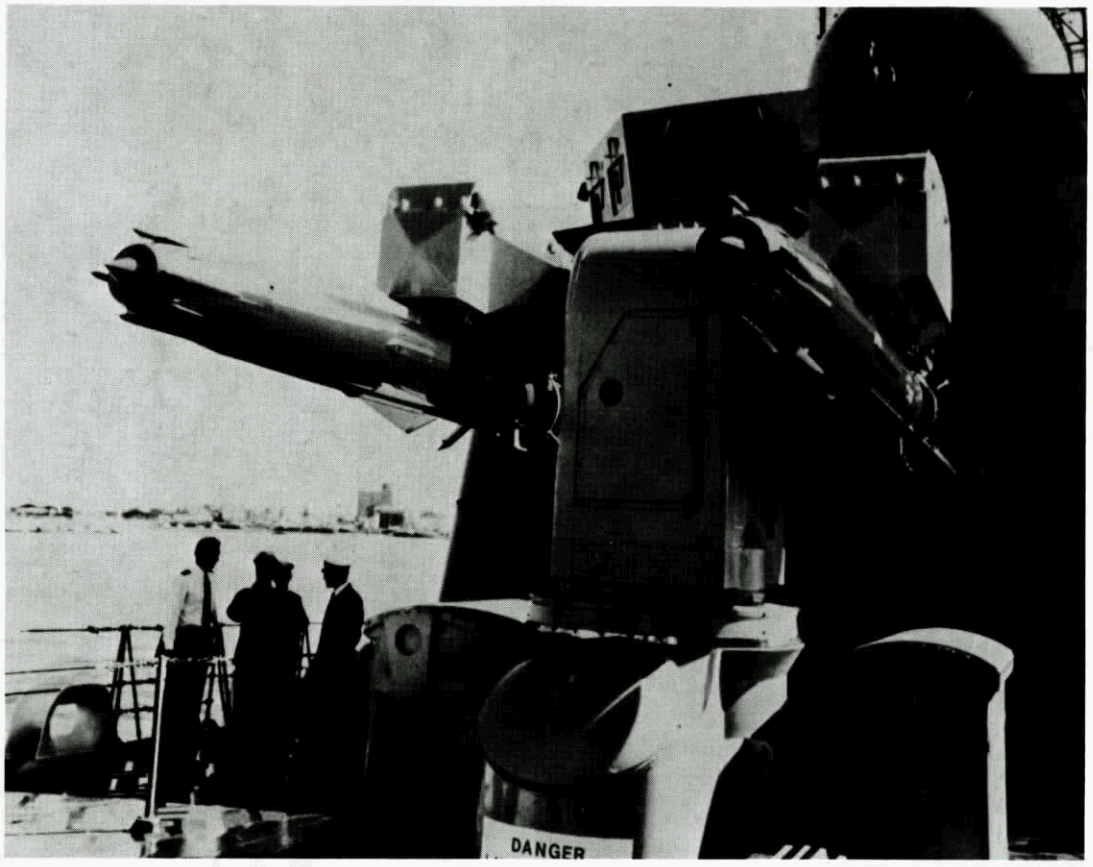

Figure 2.1: *SEA DART* surface-to-air missile

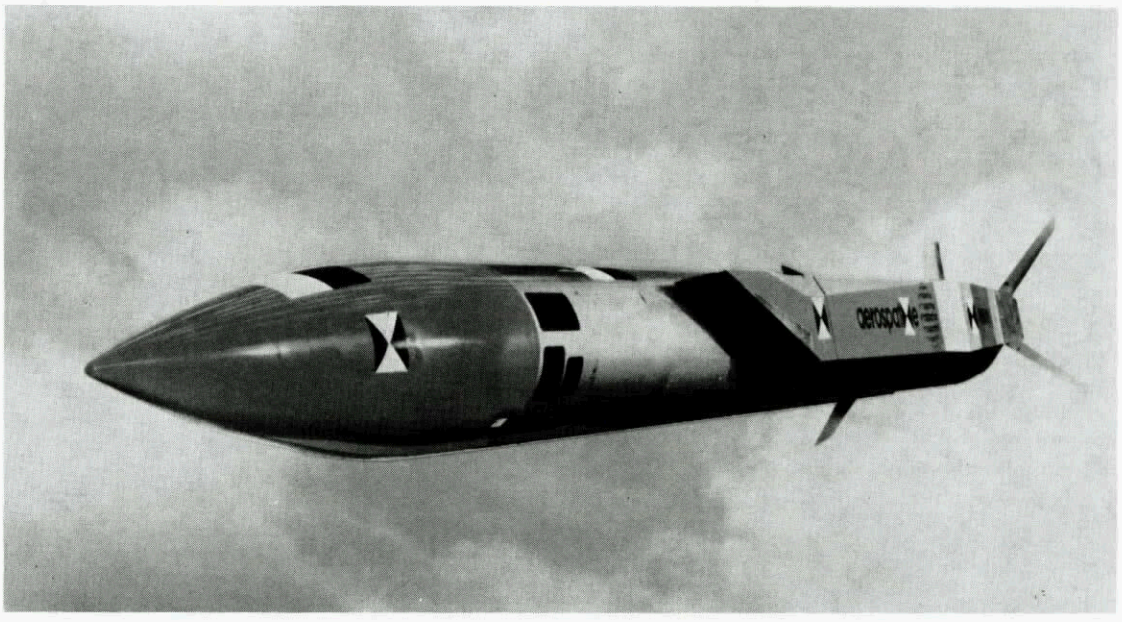

Figure 2.2: *ASMP* missile

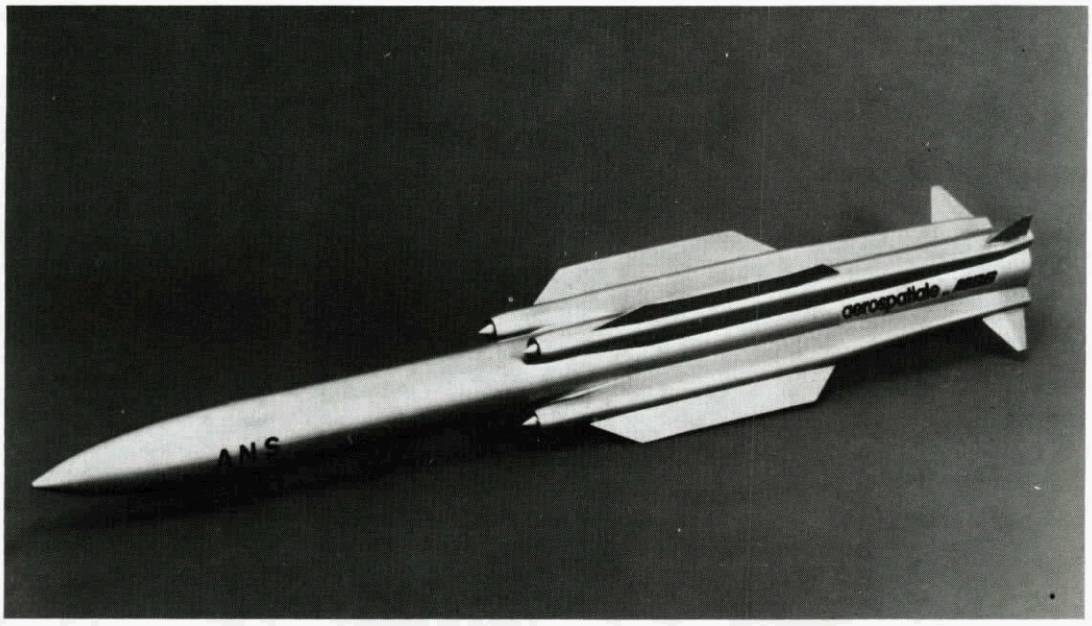

Figure 2.3: *ANS* missile

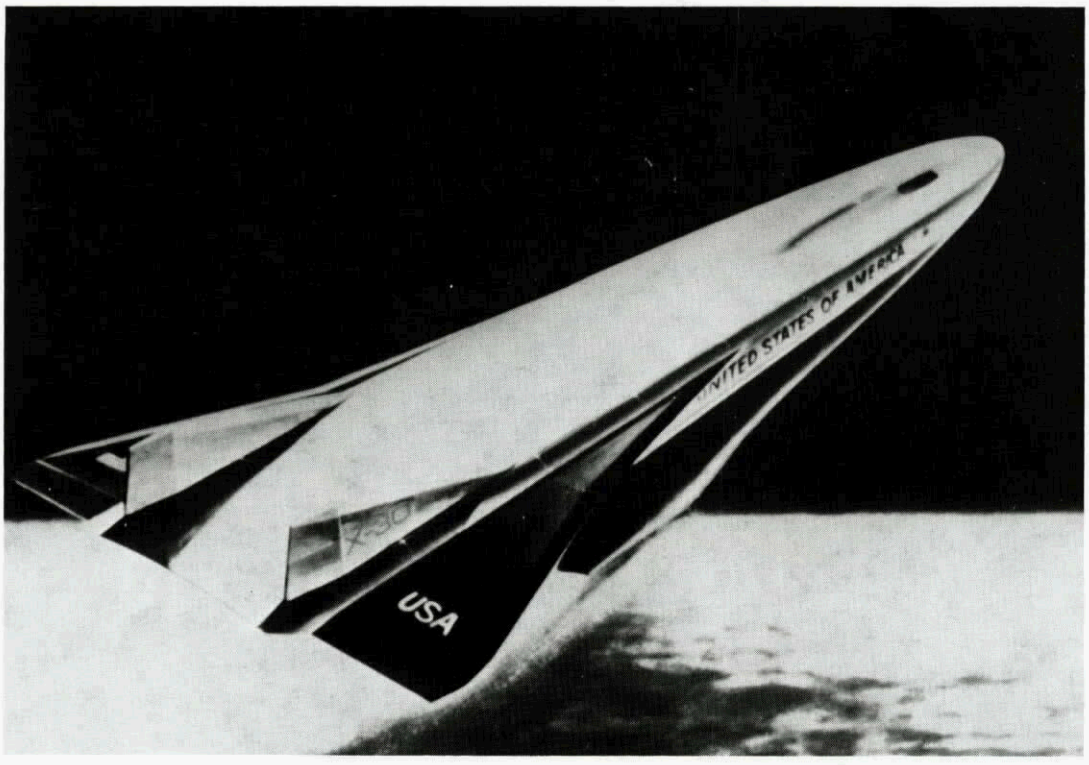

Figure 2.4: *NASP* space plane

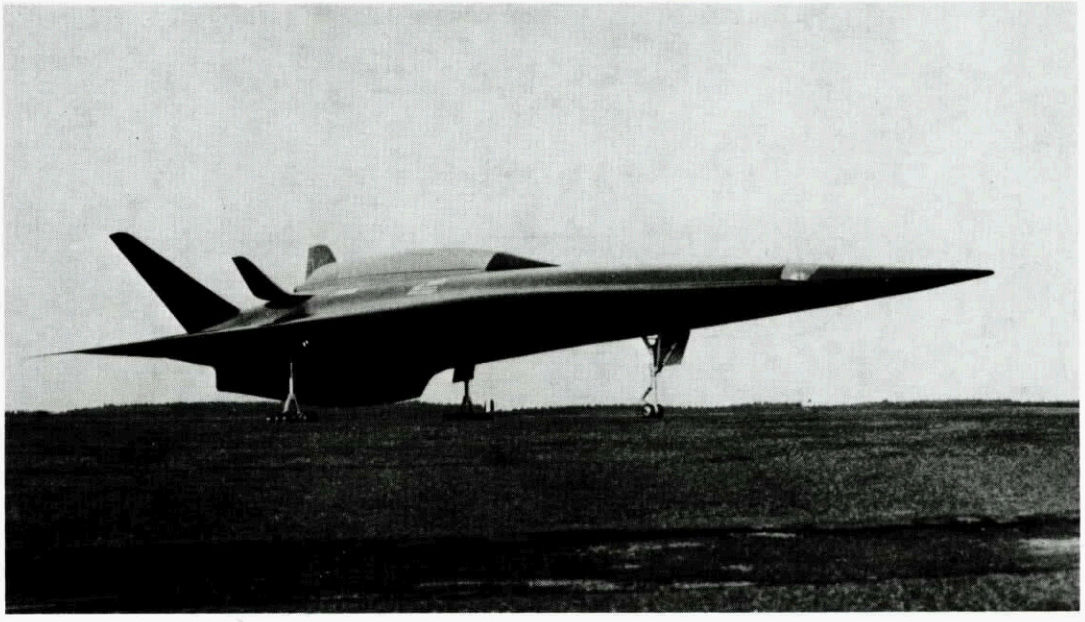

Figure 2.5: *Sänger II* space plane

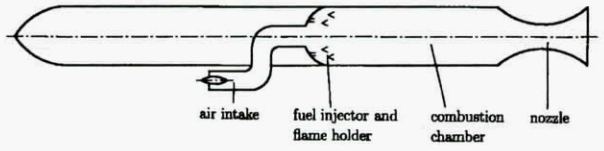

Figure 2.6: Sketch of a liquid fuel ramjet

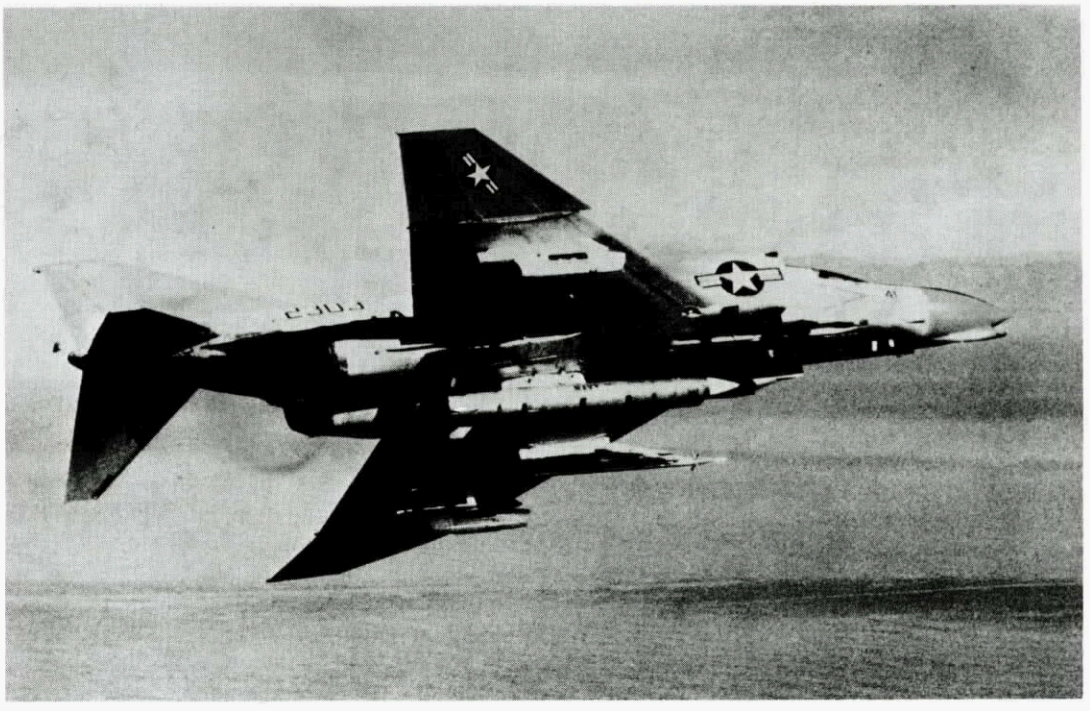

Figure 2.7: *SLAT* missile

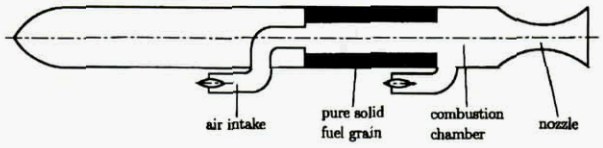

Figure 2.8: Sketch of a solid fuel ramjet

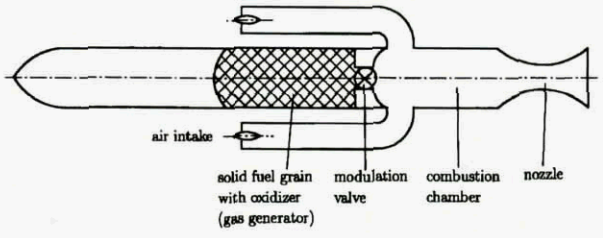

Figure 2.9: Sketch of a ducted rocket (with separate gas generator)

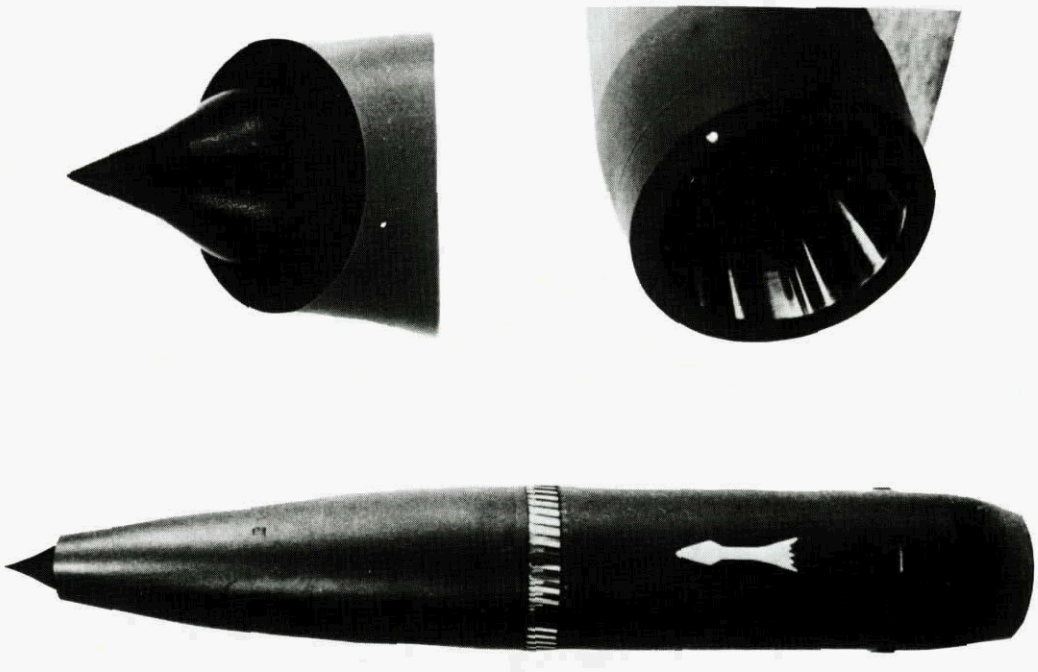

Figure 2.10: Projectile with fuel rich solid propellant ducted rocket propulsion

As the burning rate of the fuel is influenced by pressure, it is possible to regulate the gas flow.

2. **Ducted rocket with integrated gas generator (Fig. 2.12, 2.13)**
An example is the original French design, called *"Rustique"*. It has a single chamber, fuel rich solid propellant in direct contact with the combustion chamber, and wide altitude variation capability because of self-regulation qualities (as the burn rate is pressure dependent).

2.1.4 Scramjets (Supersonic Combustion)

The ramjet is without any doubt the most suitable air-breathing propulsion system for hypersonic flight in the atmosphere. Efficient operation of a ramjet is reached by subsonic combustion up to Mach 6 or 7, and supersonic combustion beyond; in the latter case, the engine is designated as a scramjet.

Theoretically, on the basis of its power performance, it could reach orbital velocities. In practice, it will be difficult to go beyond a hypersonic speed of about Mach 10 to

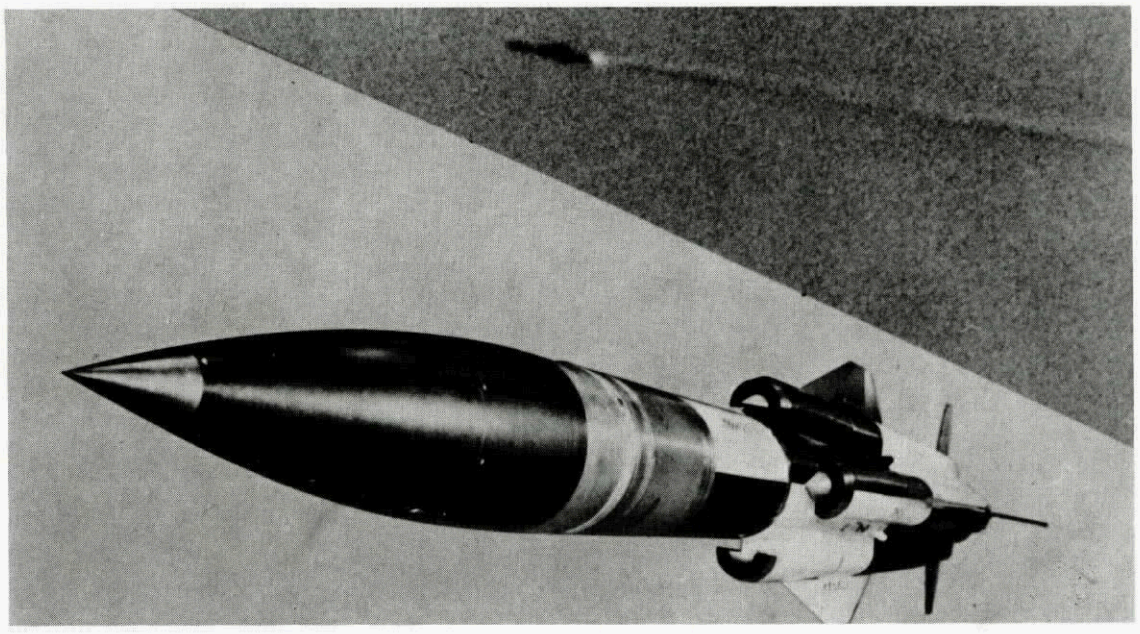

Figure 2.11: *EFA* ducted rocket missile

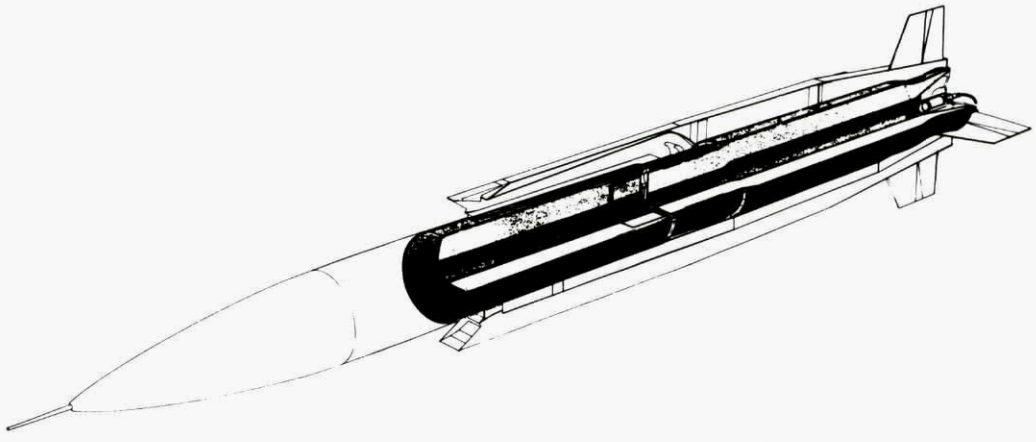

Figure 2.12: Sketch of *"Rustique"* ducted rocket missile

12, because of the sensitivity of the engine thrust to small disturbances at higher Mach numbers. However, at the present time, the complete operation envelope remains to be explored at the cost of considerable research and development efforts. Several countries have begun to consider the potential use for the scramjet and have launched ambitious programmes to develop demonstrators.

2.2 Ramjet Performance Determination

It is more difficult to evaluate the performances of air-breathing engines than those of rockets, because they vary strongly with the flight conditions (Mach number, altitude, atmospheric conditions, angle of attack, etc).

The main difficulties are discussed below.

1. **Required precision of performance determination**
   Ramjet engine net thrust, available for vehicle propul-

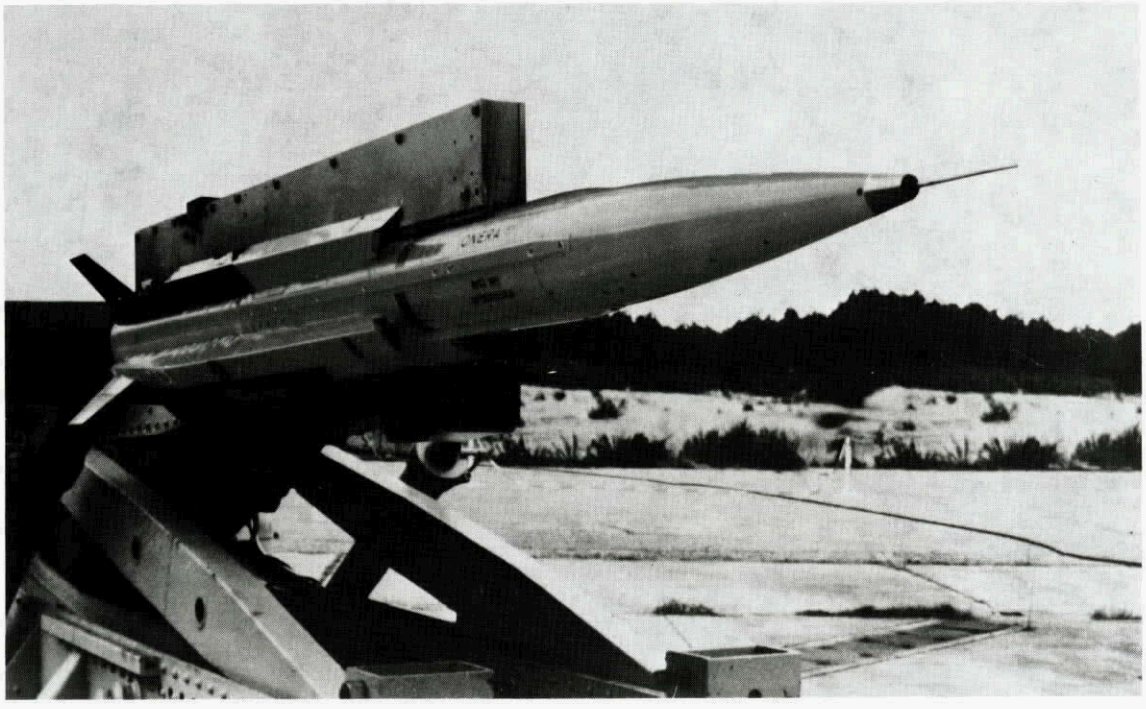

Figure 2.13: *"Rustique"* ducted rocket missile

sion is equal to the thrust generated by the nozzle minus the ram drag. This ram drag is equal to the momentum flux of the incoming air flow, and is also called inlet momentum drag.

At high flight speeds the nozzle thrust and the inlet momentum drag will have the same order of magnitude. Thus, an error in the nozzle thrust will propagate into an error in the net thrust. This increases with flight Mach number as shown in Fig. 2.14. For instance, at a flight speed of Mach 4, a 1 percent error in nozzle thrust may lead to a 3 percent error in net thrust or 3 percent in range.

2. **Engine airframe integration**
   Especially for high Mach numbers, the different components of the engine, mainly the air intake and the nozzle, are integrated in the aerodynamic configuration of the vehicle. It is therefore difficult to separate the thrust and drag terms.

3. **Specific problems for ramjets using solid fuels/propellants**
   It is more difficult to know the combustion efficiency of a solid fuel ramjet or a ducted rocket than that of a liquid fuel ramjet, because of the difficulty of mass flow measurement, and sometimes because of the presence of condensed material on the nozzle and/or in the exhaust.

2.3 Main Stages of Ramjet Development

As for any propulsion system, developing a ramjet engine goes first through successive development phases, then through detailed debugging and demonstration, and finally, acceptance testing under all flight conditions. This demands a great deal of experimental research and development.

For example, to debug one current operational ramjet powered missile and to qualify it with its equipment under all flight conditions, 600 test runs were required each year for seven years (90% of blowdown tests lasted 30 seconds and 10% lasted longer), using some 80,000 kg of liquid fuel!

In the same way as for aircraft, the current trend is to qualify the missile on the ground, in the most realistic environment possible, so that the flight tests, always very costly, have a high probability of success.

During a ramjet development, the following successive experimental steps are needed.

1. **Design test on components**
   This includes tests of air intakes in a wind tunnel, optimisation of the combustor with the help of flow visualisation techniques, etc.

2. **Connected-pipe tests**

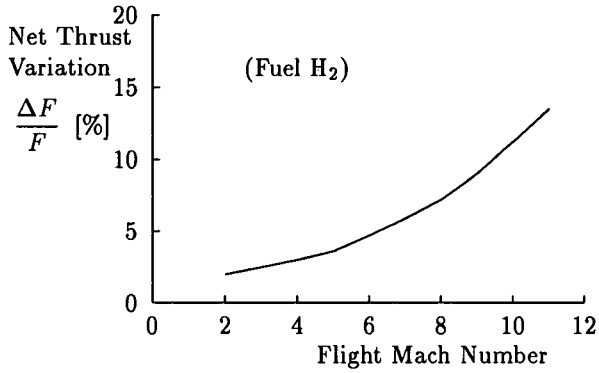

Figure 2.14: Sensitivity of net thrust to a 1% change in nozzle thrust

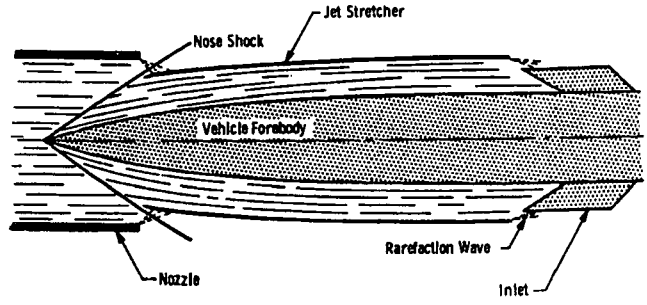

Figure 2.15: Jet stretcher concept

This is a very important step of a development, and the heart of this report. The simulation of flight conditions (velocity, altitude) is obtained with the help of different devices, such as the air heater (heat accumulation or fuel combustion). The engine is supplied with subsonic hot air, with simulation of the aerodynamic conditions at the end of the inlet diffuser. An important problem is the quality of the air entering the ramjet, for instance the percentage of water vapour. With the use of special devices, to eliminate or to compensate for the inlet momentum, it is possible to determine the ramjet nozzle thrust.

3. **Semi-free jet tests**
   The engine, including air intakes, is supplied with supersonic air coming from nozzles just in front of each inlet. The air mass flow required is roughly 50% to 100% higher than in connected-pipe tests, due to external air flow.

4. **Free jet tests**
   This is the best simulation, because the entire vehicle forebody is surrounded with supersonic air flow, as in flight. However, a free jet test installation needs to be very powerful and its cost is very high. Therefore, free jet testing is not always employed, resulting in higher risks during flight tests.

   Facility size can limit or even preclude free jet testing with a full scale forebody/inlet installed. Special test techniques are occasionally utilized to circumvent free jet size or flow rate limitations. Two prevalent techniques are the forebody simulator and jet stretcher. The forebody simulator (a contoured forebody which may be half the length of the complete forebody) provides the same inlet flow field in the free jet environment as the complete forebody in the flight environment. The jet stretcher (an aerodynamically shaped surface which simulates a free jet streamline, Fig. 2.15) extends the test rhombus of the free jet nozzle by precluding extraneous shock or expansion waves from the nozzle or jet boundary from being reflected into the flow upstream of the inlet.

5. **Flight tests**
   This is the final objective after several years of ground tests.

2.4 Need for Standardization in NATO Nations

In summary, it is seen that:

- the ramjet configurations can be various,
- the determination of performance, with good precision, is not easy,
- the ramjet test facilities are complex and costly, especially to simulate high Mach numbers, and can use many different techniques.

Many exploratory development programmes are carried only through connected-pipe testing. Connected-pipe tests also constitute the initial and a major portion of any ramjet missile propulsion development programme. The data obtained from these tests can be used to validate the designs of components such as inlets, combustors and exhaust nozzles and can also be used for some system integration (combustor-inlet coupling, etc.). The resulting data can also be used for preliminary trajectory analysis for the missile system. Thus, there is a need for comparison and recommended procedures for the connected-pipe methods used by the various NATO nations. This is the aim of this report.

3 Methods for Reporting Test Results

Established reporting standards used by the participating nations were reviewed. These included national standards and those used by individual organizations. These standards were used as a basis for the recommendations presented in this chapter. These include:

1. Identification of vehicle stations
2. General test information to be reported
3. Geometric data to be reported
4. Description of equipment and instrumentation
5. Test data to be reported, as appropriate
6. Performance data to be reported
7. Error analysis

The application of SI-units is required for reporting.

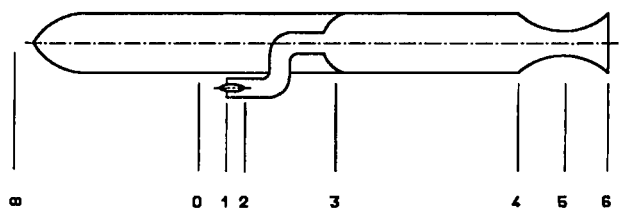

Figure 3.1: LFRJ configuration station numbers

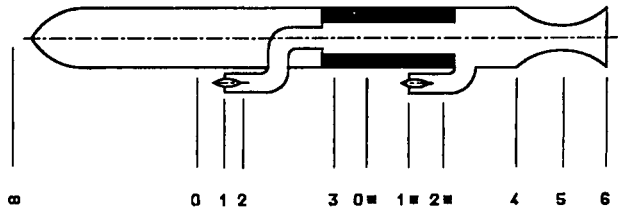

Figure 3.2: SFRJ configuration station numbers

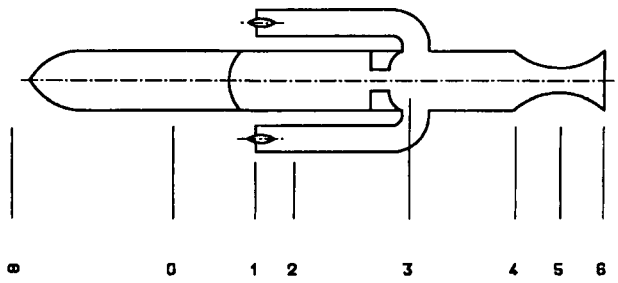

Figure 3.3: Ducted rocket configuration station numbers

3.1 Identification of Vehicle Stations

Station locations for flight conditions were specified as follows:

∞ Freestream.

0 Flow field immediately upstream of the inlet shock system

1 Inlet lip cross-section or capture station; beginning of the internal flow system

2 End point of the inlet compression process or end of the inlet diffuser

3 An appropriate position at the upstream end of combustor section

4 Downstream end of combustor section

5 Exhaust nozzle geometric throat

6 Nozzle exit

For connected-pipe test installations these station numbers should be adopted. Schematic diagrams are shown in Figures 3.1 to 3.3 which illustrate the application of station numbers to configurations which are typical of liquid fuel ramjets, solid fuel ramjets and ducted rockets. Subnumbers can be used to describe intermediate stations downstream of the primary stations defined above. For example, stations along the combustor would be identified as 3.1, 3.2, etc. Secondary inlets, such as the bypass inlet shown on the solid fuel ramjet in Figure 3.2, should be identified with an asterisk (*), with further description as deemed necessary by the author.

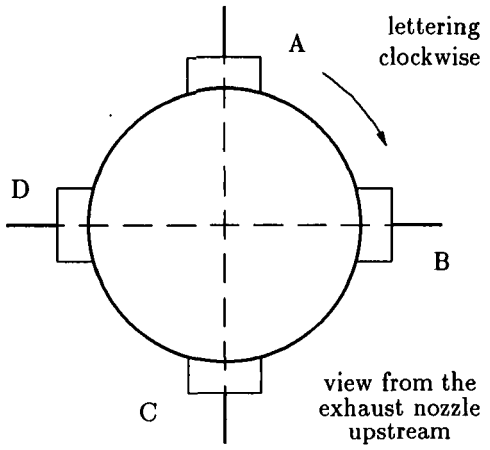

Figure 3.4: Example of station letters for multiple inlets

For multiple inlets at a common combustor station or multiple nozzle configurations, station numbers should be followed by capital letters which distinguish the individual components, beginning with "A" at the first component to be identified from the top of the vehicle cross-section, proceeding in a clockwise direction when looking upstream from the exhaust nozzle (Fig. 3.4).

3.2 General Test Information to be Reported

The information listed beneath each topic below should be reported and described, as appropriate.

- Fuel/Propellant:
  - Chemical formula(s) representing the composition
  - Heat of formation at 298.15 K
  - Enthalpy at initial temperatures
  - Stoichiometric fuel/air ratio
  - Density at 298.15 K
- Air:
  - Chemical formula representing air
  - If vitiated air is used, also include:
    - ⋆ Fuel used for the vitiator (fuel defined as above)
    - ⋆ Oxygen make-up (vitiator oxidizer and replenishment)
    - ⋆ Composition of vitiated air
- Corrections and assumptions made to arrive at the final test results may include methods for:
  - Determining combustion efficiency
  - Determining pressure losses
  - Determining fuel/propellant mass flow rate
  - Time averaging
  - Area averaging
- Special measurements, such as gas sampling, spectroscopy, etc. should be described as well.

3.3 Geometric Data to be Reported

- A schematic representation to describe the geometry of the experimental hardware, as required, including appropriate station numbers
- Geometric flow area or dimensions characterizing the flow area for the applicable stations, including area variations during the test, if any
- Corrective coefficients for flow area, if used for performance calculations, such as the nozzle discharge coefficient
- Air injection configuration (coaxial, multiple inlets, side dump, etc.)
- Air injection angle relative to the ramcombustor center axis
- Fuel injection configuration
- Fuel injection angle, relative to the ramcombustor center axis
- Exhaust nozzle internal geometry
- Afterbody and external nozzle geometry, as appropriate
- Axial dimensions as required
- Type of ramburner construction and materials, including type and extent of thermal protection

3.4 Description of Equipment and Instrumentation

While it is generally accepted that information about the related test equipment and instrumentation is important to properly document an experimental investigation, it is not essential for the purpose of determining ramjet performance. It is, however, considered essential to report the type and location of all measurements required for performance calculations. The locations should be indicated at

each relevant station or substation by a sketch or written description.

It is assumed that the instrumentation and the associated treatment of the data comply with the state of the art for obtaining the required physical properties. For example, it is assumed that thermocouple readings are corrected for recovery factor and radiation effects, if necessary for an accurate temperature measurement.

3.5 Test Data to be Reported, as Appropriate

- Mass flow rates for air, vitiator fuel, make-up oxygen, and ramcombustor fuel or propellant
- Actual compositions, such as air, vitiated air and fuels, if measured
- Inlet profiles, such as total pressures, velocities and temperatures, if known
- Equivalence ratio
- Burning time
- Fuel/propellant initial temperature
- Fuel regression rate
- Force measurement, corrected for external effects
- Measured nozzle throat area variations during test
- Mach numbers at Stations 2, 3 and 4, including a description of the method(s) of calculation
- Static and total pressures and temperatures at Stations 2, 3 and 4. Indicate if measured or describe method of calculation
- Specific impulse i^* or actual characteristic velocity c^* at Station 5
- Measured hardware temperature, if used in performance calculations
- Measured values used in heat loss calculations, if accomplished
- Amplitudes and frequencies of pressure oscillations, if recorded. Identify measurement locations with station number and include modes of oscillation, if known
- Exhaust gas composition, if known
- Other measurements, as appropriate
- General comments, to include descriptions of items unique to the experiment which may not be well known to others

3.6 Performance Data to be Reported

- Combustion efficiencies
- Expulsion efficiency
- Total pressure losses
- Nozzle efficiency
- Isentropic exponent $\gamma_{p,s}$ (refer to appendix B)
- Rich and lean flammability limits, if obtained
- Stability limits, if encountered
- General remarks regarding items which could affect performance

3.7 Uncertainty Analysis Methodology

All test data have errors or inaccuracies. A means for quantifying these inaccuracies is identified in this section and discussed in Appendix A. The accepted practice in the technical community is to express such measurement inaccuracies as an "uncertainty" which is obtained by an uncertainty or error analysis. Error analysis quantifies the uncertainty for test data and serves as an invaluable engineering tool in the tasks of designing measurement systems, ensuring compliance to data accuracy requirements, and interpreting test results (e.g., AGARD-PEP Working Group 15, Uniform Engine Test Programme ([1] and [2])). The methodology was developed by R. B. Abernethy and J. W. Thompson [3] and is used by the International Standards Organization [4], by the American National Standard Institute and American Society of Mechanical Engineers [5], and by the Instrument Society of America [6].

The methodology used to determine test data uncertainty is based on quantifying elemental errors in the measuring system for each Basic Measurement (e.g., pressure, temperature, force, length and time), classifying the errors into two categories, either as precision (random or scatter error) or bias (fixed or offset error), and propagating the errors by using Influence Coefficients (determined from Sensitivity Analysis) into an estimate of uncertainty for Performance Parameters.

3.8 Error Analysis

An error analysis provides a detailed layout for error bookkeeping and auditing which yields uncertainties for the Ba-

Pressure:	±0.2% to ±0.5% of reading
Temperature:	±0.2% to ±0.6% of reading
Fuel flow:	±0.4% to ±1.0% of reading
Area:	±0.4% to ±0.2% of reading
Force (load cell):	±0.2% to ±0.5% of reading

Table 3.1: Typical measurement uncertainties in ground test facilities

Thrust:	±0.2% to ±1.0% of calc. val.
Airflow:	±0.4% to ±1.0% of calc. val.
Total Pressure Loss:	±0.5% to ±2.0% of calc. val.
Combustion Efficiency:	±2.0% to ±5.0% of calc. val.

Table 3.2: Typical performance parameter uncertainties

sic Measurements and Performance Parameters, and identifies the contribution of each error source to the total uncertainty level. Typical measurement uncertainties in ground test facilities are given in Table 3.1.

Representative detailed layouts (or audits) of error sources for the Basic Measurements are presented in Appendix A (Tables A.1 through A.4, respectively). These error analyses results and Influence Coefficients (determined by a Sensitivity Analysis using equations which calculate the Performance Parameters) provide an error propagation basis (i.e., bookkeeping layout) which yields the uncertainties of Performance Parameters. A representative layout for any specific Performance Parameter at a selected test condition is presented in Appendix A (Table A.5). Typical Performance Parameter uncertainties are given in Table 3.2.

Measurement uncertainties are strongly influenced by ramjet operating conditions (i.e., altitude, Mach number and power setting) and by test goals, resources and schedules. It is important to note that the above uncertainty values represent a range from the best uncertainties that can be achieved to values that can be obtained using everyday measurement practices. Of course, much larger values of uncertainty will result if any part of the measurement process is carelessly executed.

4 Theoretical Performance Determination

The theoretical performance determination of ramjets is based on an ideal combustion process which assumes chemical equilibrium. Computer codes that were originally developed to evaluate the rocket motor combustion process are used to model the ramjet combustion process. The codes however are based on a flow velocity of zero in the combustion chamber, since in a (nozzled) rocket engine the Mach number is small. However, in a ramjet combustor substantial flow velocities may be encountered (up to about Mach 0.8). This requires the use of stagnation flow properties as input to the codes instead of static flow conditions. Some features of these codes and their application to the ramjet combustion and vitiated air heater processes are discussed in this chapter.

Two codes are most frequently used for performance determination. Codes based on NASA CET89 [7, 8, 9] are in use by organisations in all countries while the Naval Air Warfare Center Weapons Division (formerly Naval Weapons Center) Propellant Evaluation Program (PEP) is a code [10] used by many organisations in the United States.

Test cases were developed to compare thermochemical properties of ramjet reacting flows predicted by these codes as applied by different organisations. The differences in code outputs are discussed.

Combustor performance can be affected by combustion instability and heat loss and may also be driven by plume signature requirements. Several references are given in the bibliography [11]–[14] that are used to predict combustion instability and plume signature. Two-phase flow is addressed by some of these codes.

4.1 List of Theoretically Determined Parameters for Performance Calculations

Many parameters were identified that may be required in order to calculate performance. Some of these parameters are difficult to measure or determine experimentally and, therefore, are theoretically calculated. They are listed and described below:

Station 2:

- Molecular Weight ($\mathcal{M}_2$)
- Mole Fraction of Species (χ_2)
- Isentropic Exponent (γ_2)

Station 4:

- Stagnation Temperature (T_{t4})
- Molecular Weight ($\mathcal{M}_4$)
- Mole Fraction of Species (χ_4)
- Isentropic Exponent (γ_4) may be defined three ways:
  - $\gamma_{f4} = c_p(T_4)/c_v(T_4)$ is the frozen isentropic exponent
  - $\gamma_{s4} = -(\partial \ln p/\partial \ln v)|_{s4}$ or $-\gamma/(\partial \ln v/\partial \ln p)|_{T4}$ is for local equilibrium (Appendix B)
  - $\gamma_{p,4-5}$ is a process isentropic exponent from station 4 to station 5 expressed as $\ln(p_4/p_5)/(\ln(p_4/p_5) - \ln(T_4/T_5))$

Station 5:

- Static Pressure (p_5)
- Static Temperature (T_5)
- Characteristic Velocity (c_5^*)
- Stagnation Temperature (T_{t5})
- Molecular Weight ($\mathcal{M}_5$)
- Mole Fraction of Species (χ_5)
- Isentropic Exponent (γ_{f5}, γ_{s5} or $\gamma_{p,4-5}$)

Station 6:

- Static Pressure (p_6)
- Static Temperature (T_6)
- Specific Impulse (i_{sp})
- Molecular Weight ($\mathcal{M}_6$)

- Mole Fraction of Species (χ_6)
- Isentropic Exponent (γ_{f6}, γ_{s6} or $\gamma_{p,5-6}$)
- Specific Heat (c_{p6})
- Thrust Coefficient (c_F)

4.2 Description of Aerothermochemical Equilibrium Codes

The aerothermochemical equilibrium codes which are in use are listed below. Contacts and addresses for obtaining these codes are given in Table 4.1.

1. The NASA CET89 [7, 8, 9] computer program is used for calculations involving chemical equilibria in complex systems. The method applied is based on minimization of the Gibbs free energy. The program permits calculations such as:
   - Chemical equilibrium for assigned thermodynamic states
     - Temperature and pressure
     - Enthalpy and pressure
     - Entropy and pressure
     - Temperature and volume or density
     - Internal energy and volume or density
     - Entropy and volume or density
   - Theoretical rocket performance
     - Frozen flow
     - Equilibrium flow
   - Chapman-Jouguet detonations
   - Shock tube parameter calculation

   The program considers condensed species as well as gaseous species. Condensed and gaseous species are supposed to have the same velocity and temperature.

2. PEP code [10] was developed for the calculation of high-temperature thermodynamic properties and performance characteristics of propellant systems. Determination of chemical equilibrium is accomplished by a combination of two methods [15]–[20]. An optimized basis, which is a subset of molecular species, is chosen. The chemical system is then divided into a number of subsystems, each relating a nonbasis species to the basis. The subsystem with the greatest discrepancy in its equilibrium relationship is corrected stoichiometrically until convergence is obtained. The program permits calculations such as:
   - Chemical equilibrium for assigned thermodynamic states
     - Temperature and pressure
     - Enthalpy and pressure
     - Entropy and pressure
     - Temperature and volume or density
     - Internal energy and volume or density
     - Entropy and volume or density
   - Theoretical rocket performance
     - Frozen flow
     - Equilibrium flow

   This code was revised to run on a personal computer (IBM compatible) in 1989.

Other codes that may be used are:

1. The COPPELIA code [21] is based on the NASA CET89 code (NASA CEC 71 version). It is more complete and extended than the NASA CEC 71 code. It has limited distribution.

2. The STANJAN [22] program is used to calculate chemical equilibrium in a complex system, including several phases. The calculation technique is based on the method of element potentials. The method of element potential uses theory to relate the mole fractions of each species to quantities called element potentials. There is one element potential for each independent atom in the system, and these element potentials, plus the total number of moles in each phase, are the only variables that must be adjusted for the solution. In large problems, that is in cases with many species, this number of element potentials is a much smaller number than the number of species, and hence far fewer variables need to be adjusted. The program assumes that the gas phase is a mixture of ideal gases and that condensed phases are ideal solutions. The program, called STANJAN because of its roots at Stanford and its connection with the JANAF thermochemical data tables, is an interactive program designed for use with either personal or mainframe computers. Thermodynamic cycle analysis is easily executed with STANJAN, because the user may specify the state parameters in a variety of ways including:
   - Temperature and pressure
   - Pressure and entropy
   - Enthalpy and pressure same as last run
   - Volume and entropy same as last run

3. The Aerotherm Chemical Equilibrium (ACE) [23] computer program is a versatile code for calculating quantities of importance for many thermochemical processes. It is well adapted to study ablative processes. Closed and open systems (i.e, constant volume and constant pressure) can be handled. The relative amount of each chemical element in the system is specified for closed systems. The relative amounts

of chemical elements depend on various mass transfer rates for open systems. Systems may be treated in chemical equilibrium or certain reactions may be kinetically controlled. It has limited distribution.

4.3 Application and Procedure for Theoretical Performance Determination

Aerothermochemical equilibrium codes may be used either interactively with a data reduction program or to generate data tables of thermochemical equilibrium properties. The tables should be of sufficient fineness such that inaccuracies do not result due to the interpolation procedure used. The codes are usually used interactively, since the computational time is no longer a major concern.

In order to calculate theoretical performance one must define the inputs to the aerothermochemical equilibrium codes, select the most appropriate calculation procedure and choose the desired outputs. Assumptions must be made in determining theoretical performance. For example, the gas velocity in the combustion chamber may be assumed to be zero and heat losses through the combustor wall as well as equilibrium (velocity and temperature) between condensed and gaseous phases may be neglected. The output data may be needed for calculation of other theoretical performance parameters.

4.4 Inputs to the Aerothermochemical Equilibrium Codes

Aerothermochemical equilibrium codes, such as NASA CET89 and PEP, require certain inputs. These inputs consist of species data, pressures, temperatures or enthalpies, mass flow rates or mass fractions, geometric areas and ingredient properties.

4.4.1 Species Thermochemical Data

Species data are obtained primarily from the JANAF Thermochemical Tables [24, 25]. The Thermophysical Properties Research Center (TPRC) provides maintenance of the tables [26]. The JANAF tables have also been supplemented from other sources [27]–[29]. The tabulated data have been put into polynomial form for use by the codes. The accuracy of both the tabulated data and the curve fits to the data can significantly affect the code output. Later versions of the codes contain improved data and/or curve fits. Therefore, care must be taken if older versions of the codes are utilized.

4.4.2 Pressure Inputs

Requirements are the stagnation pressure at station 4 (M_4 is assumed equal to zero) and the pressure ratio between stations 4 and 6. The ambient air pressure is also required, if absolute values are used. The stagnation pressure at station 4 is calculated from the static properties at station 4 and the geometric areas at stations 4 and 5.

4.4.3 Mass Flowrates and/or Mass Fractions

Mass flow rates are required to determine mixture ratios and for solution of the continuity equation at different stations. The total flowrate for vitiated air (or flowrates for air, vitiator fuel and make-up oxygen) and the flowrate for ramjet combustor fuel or ducted rocket propellant must be measured or deduced from analysis.

4.4.4 Geometric Areas

The expansion ratio (A_6/A_5) is a program input and may be corrected for boundary layer thickness when appropriate (see Section 5.2.1).

4.4.5 Compositions and Temperatures or Enthalpies of Constituents

The compositions and temperatures or enthalpies of all constituents at station 3 may be needed. These are determined from the constituent temperatures and flowrates and the inlet air temperature. Heat loss between the air heater and combustor inlet is accounted for as described in Section 4.4.5.3.

4.4.5.1 Fuel/Propellant

Fuel properties are determined from the NASA CET89 ingredient file, the PEP ingredient file, military standards, laboratory analyses, handbooks [27]–[31] and manufacturer data sheets. Occasionally, a fuel consists of several ingredients. Mass weighted calculations of ingredient properties may be used to determine the properties for the fuel.

4.4.5.2 Ideal Air

The composition of the air supplied to the air heater is usually assumed to be that of ideal air. However, for ideal

code	remarks	address
NASA CET89	NASA CET89 is disseminated under the sponsorship of the National Aeronautics and Space Administration by the Computer Software Management and Information Center (COSMIC)	COSMIC Software Information Services The University of Georgia, Computer Services Annex Athens, GA 30602 USA Program Number: LEW-15113 Program Name: 9 A CET89
PEP	PEP code is available, but distribution is limited	Naval Air Warfare Center Weapons Division Code C2776 (3276) China Lake, CA 93555 USA
COPPELIA	COPPELIA code is available, but distribution is limited	ONERA 29 Avenue de la Division Leclerc 92322 Chatillon sous Bagneux France
STANJAN		Prof. W.C. Reynolds Dept. of Mechanical Engineering Stanford University Stanford, CA 94305-3030 USA

Table 4.1: Contacts and addresses for obtaining aerothermochemical equilibrium codes

air, several compositions are in use by different organisations. A list is presented in Table 4.2. The enthalpy of air as a function of temperature is given in Table 4.3 and used to $T < 2500K$.

An evaluation of the effects of air composition on theoretical combustor performance was conducted. Different ideal airs were combusted with JP-10 hydrocarbon fuel. The predicted mole fractions for some species are listed in Table 4.4. Calculated values show only small variations. Also, the theoretical performance parameters (i.e. T_{t4}, γ_4 and $\mathcal{M}_4$) do not show significant differences for the various air compositions.

4.4.5.3 Vitiated Air

The composition and enthalpy of vitiated air can be obtained using one of several different approaches described below and depicted in Figures 4.2 and 4.3 ([32]). All methods account for heat losses that always occur between the vitiator and the combustor inlet as indicated in Figure 4.1. Chapter 8 provides a detailed discussion of vitiated air heaters. T_{t3} is assumed to be equal to T_{t2}, or the temperature at some intermediate station, since the latter can be more easily measured.

Method 1

The vitiated air is assumed to be ideal air with a temperature or enthalpy corresponding to the inlet air temperature (Table 4.3). Vitiated air properties are:

- Flowrate of the vitiated air.
- Composition of ideal air.
- Temperature or enthalpy for ideal air.

Method 2

Ideal air and vitiator combustion products (assumed complete) are input as oxidant reactants to the aerothermochemical equilibrium code at the measured T_{t2} and p_{t2}. Vitiated air properties are:

- Flowrates of ideal air and vitiator combustion products.
- Compositions of ideal air and vitiator combustion products.
- Vitiated air temperature or enthalpy, where enthalpy is given by Eq. 4.1.

$$h_{t3} = \frac{\sum_i \dot{m}_i h_i(T_{t3} = T_{t2})}{\sum_i \dot{m}_i} \qquad (4.1)$$

Species	Composition	χ_N	χ_O	χ_C	χ_{Ar}	Δh_f°, $[kJ/kg]$
N_2, O_2 and Ar	$N_{835}O_{224}Ar_5$	0.78477	0.21053	0	0.00470	0
N_2, O_2 and CO_2	$N_{54.623}O_{14.675}C_{0.010}$	0.78812	0.21174	0.00014	0	-4.187
N_2, O_2, CO_2 and Ar	$N_{156.2}O_{41.96}Ar_{0.934}C_{0.0314}$	0.78443	0.21072	0.00016	0.0049	-4.187

Table 4.2: Composition and heat of formation for ideal airs

Temperature $[K]$	Enthalpy $[kJ/kg]$	Temperature $[K]$	Enthalpy $[kJ/kg]$	Temperature $[K]$	Enthalpy $[kJ/kg]$
298	0	1050	805	1800	1704
350	52.4	1100	863	1850	1766
400	103	1150	921	1900	1828
450	154	1200	979	1950	1890
500	205	1250	1038	2000	1953
550	257	1300	1092	2050	2015
600	309	1350	1157	2100	2078
650	362	1400	1217	2150	2141
700	415	1450	1277	2200	2204
750	469	1500	1337	2250	2267
800	524	1550	1398	2300	2330
850	578	1600	1459	2350	2393
900	635	1650	1520	2400	2457
950	691	1700	1581	2450	2520
1000	748	1750	1643	2500	2584

Table 4.3: Air ($N_{835}O_{224}Ar_5$) enthalpy as function of air temperature (sea level) [32]

Formulation	T_{t2}, $[K]$	χ_{N_2}	χ_{CO_2}	χ_{H_2O}	χ_{CO}	χ_{Ar}	χ_{O_2}	χ_{HO}
$N_{835}O_{224}Ar_5$	298.15	0.729	0.126	0.108	0.014	0.009	0.006	0.003
	1500	0.703	0.084	0.091	0.052	0.008	0.020	0.014
$N_{54.623}O_{14.675}C_{0.010}$	298.15	0.736	0.127	0.108	0.013	0.0	0.007	0.003
	1500	0.710	0.085	0.091	0.050	0.0	0.021	0.014
$N_{156.2}O_{41.96}Ar_{0.934}C_{0.0314}$	298.15	0.729	0.126	0.108	0.014	0.009	0.006	0.003
	1500	0.703	0.084	0.091	0.052	0.008	0.020	0.014
$\Delta h^\circ_{f,\text{JP-10}} = -773kJ/kg$, $f/a = 0.0704$, $p_4 = 218kPa$								

Table 4.4: Some species mole fractions for combustion of JP-10 with ideal airs.

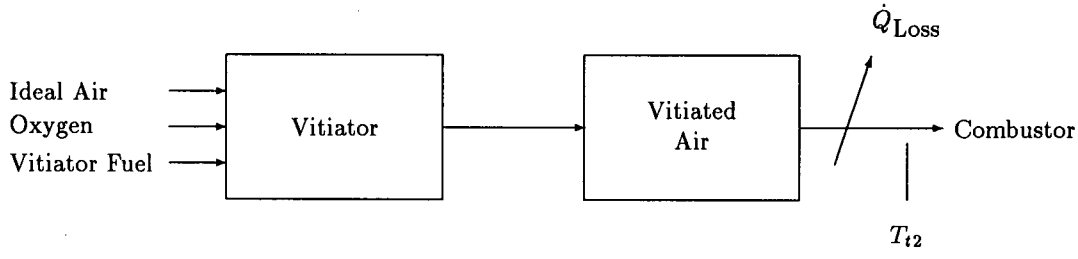

Figure 4.1: Schematic of vitiator test setup

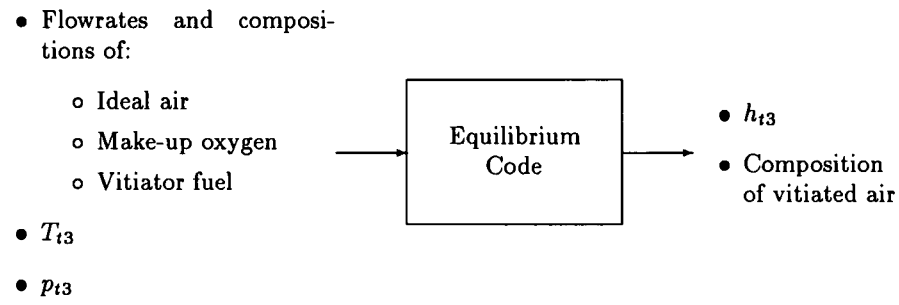

Figure 4.2: Determination of flow properties at station 3 assuming equilibrium vitiator combustion for method 3

Method 3

Input a specified temperature (T_{t3}) and pressure (p_{t3}) into an aerothermochemical equilibrium code and calculate the equilibrium flow, given the mass fractions for the air, make-up oxygen and the vitiator fuel (Figure 4.2).

Method 4

If the $T - p$ approach of Method 3 cannot be done by the code then an iterative approach can be used that gives identical results. Use an aerothermochemical equilibrium code to calculate the composition and temperature of the vitiated air for a specified pressure (p_{t3}), given the mass fractions for the air, make-up oxygen and vitiator fuel. The heat losses are considered by adjusting the enthalpies (via the heat of formation) of the vitiator ingredients until the calculated temperature matches the measured temperature at station 2 (Figure 4.3).

Test cases were used to evaluate the four vitiated air methods. Air was burned with vitiator fuels (hydrogen and methane) to obtain inlet air temperatures of 700 and $1000K$. A $100K$ temperature loss was assumed to occur between the vitiator and the combustor inlet.

The results of the vitiator enthalpy calculation for each method are tabulated (Table 4.5). Method 1 overpredicts the value of enthalpy when compared to the more rigorous approaches of Methods 2–4. This was due to the failure to account for vitiator product species. The values of vitiator enthalpy calculated from Methods 2–4 were nearly identical. It is recommended that one of these methods be used for most applications and that the use of Method 1 be restricted to conditions with a low vitiator temperature.

4.5 Results from the Aerothermochemical Equilibrium Codes

The numerical values of some theoretical performance parameters may be different depending on which equilibrium option is selected. The code outputs are also dependent on assumptions made in determining the inputs or on the calculation procedure itself. Each of these items is considered further in the following subsections.

4.5.1 Equilibrium Option

A user of any aerothermochemical equilibrium code must decide whether frozen or local equilibrium flow is more appropriate. Generally, local equilibrium is appropriate from station 4 to station 5. Condensation and recombination processes can be important between stations 5 and 6. Therefore, from station 5 to station 6 one must decide between local equilibrium, frozen or a combination of local equilibrium followed by frozen flow.

However, it is recommended to run the code first with both the local equilibrium and the frozen flow options between stations 4 and 6 to determine the difference in performance between the two modes. If a difference of more than 5% is observed in specific impulse it is recommended that the code be re-run, assuming local equilibrium flow between stations 4 and 5 and frozen flow between stations 5 and 6.

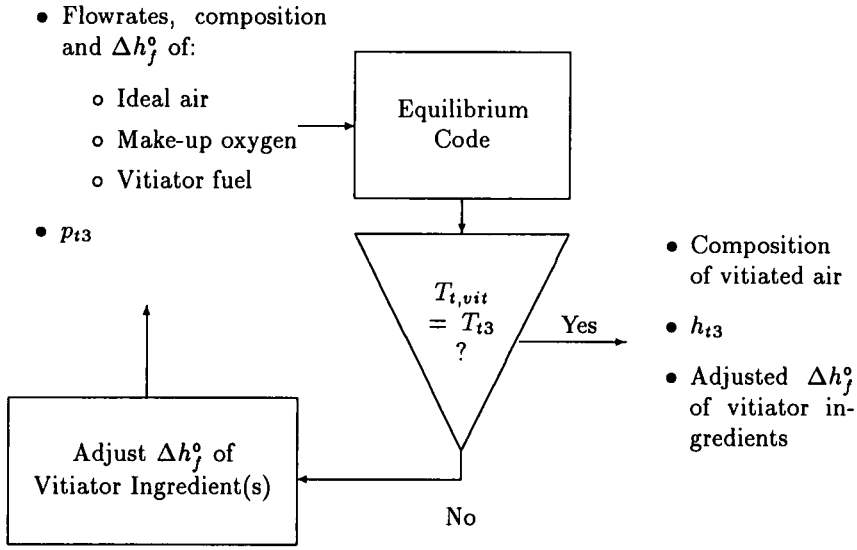

Figure 4.3: Determination of flow properties at station 3 assuming equilibrium vitiator combustion for method 4

		Product enthalpies $[kJ/kg]$		
Vitiator Fuel	Vitiator Temperature $[K]$	Method 1	Method 2	Method 3 & 4
Hydrogen	700	415.0	-112.8	-112.8
	1000	747.6	-123.2	-123.1
Methane	700	415.0	-169.4	-169.3
	1000	747.6	-216.9	-217.1

Table 4.5: Summary of product enthalpies (Air $N_{835}O_{224}Ar_5$ at $p_{t2} = 650kPa$)

4.5.2 Effects of Input Parameters on Theoretical Performance

The effects of combustor Mach number, condensed species and the aerothermochemical equilibrium code used on theoretical performance parameters were evaluated. The effects of ideal air versus vitiated air were discussed in Section 4.4.5.3, but are addressed in more detail in Chapter 7 and 8. The inputs used in this investigation are listed below.

T_{t2} $= 625K$

Δh_f° $= 0J/kg$ for $N_{835}O_{224}Ar_5$ at $298K$

Δh_f° $= 335\ kJ/kg$ for $N_{835}O_{224}Ar_5$ at $625K$

Δh_f° $= -773kJ/kg$ for $C_{10}H_{16}$ at $298K$

Δh_f° $= 0J/kg$ for Boron at $298K$

Δh_f° $= 0J/kg$ for Magnesium at $298K$

p_4 $= 218kPa$

p_5 $= 100kPa$

f/a $= 0.0704$ for $C_{10}H_{16}$

f/a $= 0.1$ for $(C_{10}H_{16})_{50\%}(B)_{40\%}(Mg)_{10\%}$

Two ramjet fuels were used in order to address the issue of condensed species. One was a liquid hydrocarbon fuel ($C_{10}H_{16}$) and the other a metallized fuel (a blend of $C_{10}H_{16}$ (50%), B (40%) and Mg (10%) by mass). Ideal air ($N_{835}O_{224}Ar_5$) rather than vitiated air (ideal air, make-up oxygen and vitiator fuel) was used to simplify the calculation procedure. The results are presented in Table 4.6.

The codes require p_{t4} as an input, but p_4 is usually the only available measurement. If it can be assumed that $M_4 = 0$ then, $p_{t4} = p_4$. However, if this assumption is not valid, then it becomes important to calculate p_{t4} and use this value as the input to the code. Specific impulse is very dependent on the value used for p_{t4} as seen from cases 1 and 4 of Table 4.6. Combustion temperatures were somewhat affected by pressure and other parameters were only slightly affected. The validity of assuming $p_{t4} = p_4$ is dependent on the parameters of interest and the combustor Mach number.

Case	Fuel	M_4	p_{t4} kPa	T_{t4} K	T_5 K	i_{sp} Ns/kg	Code
1	Liquid	0	218	2449	2271	1022	PEP
2	Liquid	0	218	2450	2269	1022	NASA CET89
3	Liquid	0.41	240	2453	2272	1072	PEP
4	Liquid	0.86	330	2465	2280	1247	PEP
5	Metallized	0	218	2709	2540	1052	PEP
6	Metallized	0.41	240	2714	2544	1112	PEP
7	Metallized	0.86	330	2733	2556	1287	PEP
8	Metallized	0.86	330	2736	2558	1288	NASA CET89

Table 4.6: Values of theoretical performance parameters

There were no significant differences (compare cases 1 and 2 or cases 7 and 8 of Table 4.6) in the calculated values obtained from the two equilibrium codes used (NASA CET89 and PEP).

4.6 Determination of the Stoichiometric Fuel/Air Ratio

The stoichiometric fuel/air ratio is required for calculating equivalence ratio (Equation 4.2) and is generally defined by the stoichiometric equation for ideal air and the fuel/propellant assuming complete combustion, regardless of whether the actual air is vitiated or not.

$$\phi = \frac{(f/a)_{meas}}{(f/a)_{stoich}} \tag{4.2}$$

Other methods are sometimes used to determine this ratio, however, since the air is almost always vitiated. Method 2 considers only the ideal air portion of the vitiated air to determine a stoichiometric fuel/air ratio. Combustion products of the vitiator are not included.

Method 3 requires the determination of a theoretical equivalence ratio for a hydrocarbon ramjet fuel (the ratio of oxidizer required for complete combustion of the vitiator and ramjet fuels to that available for combustion) according to Equation 4.3. The numerator consists of the oxidizer used in the vitiator combustor process subtracted from that required for complete combustion of all fuels at station 4. The denominator is the oxidizer available for combustion of the ramjet fuel. The oxidizer needed for complete combustion of the vitiator fuel is appropriately accounted for by this method.

$$\phi = \frac{(N_H/2.0 + N_C \times 2.0)_4 - (N_H/2.0 + N_C \times 2.0)_2}{(N_O)_2 - (N_H/2.0 + N_C \times 2.0)_2} \tag{4.3}$$

The stoichiometric fuel/air ratio may then be calculated using Equation 4.2 and the measured fuel/air ratio. This method will give a result identical to method 2, if the actual mole fraction of oxygen in the vitiated air is 0.2095.

The NASA CET89 code also provides the equivalence ratio from which the stoichiometric fuel/air ratio can be determined.

4.7 Other Aspects of Theoretical Performance Prediction

Several computer codes are available for the prediction of combustion instabilities [11]–[13], plume signature and multi-phase flow losses [14]. Any modern finite element code will calculate potential acoustic frequencies that may be excited. There are no codes for the prediction of frequencies that will be excited.

5 Required Measured Parameters

The main objective of this chapter is to specify the minimum set of parameters that should be measured to determine the performance of a ramjet engine. Typical ways of measuring these parameters are indicated. Some additional nonessential (but useful) data that can also be obtained are briefly mentioned.

5.1 Required Measured Parameters to Evaluate Ramjet Engine Performance

The measured parameters listed below use the station numbers and nomenclature specified in Chapter 3 and are valid for the liquid fuel ramjet, ducted rocket and solid fuel ramjet. The parameters are listed according to whether they are measured before and/or after a test or during a test.

5.1.1 Measurements Taken Before and/or After a Test

These measurements are the following:

A_2 geometric area at station 2

$A_{2\star}$ geometric area at station $2\star$ for solid fuel ramjet with by-pass inlets

A_4 geometric area at station 4

A_5 geometric area at station 5

A_6 geometric area at station 6, if used

A_b nozzle base area (Figure 5.1)

A_g ducted rocket gas generator throat area

$m_{f,i}$ initial mass of fuel/propellant (SFRJ and DR only)

$m_{f,f}$ final mass of fuel/propellant (SFRJ and DR only)

$T_{f,i}$ initial fuel/propellant temperature

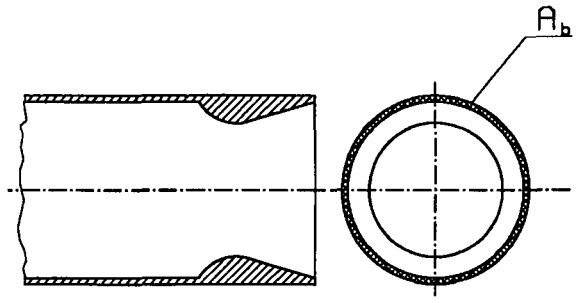

Figure 5.1: Base area for a convergent-divergent nozzle

5.1.2 Measurements Taken During a Test

Each parameter is measured as a function of time. It is assumed here that inlet conditions are measured at station 2 (and possibly station $2^\star$ for by-pass inlets). If a location beyond station 2 (or $2^\star$) is utilized then appropriate subscripts should be used.

$\dot{m}_2$ mass flow rate at station 2.
If vitiated air is used

$$\dot{m}_2 = \dot{m}_{air} + \dot{m}_{vf} + \dot{m}_{O_2} \qquad (5.1)$$

- $\dot{m}_{air}$ non vitiated air mass flow rate
- $\dot{m}_{vf}$ vitiator fuel mass flow rate
- $\dot{m}_{O_2}$ oxygen make-up mass flow rate (vitiator oxidizer and replenishment)

p_2 or p_{t2} static or total pressure at station 2

T_{t2} total temperature at station 2

For by-pass inlets with SFRJ (Figure 3.2) $\dot{m}_{2^\star}$, $p_{2^\star}$ or $p_{t2^\star}$ and $T_{t2^\star}$ are also needed.

$\dot{m}_f$ fuel or propellant mass flow rate

p_4 static pressure at station 4

p_b base pressure

p_{amb} local ambient pressure

F_{LC} load cell force

If heat losses or thermal induced area changes are to be taken into account, additional measurements are required. (For example, if a water cooled device is applied, $\dot{m}_{H_2O}$, $T_{H_2O,in}$ and $T_{H_2O,out}$ are required.)

5.2 Typical Methods for Measuring Parameters

It is assumed that mass flow rate, pressure, temperature and force are measured using conventional techniques. It is further assumed that pressures and temperatures should represent appropriate averaged values across the flow area. Special ramjet measurements are delineated below.

5.2.1 Nozzle Discharge Coefficient

The discharge coefficient is traditionally a streamline curvature correction to yield the effective flow area for one-dimensional isentropic flow.

For sonic flow the following equation can be used to estimate c_{D5} experimentally (using pre- and/or post-test air flow):

$$\dot{m}_5 = p_{t5} A_5 c_{D5} \sqrt{\frac{\gamma_5}{R_5 T_{t5}}} \left(\frac{2}{\gamma_5 + 1}\right)^{\frac{\gamma_5+1}{2(\gamma_5-1)}} \tag{5.2}$$

with

R_5 $= \mathcal{R}/\mathcal{M}_5$

$\mathcal{R}$ universal gas constant

$\mathcal{M}_5$ molecular weight at station 5

γ_5 $= \gamma_{f5}$ or $= \gamma_{s5}$ or $= \gamma_{p,4-5}$ (Appendix B)

However, it is generally very difficult to obtain an accurate value of c_{D5} because of inaccuracies in the measurements of mass flow rate, pressure and temperature and the effect of molecular weight and specific heat ratio.

If accurate values cannot be determined experimentally then c_{D5} may be estimated from reference [33].

5.2.2 Fuel Mass Flow Rates for SFRJ and DR

In the cases of the solid fuel ramjet and ducted rocket, the mass flow rate is not measured directly, but can be approximated by the methods given below.

- SFRJ:

$$\dot{m}_f = \frac{m_{f,i} - m_{f,f}}{t_b} \tag{5.3}$$

with

$m_{f,i} - m_{f,f}$ total burnt mass of fuel

t_b burn time

- DR with choked gas generator, constant injection throat area and for a constant c^*:

$$\dot{m}_f(t) = \frac{(m_{f,i} - m_{f,f}) p_{t,g}(t)}{\int_0^{t_b} p_{t,g}(t) dt} \tag{5.4}$$

with

$p_{t,g}$ gas generator total pressure
(Practically, the gas generator static pressure, p_g, is measured and used in the instantaneous fuel mass flow rate calculation Eq. 5.4.)

- DR with unchoked gas generator or choked gas generator with variable injection throat area:

$$\dot{m}_f(t) = \varrho_f S_b(t) r_b(t) \tag{5.5}$$

with

ϱ_f propellant density

S_b propellant burning surface area

r_b burning rate

The burning rate for solid propellants can be measured directly or calculated with a burning law, generally expressed by:

$$r_b = a p_g^n \tag{5.6}$$

with

a a parameter which depends primarily upon propellant temperature

n pressure exponent

The parameters a and n can be a function of pressure and initial propellant temperature.

For solid propellant configurations with varying burning area, there is a relation between burning grain area and burnt thickness such that $S_b(t) = f(E_b(t))$ where this last value is obtained by

$$E_b(t) = \int_0^t r_b(t) dt \tag{5.7}$$

The method also requires knowledge of the relation between the burning rate and the gas generator pressure.

5.3 Useful Data not Essential for Performance Calculations

For a better understanding of ramjet engine behaviour, other useful data, although not essential, are frequently taken. For instance:

- Combustor surface temperature (e.g thermocouple, pyrometer, IR thermography).
- Direct instantaneous measurements of DR and SFRJ fuel regression rate (e.g ultrasonic or X ray methods).
- Exhaust plume signature (e.g temperature, IR, particle size).
- Local flowfield (e.g velocity, temperature, distortion, turbulence).

5.4 Pressure Oscillations and Combustion Instabilities

The analysis of pressure oscillations and combustion instabilities is a difficult problem and requires a specific detailed description. Nevertheless, it is generally assumed that unsteady pressure measurements are made (e.g piezoelectric transducers) at locations on the combustor wall (water cooled transducers) and/or the inlet ducts.

From the signal-time histories that are obtained, frequency, amplitude and phase data can be determined.

6 Experimental Performance Evaluation

The performance evaluation of ramjet motors is accomplished with the help of characteristic parameters. Usually these parameters are determined by a combination of measurement and analytical calculation. Typical ramcombustor performance parameters are:

- Combustion efficiency
- Total pressure loss
- Nozzle expansion efficiency
- Expulsion efficiency of the fuel tank or gas generator

In addition, other parameters characterizing the operational function or limits of the engine may be used. They include ignition limits, blow-off limits and combustion stability. The latter parameters are not addressed in this report.

6.1 Assumptions and Procedures

Required measured parameters are listed in Chapter 5. These parameters are used as the data base for the calculations which can be performed using the equations in this chapter.

Furthermore, for the calculation procedure several assumptions are necessary:

- One dimensional flow.
- Mass flow at station 4 is the same as at station 5: $\dot{m}_4 = \dot{m}_5$. That means that the complete mass flow of the combustor is expanded through the nozzle. In the following sections either $\dot{m}_4$ or $\dot{m}_5$ are used, depending on which is most appropriate to the context.
- Total pressure losses between stations 4 and 5 are neglected: $p_{t4} = p_{t5}$
- Heat losses between stations 4 and 5 are neglected: $T_{t4} = T_{t5}$.
- Between stations 4 and 5 isentropic, equilibrium flow is assumed.
- Normally, the Mach number at station 5 is $M_5 = 1$. The nozzle throat is choked.

The evaluation process necessitates knowledge of the composition of the combustion gases. In principle, a chemical analysis of the combustion products is needed. Because of the high effort that this would entail, and in order not to introduce additional sources of error, this procedure is avoided in most cases. Instead, it is assumed that the composition of the combustion gases is the same as in the case of chemical equilibrium. Concerning the physical model, upon which the evaluation process is based, this means that the energy losses of incomplete reactions are substituted by simple heat losses. Only in the case of highly incomplete reaction within the combustion chamber will this assumption lead to noticeable errors of evaluation: the better the efficiency, the truer the assumption.

Referring to the calculation procedures, there are two approaches possible.

One is to relate stagnation to static properties (Appendix B). Any use of γ-values is to some extent inaccurate, but the inaccuracies are small. It is recommended in this procedure to use the γ_p between the chamber stagnation and static throat conditions.

The more correct procedure is to extract from the aerothermochemical equilibrium calculation the direct relationship between the several parameters. This does not require the determination of γ-values. The normal approach is to apply the theoretical values of adiabatic combustion. A refinement, by using a plausible average combustion efficiency in the theoretical calculation, may be reasonable in some cases. The effort of a true iteration is usually not worthwhile.

6.2 Combustion Efficiency

In general, an efficiency definition compares a measured performance value with a theoretically evaluated one. The resulting value gives information about the quality of the examined process. Hence, the general formula is:

$$\eta = \frac{\text{experimentally determined value}}{\text{theoretically determined value}}$$

where the numerator and denominator consist of characteristic performance parameters. Due to practical or traditional reasons, several definitions of combustion efficiency are in use. Presented herein are combustion efficiencies

based on characteristic velocity (η_{c^*}), vacuum specific impulse (η^*_{vac}), temperature rise ($\eta_{\Delta T}$) and equivalence ratio (η_ϕ).

Incomplete combustion of ramjet fuel (with some fuel unburned) in fuel-rich situations results in a nonequilibrium combustion temperature that is higher than the theoretical equilibrium combustion temperature. Thus, combustion efficiencies greater than unity may be calculated when $\phi > 1$.

There are two basic ways to determine combustion efficiency, either by measured static chamber pressure or by measured thrust. Both ways can be executed utilizing isentropic exponents (Appendix B) or, as recommended in 6.1, by utilizing parameters derived from the aerothermochemical equilibrium code, not using γ-values. The resulting four methods are outlined below.

Derivations of the equations utilized in this chapter are given in Appendix C.

6.2.1 Efficiency Based on Characteristic Velocity

The c^* efficiency compares the characteristic velocities of the exhaust jet derived from experiment and from theory.

$$\eta_{c^*} = \frac{c^*_{exp}}{c^*_{th}} \tag{6.1}$$

c^*_{exp} given by:

$$c^*_{exp} = \frac{p_{t4} A_5 c_{D5}}{\dot{m}_4} \tag{6.2}$$

where

c^*_{th} is calculated with the aerothermochemical equilibrium code

c_{D5} is the discharge coefficient at station 5

$\dot{m}_4$ is given by:

$$\dot{m}_4 = \dot{m}_{air} + \dot{m}_{vit} + \dot{m}_f$$

The methods to determine the total pressure p_{t4} are as follows:

1. Based on measured static pressure utilizing γ:

   In this case, M_4 must first be calculated.

$$M_4 = \frac{c_{D5} A_5}{A_4} \left(\frac{2}{\gamma_{p,s}+1} + \frac{\gamma_{p,s}-1}{\gamma_{p,s}+1} M_4^2 \right)^{\frac{\gamma_{p,s}+1}{2(\gamma_{p,s}-1)}} \tag{6.3}$$

   Then

$$p_{t4} = p_{4,exp} \left(1 + \frac{\gamma_{p,s}-1}{2} M_4^2 \right)^{\frac{\gamma_{p,s}}{\gamma_{p,s}-1}} \tag{6.4}$$

2. Based on measured static pressure without using γ:

   p_{t4} can be determined using the following expression

$$p_{t4} = \left(\frac{p_{t4}}{p_4} \right)_{th} p_{4,exp} \tag{6.5}$$

   where $(p_{t4}/p_4)_{th}$ is obtained from an aerothermochemical equilibrium code for a specified area ratio $A_4/(A_5 c_{D5})$.

3. Based on measured thrust utilizing γ:

   In the case of thrust measurement with a convergent nozzle the total pressure at station 4 (assumed = p_{t5}) can be determined from the following equation:

$$p_{t4} = \frac{F_5 + p_{amb} A_5}{(1+\gamma_{p,s} c_{D5}) A_5} \left(\frac{\gamma_{p,s}+1}{2} \right)^{\frac{\gamma_{p,s}}{\gamma_{p,s}-1}} \tag{6.6}$$

   F_5 is the load cell thrust, corrected for base pressure force and preloads on the thrust stand

4. Based on measured thrust without utilizing γ:

   p_{t4} $(= p_{t5})$ is given by:

$$p_{t4} = \left(\frac{c^*}{i^*_{vac}} \right)_{th} \frac{F_5 + p_{amb} A_5}{A_5 c_{D5}} \tag{6.7}$$

6.2.2 Efficiency Based on Vacuum Specific Impulse

$\eta_{i^*_{vac}}$ describes the relation of an experimental vacuum specific impulse to the theoretical value:

$$\eta_{i^*_{vac}} = \frac{i^*_{vac,exp}}{i^*_{vac,th}} \tag{6.8}$$

i^*_{vac} is defined as the thrust per unit mass flow of a convergent nozzle discharging into a vacuum. This value is identical with the stream thrust per unit mass flow in the sonic throat:

$$i^*_{vac} = \frac{F_{S5}}{\dot{m}_5} \tag{6.9}$$

$i^*_{vac,th}$ can be obtained using an aerothermochemical equilibrium code and the following equation:

$$i^*_{vac,th} = \frac{\dot{m}_5 c_5 + p_5 A_5}{\dot{m}_5} \tag{6.10}$$

$i^*_{vac,exp}$ can be derived from one of the following techniques:

1. Based on measured static pressure using γ:

$$i^{\star}_{vac,exp} = \frac{p_{t4}A_5}{\dot{m}_4}\left(\frac{2}{\gamma_{p,s}+1}\right)^{\frac{\gamma_{p,s}}{\gamma_{p,s}-1}}(1+\gamma_{p,s}c_{D5}) \tag{6.11}$$

where p_{t4} is obtained from Eqs. 6.3 and 6.4.

2. Based on measured pressure without using γ:

$$i^{\star}_{vac,exp} = c^{\star}_{exp}\left(\frac{i^{\star}_{vac}}{c^{\star}}\right)_{th} \tag{6.12}$$

where $c^{\star}_{exp}$ is calculated with Eqs. 6.2 and 6.5.

3. Based on measured thrust using γ:
In this particular case method 3 does not exist because γ does not appear in the resulting expression.

4. Based on measured thrust without using γ:

$$i^{\star}_{vac,exp} = \frac{F_5 + p_{amb}A_5}{\dot{m}_5} \tag{6.13}$$

There exists another method using measured static pressure in the sonic throat:

$$i^{\star}_{vac,exp} = (\gamma_{p,s}c_{D5}+1)\frac{p_5 A_5}{\dot{m}_5} \tag{6.14}$$

This approach is not often used due to the difficulties of measuring p_5.

The efficiencies $\eta_{i^{\star}_{vac}}$ and $\eta_{c^{\star}}$ are directly equivalent.

Note that the use of either efficiency depends on the type of measurement. If the test arrangement has a convergent nozzle and thrust is measured, the evaluation based on $i^{\star}_{vac}$ is more straight forward. If only pressure is measured, it is more appropriate to use $c^{\star}$.

6.2.3 Efficiency Based on Temperature Rise

The value $\eta_{\Delta T}$ shows the experimental stagnation temperature rise in comparison to the theoretical temperature rise in the combustion chamber:

$$\eta_{\Delta T} = \frac{T_{t4,exp} - T_{t2}}{T_{t4,th} - T_{t2}} \tag{6.15}$$

where

$T_{t4,th}$ can be obtained from an aerothermochemical equilibrium code.

In principle $T_{t4,exp}$ can be measured directly (total temperature probes, calorimeters etc.) but good results are difficult to achieve. In most cases the total temperature at station 4 is determined directly from the experimentally obtained characteristic velocity and/or vacuum specific impulse, using one of the following methods:

1. pressure measurement at station 4 using γ:

$$T_{t4,exp} = \gamma_{p,s}\left(\frac{2}{\gamma_{p,s}+1}\right)^{\frac{\gamma_{p,s}+1}{\gamma_{p,s}-1}}\frac{c^{\star 2}_{exp}}{R_{4,exp}} \tag{6.16}$$

or:

$$T_{t4,exp} = \frac{\gamma_{p,s}}{2(\gamma_{p,s}+1)}\frac{i^{\star 2}_{vac,exp}}{R_{4,exp}} \tag{6.17}$$

For practical reasons, $R_{4,exp}$ is replaced by $R_{4,th}$ obtained from an aerothermochemical equilibrium code. $c^{\star}_{exp}$ is obtained from Eqs. 6.2–6.4 and $i^{\star}_{vac,exp}$ from Eq. 6.11.

2. pressure measurement at station 4 without using γ:

$$T_{t4,exp} = \left(\frac{T_{t4}R_4}{c^{\star 2}}\right)_{th}\frac{c^{\star 2}_{exp}}{R_{4,exp}} \tag{6.18}$$

or:

$$T_{t4,exp} = \left(\frac{T_{t4}R_4}{i^{\star 2}_{vac}}\right)_{th}\frac{i^{\star 2}_{vac,exp}}{R_{4,exp}} \tag{6.19}$$

The same comment on $R_{4,exp}$ as given above applies here also. $c^{\star}_{exp}$ is obtained from Eqs. 6.2 and 6.5 and $i^{\star}_{vac,exp}$ from Eq. 6.12.

3. thrust measurement using γ:
Use Eq. 6.16 together with Eq. 6.2 and Eq. 6.6 to obtain $T_{t4,exp}$.

4. thrust measurement without using γ:
Use Eq. 6.19 together with Eq. 6.13 to obtain $T_{t4,exp}$.

6.2.4 Efficiency Based on Equivalence Ratio

The efficiency of a combustion process can be characterized by comparison of the experimentally injected equivalence ratio ϕ_{inj} against the theoretical value ϕ_b which is necessary to gain the experimentally determined performance ($c^{\star}$, $i^{\star}_{vac}$).

$$\eta_{\phi} = \frac{\phi_b}{\phi_{inj}} \tag{6.20}$$

with:

$$\phi_{inj} = \left(\frac{\dot{m}_f}{\dot{m}_{air}}\right)_{exp}\frac{1}{(f/a)_{stoich}} \tag{6.21}$$

For example, an aerothermochemical equilibrium code is used to generate the theoretical relationship between $c^{\star}$ and ϕ (Fig. 6.1). The figure is entered with $c^{\star}_{exp}$ to obtain ϕ_b. Normally, this technique is used for experimentally injected equivalence ratios $\phi \leq 1$. $c^{\star}$ varies insignificantly with small changes in pressure. Therefore, p_{t4} obtained using any of the above mentioned methods is suitable for input to the code.

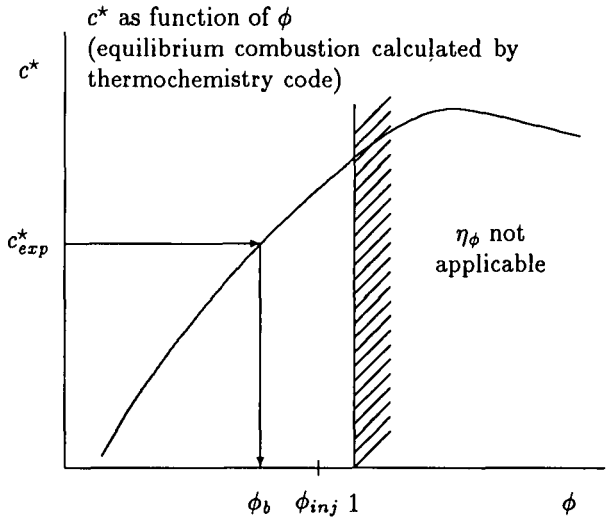

Figure 6.1: Principle of determination of ϕ_b from $c^* = f(\phi)$

6.3 Additional Performance Parameters

6.3.1 Pressure Losses

Usually, pressure losses are characterized by the ratio of total pressures:

$$\frac{p_{t4}}{p_{t2}} \tag{6.22}$$

or by the relative difference of total pressures:

$$\frac{p_{t2} - p_{t4}}{p_{t2}} \tag{6.23}$$

Pressure losses occur at different places in the ramjet engine. The above mentioned pressure ratios give only global values. The following pressure losses may be found in a ramjet engine:

- aerodynamic stagnation pressure losses caused by
  - sudden expansion (dump) from station 2 up to station 4 (Carnot diffusor)
  - wall friction
  - flow turning
  - fuel injector and flameholder drag
- stagnation pressure losses caused by combustion

Direct measurement of the total pressures with rakes of pitot-tubes mostly leads to complicated test arrangements. The pitot-tubes must be cooled and, because of this, they become bulky. Therefore, there is a risk that the test results may be affected by blockage of the chamber cross-section. If metallized propellants are used the severe problem arises to protect the orifices from being clogged by the combustion products. Therefore, in most cases the total pressures are derived from the measurements of static wall pressures or thrust.

In the following sections the equations for determination of the total pressures are presented.

6.3.1.1 Evaluation of p_{t2}

p_{t2} may be determined using

$$p_{t2} = p_2 \left(1 + \frac{\gamma_2 - 1}{2} M_2^2\right)^{\frac{\gamma_2}{\gamma_2 - 1}} \tag{6.24}$$

M_2 is found as the subsonic solution of the following relation:

$$M_2 \sqrt{1 + \frac{\gamma_2 - 1}{2} M_2^2} = \frac{\dot{m}_2}{p_2 A_2} \sqrt{\frac{R_2 T_{t2}}{\gamma_2}} \tag{6.25}$$

Referring to section 6.1 it is best to use the process γ between stagnation and static conditions at station 2. Low Mach number and moderate temperatures at station 2 permit the process γ to be replaced by γ values obtained from air tables at the measured temperature T_{t2}.

6.3.1.2 Evaluation of p_{t4}

The total pressure at station 4 can be derived from measurements either of static pressure p_4 or of the thrust. In addition, the evaluation of p_{t4} can be done with or without utilizing isentropic exponents, using the formulas presented in Section 6.2.1.

6.3.2 Expulsion Efficiency

The expulsion efficiency characterizes the completeness of the fuel/propellant utilization and has the following definition:

$$\eta_{ex} = \frac{m_{f,inj}}{m_{f,i}} = 1 - \frac{\Delta m_f}{m_{f,i}} \tag{6.26}$$

$m_{f,i}$ is the total stored propellant, Δm_f is the residue of the fuel/propellant in the tank system, gas generator or combustor (in the case of the solid fuel ramjet) after use.

The liquid fuel ramjet has a rather high expulsion efficiency of about 0.98. Fuel residues are due to wetting of the bladder, remainder in pipes and pumps, etc.

High expulsion efficiencies are not easily obtained for solid propellant ducted rocket gas generators. However, with a proper design of the propellant and gas generator an expulsion efficiency of above 0.96 is possible.

The expulsion problems are even more critical in the case of the solid fuel ramjet, primarily due to non-uniform burning of the fuel grain. Generally, the expulsion efficiency will remain below 0.95.

6.3.3 Nozzle expansion efficiency

In section 6.1 the evaluation of ramcombustor performance was based on the assumption that the flow within the convergent part of the nozzle was isentropic. This idealization is admissible since the losses within a well-shaped convergent nozzle are small. Moreover, the idealization of the flow process in the subsonic part of the nozzle does not suppress these small losses, but only shifts them to the performance balance of the combustor.

The losses within the supersonic part of the thrust nozzle can be higher. Losses are caused by:

1. wall friction
2. divergence and local shocks
3. heat transfer to the wall
4. two-phase flow effects
5. incomplete recombination (or dissociation)

The first two types of losses are approximately proportional to the exit stream thrust and are usually considered by the expansion efficiency φ_D, being defined as follows (assuming no base drag):

$$\begin{aligned} \varphi_D &= \frac{(p_6 A_6 + \dot{m}_6 c_6)_{exp}}{(p_6 A_6 + \dot{m}_6 c_6)_{th}} \\ &= \frac{F_6 + p_{amb} A_6}{[p_6 A_6 (1 + \gamma_6 M_6^2)]_{th}} \end{aligned} \qquad (6.27)$$

where F_6 equals the load cell thrust corrected for any preloads on the thrust stand and base pressure forces.

In the regime of moderate supersonic speeds up to about Mach 4, the aerodynamic types of losses ("1" and "2") are dominant, and the expansion efficiency is a useful tool to determine the effective thrust from the theoretical values calculated with the aerothermochemical equilibrium code. With well shaped thrust nozzles, expansion efficiencies of about 0.98 are possible.

In the hypersonic flight regime, the nozzle performance losses due to incomplete recombination have increasing significance, and have to be calculated or at least estimated by appropriate methods before the expansion efficiency is applied.

The wall heat transfer is of noticeable influence only in the case of heat-sink or active cooling and then has to be considered.

The two-phase flow effects which significantly reduce the performance of solid propellant rocket motors are of minor importance in the case of ramjets. Due to the high dilution by nitrogen, the solid mass fraction of ramjet exhaust is always small, even if metals are applied as a fuel compound. Nevertheless, the negative influence has to be considered and it is recommended to reduce the expansion efficiency by about one percentage point if a highly metallized propellant is used.

7 Sample Calculations

Sample calculations are provided to assist the reader with applications of methodologies established in this report. All aerothermochemical equilibrium calculations were performed with the help of the NASA CET89 code [9] according to the assumptions as outlined in Chapter 6. Results from four cases are presented. Case 1 is for a LFRJ performance without vitiation heating of the test air medium (ideal air). For this case, calculation results are provided for combustion efficiency based on characteristic velocity, vacuum specific impulse, temperature rise and equivalence ratio. Each efficiency parameter is computed both from measured static combustor pressure and measured sonic thrust. For each type of measurement calculations were made with and without $\gamma_{p,s}$. Therefore, results of the four computational methods are presented. Case 2 is a sample calculation for LFRJ performance when a vitiated air heater is employed. Cases 3 and 4 are sample calculations only for mass flow rates for the DR and SFRJ, respectively, because the remaining calculations are identical to those of the LFRJ. Tables 7.1 and 7.2 present a summary of the equations necessary for the calculation of the performance parameters using the four methods presented in Chapter 6.

Combustor and nozzle heat losses are neglected in the theoretical calculations of the following examples. For all calculations the actual input and output files for the NASA CET89 are given in Appendix D.

7.1 LFRJ Performance with Ideal Air (Case 1)

This case is for a kerosene-fueled LFRJ tested in an ideal air test medium (no vitiator). Detailed procedures are presented only for the method "measured static combustor pressure without using γ". However, numerical results for all four methods are summarized in Table 7.3.

7.1.1 Calculation Procedure

The following describes a methodology that can be followed to calculate the efficiency parameters and is organized in the order the information is required, and the order of Chapter 3, Methods for Reporting Test Results.

7.1.1.1 General test information

- Fuel: $C_{10}H_{20}$ kerosene
- Air: $N_{156.2}O_{41.96}Ar_{0.934}C_{0.0314}$

7.1.1.2 Geometric data

- Flow areas

$$A_2 = 0.010325\ m^2$$
$$A_4 = 0.022698\ m^2$$

- Exhaust nozzle (Fig. 5.1 and C.1)

$$A_5 = 0.012668\ m^2$$
$$c_{D5} = 0.996$$
$$A_b = 0.004304\ m^2$$

7.1.1.3 Measured test data

- Mass flows

$$\dot{m}_{vf} = 0.0\ kg/s$$
$$\dot{m}_{O_2} = 0.0\ kg/s$$
$$\dot{m}_{air} = 6.692\ kg/s$$
$$\dot{m}_f = 0.311\ kg/s$$

- Thrust stand forces

$$F_{LC} = 13400\ N$$
$$F_{tare} = 5000\ N$$

- Pressures and temperatures

$$p_{amb} = 101300\ Pa$$
$$p_2 = 650200\ Pa$$
$$p_4 = 568800\ Pa$$
$$p_5 = 341203\ Pa$$
$$p_b = 78065\ Pa$$
$$T_{t2} = 606\ K$$
$$T_f = 298.15\ K$$

Method	1		2	
Calculation Procedure	p_4 with γ		p_4 without γ	
Parameter	Equation	Source	Equation	Source
M_2	$M_2\sqrt{1+\frac{\gamma_2-1}{2}M_2^2}=\left(\frac{\dot{m}_2}{p_2A_2}\right)\sqrt{\frac{R_2T_{t2}}{\gamma_2}}$	Eq. 6.25	Method 1	
p_{t2}	$p_{t2}=p_2\left(1+\frac{\gamma_2-1}{2}M_2^2\right)^{\frac{\gamma_2}{\gamma_2-1}}$	Eq. 6.24	Method 1	
T_{t4}, p_{t4} 1^{st} It.	$p_{t4}=p_{4,exp},\ T_{t4}=T_4$		Method 1	
$\gamma_{p,s}$	$\gamma_{p,s}=\frac{\ln(p_{t4}/p_{5,th})}{\ln(p_{t4}/p_{5,th})-\ln(T_{t4}/T_{5,th})}$	Eq. B.10	not required	
M_4	$M_4=\frac{c_{D5}A_5}{A_4}\left(\frac{2}{\gamma_{p,s}+1}+\frac{\gamma_{p,s}-1}{\gamma_{p,s}+1}M_4^2\right)^{\frac{\gamma_{p,s}+1}{2(\gamma_{p,s}-1)}}$	Eq. 6.3	not required	
p_{t4}	$p_{t4}=p_4\left(1+\frac{\gamma_{p,s}-1}{2}M_4^2\right)^{\frac{\gamma_{p,s}}{\gamma_{p,s}-1}}$	Eq. 6.4	$p_{t4}=\left(\frac{p_{t4}}{p_4}\right)_{th}p_{4,exp}$	Eq. 6.5
rerun aerothermochemistry code using p_{t4}; yields new theoretical values				
$R_{4,exp}$	$R_{4,exp}=R_{4,th}$		Method 1	
c^*_{exp}	$c^*_{exp}=\frac{p_{t4}A_5c_{D5}}{\dot{m}_4}$	Eq. 6.2	Method 1	
$T_{t4,exp}$	$T_{t4,exp}=\gamma_{p,s}\left(\frac{2}{\gamma_{p,s}+1}\right)^{\frac{\gamma_{p,s}+1}{\gamma_{p,s}-1}}\frac{c^{*2}_{exp}}{R_{4,exp}}$	Eq. 6.16	$T_{t4,exp}=\left(\frac{T_{t4}R_4}{c^{*2}}\right)_{th}\frac{c^{*2}_{exp}}{R_{4,exp}}$	Eq. 6.18
recalculate $\gamma_{p,s}$, M_4 and p_{t4} — iterate to desired accuracy				
$i^*_{vac,exp}$	$i^*_{vac,exp}=\frac{p_{t4}A_5}{\dot{m}_4}\left(\frac{2}{\gamma_{p,s}+1}\right)^{\frac{\gamma_{p,s}}{\gamma_{p,s}-1}}(1+\gamma_{p,s}c_{D5})$	Eq. 6.11	$i^*_{vac,exp}=c^*_{exp}\left(\frac{i^*_{vac}}{c^*}\right)_{th}$	Eq. 6.12
ϕ_b	p_{t4}, c^*_{exp} and code	Fig. 7.1	Method 1	
$(f/a)_{stoich}$	$(f/a)_{stoich}=\frac{(\dot{m}_f/\dot{m}_{air})_{exp}}{\phi}$		Method 1	
ϕ_{inj}	$\phi_{inj}=\frac{(\dot{m}_f/\dot{m}_{air})_{exp}}{(f/a)_{stoich}}$	Eq. 6.21	Method 1	
η_{c^*}	$\eta_{c^*}=\frac{c^*_{exp}}{c^*_{th}}$	Eq. 6.1	Method 1	
$\eta_{i^*_{vac}}$	$\eta_{i^*_{vac}}=\frac{i^*_{vac,exp}}{i^*_{vac,th}}$	Eq. 6.8	Method 1	
$\eta_{\Delta T}$	$\eta_{\Delta T}=\frac{T_{t4,exp}-T_{t2}}{T_{t4,th}-T_{t2}}$	Eq. 6.15	Method 1	
η_ϕ	$\eta_\phi=\frac{\phi_b}{\phi_{inj}}$	Eq. 6.20	Method 1	
p_{t4}/p_{t2}	$\frac{p_{t4}}{p_{t2}}$	Eq. 6.22	Method 1	
$(p_{t2}-p_{t4})/p_{t2}$	$\frac{p_{t2}-p_{t4}}{p_{t2}}$	Eq. 6.23	Method 1	
All required theoretical values are obtained from the NASA CET89 code: p_{t4}/p_4, $R_{4,th}$, R_2, γ_2, ϕ, $T_{t4,th}$, $p_{5,th}$, c^*_{th}, i^*_{vac}				

Table 7.1: Summary of equations for performance calculations

7.1.1.4 Preliminary Calculations

The following preliminary calculations must be made to provide inputs for the efficiency parameter equations in Chapter 6:

- Fuel enthalpy Enthalpy of fuel

$$\begin{aligned} h_f &= \text{book value at measured } T_f \\ &= -2016.6\ kJ/kg \end{aligned}$$

Since the aerothermochemical equilibrium code requires enthalpy units in $cal/mole$:

$$\begin{aligned} h_f &= -2016.6\frac{kJ}{kg}\times\frac{1000\ cal}{4.184\ kJ}\times \\ &\quad \frac{1\ kg}{1000\ g}\times 140.27\frac{g}{mole} \\ &= -67607\frac{cal}{mole} \end{aligned}$$

- Nozzle stream thrust (Eqs. C.25 – C.26)

$$\begin{aligned} F_{meas} &= F_{LC}-F_{tare} \\ &= 13400-5000 \\ &= 8400\ N \end{aligned}$$

Method	3		4	
Calculation Procedure	F_5 with γ		F_5 without γ	
Parameter	Equation	Source	Equation	Source
M_2	Method 1		Method 1	
p_{t2}	Method 1		Method 1	
T_{t4}, p_{t4} 1^{st} It.	Method 1		Method 1	
$\gamma_{p,s}$	Method 1		not required	
M_4	Method 1		not required	
p_{t4}	$p_{t4} = \frac{F_5 + p_{amb}A_5}{(1+\gamma_{p,s}c_{D5})A_5}\left(\frac{\gamma_{p,s}+1}{2}\right)^{\frac{\gamma_{p,s}}{\gamma_{p,s}-1}}$	Eq. 6.6	$p_{t4} = \left(\frac{c^*}{i^*_{vac}}\right)_{th}\frac{F_5 + p_{amb}A_5}{A_5 c_{D5}}$	Eq. 6.7
rerun aerothermochemistry code using p_{t4}; yields new theoretical values				
$R_{4,exp}$	Method 1		Method 1	
c^*_{exp}	Method 1		Method 1	
$T_{t4,exp}$	Method 1		Method 2	
recalculate $\gamma_{p,s}$, M_4 and p_{t4} — iterate to desired accuracy				
$i^*_{vac,exp}$	no procedure		$i^*_{vac,exp} = \frac{F_5 + p_{amb}A_5}{\dot{m}_5}$	Eq. 6.13
ϕ_b	Method 1		Method 1	
$(f/a)_{stoich}$	Method 1		Method 1	
ϕ_{inj}	Method 1		Method 1	
η_{c^*}	Method 1		Method 1	
$\eta_{i^*_{vac}}$	Method 1		Method 1	
$\eta_{\Delta T}$	Method 1		Method 1	
η_ϕ	Method 1		Method 1	
p_{t4}/p_{t2}	Method 1		Method 1	
$(p_{t2} - p_{t4})/p_{t2}$	Method 1		Method 1	
All required theoretical values are obtained from the NASA CET89 code: p_{t4}/p_4, $R_{4,th}$, R_2, γ_2, ϕ, $T_{t4,th}$, $p_{5,th}$, c^*_{th}, i^*_{vac}				

Table 7.2: Summary of equations for performance calculations (cont'd)

$$\begin{aligned} F_5 &= F_{meas} - A_b(p_b - p_{amb}) \\ &= 8400 - 0.004304(78065 - 101300) \\ &= 8500\ N \end{aligned}$$

- Station 2 conditions
  With tables or an aerothermochemical equilibrium code (Fig. D.1), determine the following at station 2
  - inputs: p_{t2} (assumed equal to measured p_2), T_{t2}, air composition
  - output:

$$\begin{aligned} \mathcal{M}_2 &= 28.965\ kg/kmole \\ \gamma_2 &= 1.3750 \\ h_2 &= h_{t2} = h_{air} \end{aligned}$$

$$= 310.9\ kJ/kg$$

converting to $cal/mole$:

$$\begin{aligned} h_{air} &= 310.9\frac{kJ}{kg} \times \frac{1000\ cal}{4.184\ kJ} \times \\ &\quad \frac{1\ kg}{1000\ g} \times 28.965\frac{g}{mole} \\ &= 2152.4\frac{cal}{mole} \end{aligned}$$

$$\begin{aligned} R_2 &= \frac{\mathcal{R}_2}{\mathcal{M}_2} \\ &= \frac{8314.51}{28.965} \\ &= 287.05\ \frac{J}{kg\ K} \end{aligned}$$

- Chamber total pressure (p_{t4})

  The process for determining p_{t4} requires several sequential runs of the aerothermochemical equilibrium code. Method 2 (Table 7.1) is being used for the sample calculation. However, for clarity, the required processes to obtain p_{t4} for all four methods are shown.

  For all methods, run the aerothermochemical equilibrium code using a measurement or estimate of p_4 (in this example $p_4 = 568800\ Pa$) as a first approximation to generate p_{t4}.

  - input (Fig. D.2): p_4, $A_4/(A_5 c_{D5})$, $\dot{m}_{air}/\dot{m}_f$, h_{air}, h_f

$$\begin{aligned}\frac{A_4}{A_5 c_{D5}} &= \frac{0.022698}{0.012668 \times 0.996} \\ &= 1.7990 \\ &= \texttt{SUBAR(1)}\end{aligned}$$

$$\begin{aligned}\frac{\dot{m}_{air}}{\dot{m}_f} &= \frac{6.692}{0.311} \\ &= 21.5177 \\ &= \texttt{MIX(1)}\end{aligned}$$

  - output (Fig. D.2):

$$\begin{aligned} p_{5,th} &= 314560\ Pa \\ \left(\frac{p_{t4}}{p_4}\right)_{th} &= 1.0793 \\ T_{4,th} &= 2065.80\ K \\ T_{5,th} &= 1834.46\ K \\ c^*_{th} &= 1170\ m/s \\ i^*_{vac,th} &= 1462.1\ Ns/kg \\ \phi &= 0.6877 \end{aligned}$$

  - obtain first estimate for the chamber-to-throat process γ ($\gamma_{p,s}$):
    with $p_{t4} = p_4$ and $T_{t4} = T_4$

$$\begin{aligned}\frac{p_{t4}}{p_{5,th}} &= \frac{568800}{314560} \\ &= 1.8082\end{aligned}$$

$$\begin{aligned}\frac{T_{t4}}{T_{5,th}} &= \frac{2065.80}{1834.46} \\ &= 1.1261\end{aligned}$$

    From Eq. B.10:

$$\begin{aligned}\gamma_{p,s} &= \frac{\ln(p_{t4}/p_{5,th})}{\ln(p_{t4}/p_{5,th}) - \ln(T_{t4}/T_{5,th})} \\ &= \frac{\ln(1.8082)}{\ln(1.8082) - \ln(1.1261)} \\ &= 1.2508\end{aligned}$$

Method 1: using measured p_4 and γ

  - determine the combustor Mach number using Eq. 6.3

$$\begin{aligned}M_4 &= \frac{c_{D5}A_5}{A_4} \times \left(\frac{2}{\gamma_{p,s}+1} + \frac{\gamma_{p,s}-1}{\gamma_{p,s}+1}M_4^2\right)^{\frac{\gamma_{p,s}+1}{2(\gamma_{p,s}-1)}} \\ &= \frac{0.996 \times 0.012668}{0.022698}\left(\frac{2}{1.2508+1} + \frac{1.2508-1}{1.2508+1}M_4^2\right)^{\frac{1.2508+1}{2(1.2508-1)}} \\ &= 0.3504\end{aligned}$$

  - compute p_{t4} using Eq. 6.4:

$$\begin{aligned}p_{t4} &= p_4\left(1 + \frac{\gamma_{p,s}-1}{2}M_4^2\right)^{\frac{\gamma_{p,s}}{\gamma_{p,s}-1}} \\ &= 568800 \times \left(1 + \frac{1.2508-1}{2}0.3504^2\right)^{\frac{1.2508}{1.2508-1}} \\ &= 613838\ Pa\end{aligned}$$

  - rerun the aerothermochemical equilibrium code using $p_{t4} = 613838\ Pa$ (all other input data unchanged)
    output (Fig. D.3):

$$\begin{aligned} p_{5,th} &= 339460\ Pa \\ T_{t4,th} &= 2066.02\ K \\ T_{5,th} &= 1834.49\ K \\ c^*_{th} &= 1170\ m/s \\ i^*_{vac,th} &= 1462.1\ Ns/kg \\ \mathcal{M}_4 &= 28.909\ kg/kmole \end{aligned}$$

  - recalculate $\gamma_{p,s}$ using Eq. B.10:

$$\gamma_{p,s} = 1.2510$$

    and p_{t4} using Eq. 6.3 and 6.4

$$p_{t4} = 613845\ Pa$$

  - perform additional iterations for increased accuracy, only if the successive values in p_{t4} differ significantly

Method 2: using measured p_4 without γ

  - calculate combustor total pressure using Eq. 6.5

$$\begin{aligned}p_{t4} &= \left(\frac{p_{t4}}{p_4}\right)_{th} p_{4,exp} \\ &= 1.0793 \times 568800 \\ &= 613906\ Pa\end{aligned}$$

  - rerun aerothermochemical equilibrium code at $p_{t4} = 613906 Pa$ (all other input data unchanged)

output (Fig. D.4):

$$\begin{aligned} p_{t4}/p_4 &= 1.0793 \\ T_{t4,th} &= 2066.02\ K \\ T_{5,th} &= 1834.49\ K \\ c^*_{th} &= 1170\ m/s \\ i^*_{vac,th} &= 1462.1\ m/s \\ \mathcal{M}_4 &= 28.909\ kg/kmole \end{aligned}$$

Method 3: using measured thrust and γ

- calculate chamber total pressure using Eq. 6.6

$$\begin{aligned} p_{t4} &= \frac{F_5 + p_{amb}A_5}{(1+\gamma_{p,s}c_{D5})A_5}\left(\frac{\gamma_{p,s}+1}{2}\right)^{\frac{\gamma_{p,s}}{\gamma_{p,s}-1}} \\ &= \frac{8500 + 101300 \times 0.012668}{(1+1.2508 \times 0.996)0.012668} \times \\ &\quad \left(\frac{1.2508+1}{2}\right)^{\frac{1.2508}{1.2508-1}} \\ &= 619848\ Pa \end{aligned}$$

- rerun aerothermochemical equilibrium code using $p_{t4} = 619848\ Pa$ (all other input unchanged)
  output (Fig. D.5):

$$\begin{aligned} p_{5,th} &= 342780\ Pa \\ T_{t4,th} &= 2066.05\ K \\ T_{5,th} &= 1834.50\ K \\ c^*_{th} &= 1170\ m/s \\ i^*_{vac,th} &= 1462.1\ Ns/kg \\ \mathcal{M}_4 &= 28.906\ kg/kmole \end{aligned}$$

- calculate $\gamma_{p,s}$ using Eq. B.10

$$\gamma_{p,s} = 1.2510$$

and p_{t4} using Eq. 6.6

$$p_{t4} = 619884\ Pa$$

- reiterate if required

Method 4: using measured thrust without γ

- calculate chamber total pressure using Eq. 6.7

$$\begin{aligned} p_{t4} &= \left(\frac{c^*}{i^*_{vac}}\right)_{th}\frac{F_5 + p_{amb}A_5}{A_5 c_{D5}} \\ &= \left(\frac{1170}{1462.1}\right) \times \\ &\quad \frac{8500 + 101300 \times 0.012668}{0.012668 \times 0.996} \\ &= 620477\ Pa \end{aligned}$$

- rerun aerothermochemical equilibrium code using $p_{t4} = 620477\ Pa$ (all other input unchanged)
  output (Fig. D.6):

$$\begin{aligned} T_{t4,th} &= 2066.05\ K \\ c^*_{th} &= 1170\ m/s \\ i^*_{vac,th} &= 1462.1\ Ns/kg \\ \mathcal{M}_4 &= 28.906\ kg/kmole \end{aligned}$$

- reiterate if required

- Stoichiometric fuel/air ratio
  using Eqs. 4.2 and 4.3 and ϕ from Fig. D.2

$$\begin{aligned} \left(\frac{f}{a}\right)_{exp} &= \frac{\dot{m}_f}{\dot{m}_{air}} \\ &= \frac{0.311}{6.692} \\ &= 0.04647 \end{aligned}$$

$$\begin{aligned} \left(\frac{f}{a}\right)_{stoich} &= \frac{\left(\frac{f}{a}\right)_{exp}}{\phi} \\ &= \frac{0.04647}{0.6877} \\ &= 0.06757 \end{aligned}$$

- Mass flows

$$\begin{aligned} \dot{m}_2 &= \dot{m}_{air} \\ &= 6.692\ kg/s \\ \dot{m}_4 &= \dot{m}_5 = \dot{m}_2 + \dot{m}_f \\ &= 6.692 + 0.311 \\ &= 7.003\ kg/s \end{aligned}$$

7.1.1.5 Performance Calculation

The performance parameters can now be calculated by employing the equations of Chapter 6 and using the output shown in Fig. D.1 for Station 2 and Figs. D.2 and D.4 for Stations 4 and 5. All required equations are given in column 2 of Table 7.1. Results are presented in Table 7.3.

- Combustion Efficiency

1. Efficiency based on characteristic velocity, η_{c^*}
   Using Eq. 6.2

$$\begin{aligned} c^*_{exp} &= \frac{p_{t4}A_5 c_{D5}}{\dot{m}_4} \\ &= \frac{613906 \times 0.012668 \times 0.996}{7.003} \\ &= 1106.08\ m/s \end{aligned}$$

From Eq. 6.1

$$\begin{aligned} \eta_{c^*} &= \frac{c^*_{exp}}{c^*_{th}} \\ &= \frac{1106.08}{1170} \\ &= 0.9454 \end{aligned}$$

Method		1	2	3	4
Calculation Procedure		p_4 using γ	p_4 without using γ	F_5 using γ	F_5 without using γ
M_2	-	0.351			
p_{t2}	Pa	706824			
$\gamma_{p,s}$ 1^{st} iter.	-	1.2508	-	1.2508	-
M_4	-	0.350	-	0.350	-
p_{t4}	Pa	613838	613906	619848	620477
$R_{4,exp}$	$J/kg/K$	287.6	287.6	287.6	287.6
c^*_{exp}	m/s	1106	1106	1117	1118
$T_{t4,exp}$	K	1843	1846	1879	1886
$\gamma_{p,s}$ 2^{st} iter.	-	1.2510	-	1.2510	-
$i^*_{vac,exp}$	Ns/kg	1383	1382	-	1397
ϕ_b	-	0.567	0.568	0.587	0.587
$(f/a)_{stoich}$	-	0.0676	0.0676	0.0676	0.0676
ϕ_{inj}	-	0.688	0.688	0.688	0.688
η_{c^*}	-	0.945	0.945	0.955	0.955
η_{i^*}	-	0.945	0.945	-	0.955
$\eta_{\Delta T}$	-	0.847	0.850	0.872	0.877
η_ϕ	-	0.825	0.825	0.853	0.856
p_{t4}/p_{t2}	-	0.868	0.869	0.877	0.878
$(p_{t2}-p_{t4})/p_{t2}$	-	0.132	0.132	0.123	0.122

Table 7.3: LFRJ performance with ideal air (Case 1)

2. Efficiency based on vacuum specific impulse, $\eta_{i^*_{vac}}$

From Eq. 6.12

$$\begin{aligned} i^*_{vac,exp} &= c^*_{exp}\left(\frac{i^*_{vac}}{c^*}\right)_{th} \\ &= 1106.08\left(\frac{1462.1}{1170}\right) \\ &= 1382.22\ m/s \end{aligned}$$

From Eq. 6.8

$$\begin{aligned} \eta_{i^*_{vac}} &= \frac{i^*_{vac,exp}}{i^*_{vac,th}} \\ &= \frac{1382.22}{1462.1} \\ &= 0.9454 \end{aligned}$$

3. Efficiency based on temperature rise, $\eta_{\Delta T}$

with $R_{4,exp} = R_{4,th}$ and Eq. 6.18

$$\begin{aligned} R_{4,th} &= \frac{\mathcal{R}}{\mathcal{M}_4} \\ &= \frac{8314.51}{28.909} \\ &= 287.61\ J/kg/K \end{aligned}$$

$$\begin{aligned} T_{t4,exp} &= \left(\frac{T_{t4}R_4}{c^{*2}}\right)_{th}\frac{c^{*2}_{exp}}{R_{4,exp}} \\ &= \left(\frac{2066.02\times 287.61}{(1170)^2}\right)\times\frac{1106.08^2}{287.61} \\ &= 1846.44\ K \end{aligned}$$

Using Eq. 6.15.

$$\begin{aligned} \eta_{\Delta T} &= \frac{T_{t4,exp}-T_{t2}}{T_{t4,th}-T_{t2}} \\ &= \frac{1846.44-606}{2066-606} \\ &= 0.8496 \end{aligned}$$

4. Efficiency based on equivalence ratio, η_ϕ

A plot of theoretical characteristic velocity (c^*_{th}) versus equivalence ratio (ϕ) has to be generated using the aerothermochemical equilibrium code as shown in Fig. D.7 and 7.1. This is achieved by using the input file Fig. D.7 while varying the ratio between $\dot{m}_{air}$ and $\dot{m}_f$. The equivalence ratio (ϕ_b) necessary to theoretically produce the measured c^*_{exp} is determined from this plot.

$$\phi_b = 0.5675$$

Using Eq. 6.21

$$\begin{aligned} \phi_{inj} &= \left(\frac{\dot{m}_f}{\dot{m}_{air}}\right)_{exp}\frac{1}{(f/a)_{stoich}} \\ &= \left(\frac{0.311}{6.692}\right)\frac{1}{0.06757} \\ &= 0.6878 \end{aligned}$$

Using Eq. 6.20

$$\eta_\phi = \frac{\phi_b}{\phi_{inj}}$$

c^* $(\frac{m}{s})$	1094	1097	1100	1103	1106	1109
ϕ	0.550	0.555	0.560	0.565	0.570	0.575
c^* $(\frac{m}{s})$	1112	1115	1118	1120	1123	
ϕ	0.580	0.585	0.590	0.595	0.600	

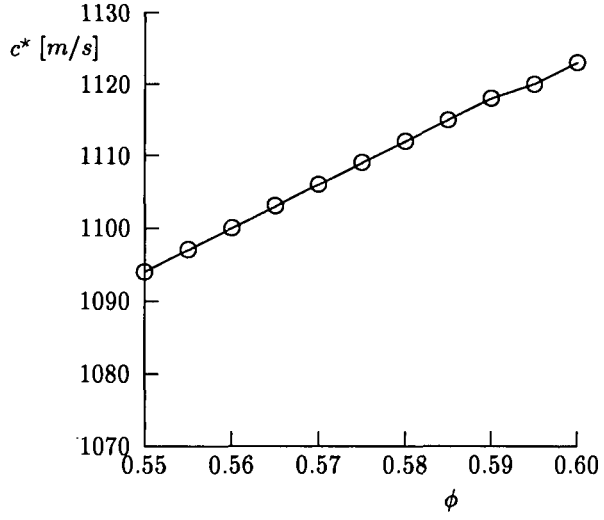

Figure 7.1: Determination of ϕ_b from $c^* = f(\phi)$

$$= \frac{0.5675}{0.6878}$$
$$= 0.8251$$

- Combustor total pressure loss
  - calculate the Mach number at station 2 using Eq. 6.25:

$$M_2\sqrt{1+\frac{\gamma_2-1}{2}M_2^2} = \frac{\dot{m}_2}{p_2 A_2}\sqrt{\frac{R_2 T_{t2}}{\gamma_2}}$$

$$M_2\sqrt{1+\frac{1.3750-1}{2}M_2^2} =$$
$$\frac{6.692}{650200 \times 0.010325} \times \sqrt{\frac{287.05 \times 606}{1.3750}}$$
$$M_2 = 0.3505$$

  - calculate the total pressure at station 2 using Eq. 6.24:

$$p_{t2} = p_2\left(1+\frac{\gamma_2-1}{2}M_2^2\right)^{\frac{\gamma_2}{\gamma_2-1}}$$
$$= 650200 \times \left(1+\frac{1.3750-1}{2}0.3505^2\right)^{\frac{1.3750}{1.3750-1}}$$
$$= 706824\ Pa$$

  - calculate the total pressure ratio

$$\frac{p_{t4}}{p_{t2}} = \frac{613906}{706824}$$
$$= 0.8685$$

  - calculate the relative difference of the total pressure

$$\frac{p_{t2}-p_{t4}}{p_{t2}} = \frac{706824-613906}{706824}$$
$$= 0.1315$$

7.1.2 Discussion of Results

Combustion efficiencies for Case 1, LFRJ performance with ideal air, are tabulated in Table 7.3 and the influence coefficients and uncertainty levels are summarized at the end of this section in Table 7.12.

Considering first the results in Table 7.3, one can see that the various performance parameter calculations yield different numerical values. For example, the η_{c^*} and $\eta_{i^*_{vac}}$ for Case 1 are $\approx$ 95 %, however, $\eta_{\Delta T}$ is $\approx$ 85 % and η_ϕ is $\approx$ 83 %. The main reason for the differences between the higher values (η_{c^*} and $\eta_{i^*_{vac}}$) and the lower values ($\eta_{\Delta T}$ and η_ϕ) is the range over which the parameters can vary. This demonstrates that when examining the combustion efficiency calculated for a ramjet, one must first understand the efficiency parameter that is being used.

The influence coefficients information presented in Table 7.12 is more important to the reader than the uncertainty levels, which are presented merely to demonstrate the uncertainty methodology. The influence coefficients reflect the sensitivity of performance calculation methods to input parameters. Critical input parameters can be identified which are independent of facilities or measurement systems. For example, for the $\eta_{\Delta T}$ based on combustor pressure, the input parameters with the most influence on uncertainty (greatest influence coefficients) are $\dot{m}_{air}$, p_4, c_{D5} and A_5, whereas for the $\eta_{\Delta T}$ based on thrust, $\dot{m}_{air}$ and F_5 have the largest influence coefficients.

The reader should be careful not to generalize conclusions from the uncertainty levels in Table 7.12. Uncertainty levels are highly dependent on each test facility, measurement system, calculation methods, installation effects and environmental conditions. The error sources utilized herein to estimate uncertainties are not necessarily typical values for the entire operating range. Table 7.12 shows a difference between the uncertainty levels of the first two parameters (η_{c^*} and $\eta_{i^*_{vac}}$) and the second two ($\eta_{\Delta T}$ and η_ϕ). However, a 1 % uncertainty in η_{c^*} or $\eta_{i^*_{vac}}$ is 2 % of the entire range for these performance parameters. With $\eta_{\Delta T}$ and η_ϕ, a 1 % uncertainty is 1 % of the range of these parameters.

Error analysis is an essential engineering tool for designing measurement systems, selecting calculation methods, identifying critical data validation requirements, ensuring compliance with test data requirements, interpreting test results, and providing a bookkeeping process for certifying

		Type Error (%)		Description of Error Sources
		b	s	
Standards Calibration Hierarchy	.....	0.12		b_1- Standard lab calibration, including traceability to national standards
Data Acquisition	Calibration System Errors			
	• Reference Source	*		b_2- Determination of reference pressure
	• Sensor			
	– Hysteresis		(s_7)	s_3- Sensor hysteresis (combined with s_7)
	– Non-linearity	(b_8)		b_8- Sensor non-linearity (combined with b_8)
	– Repeatability		(s_7)	s_5- Sensor repeatability (combined with s_7)
	Recording System Errors			
	• Sampling		*	s_6- Data variations due to facility or engine instabilities
	• Channel	0.15	0.15	b_7 & s_7- Signal conditioning, electrical calibrations and digital systems
Data Reduction	Data Processing Errors	0.05		b_8- Curve fits of calibration data
Other Effects	Installation Effects Errors			
	• Pressure Probe	*		b_7- Design/fabrication of probes
	Environmental Effects Errors			
	• Temperature		*	s_{10}- Temperature change effect on sensor
	• Vibration	*		b_{11}- Vibration effect on sensor
	Root Sum Square	0.20	0.15	

* Negligible Error

Table 7.4: Pressure measurement error sources (Case 1)

results. Pre-test error analysis allows corrective action to be taken prior to the test to reduce uncertainties that appear too high. In practice, it is an iterative procedure to tailor the entire process and minimize uncertainty levels. Post-test error analyses, which are based on actual test results,

- permit refinement of final uncertainty levels,
- check for consistency of redundant measurements,
- identify data validation problems.

7.1.3 Uncertainty Analysis

Representative uncertainties were determined using the methodology defined in Section 3.7 and Appendix A. Results are presented for input parameters (both measured and calculated) and performance parameters. Representative uncertainties for measured parameters of pressure, temperature, force (load cell), area and fuel flow rate are presented in Tables 7.4 through 7.8. Next, the uncertainties of calculated input parameters were determined by error propagation using appropriate measured parameter uncertainties and Influence Coefficients for airflow rate (Table 7.9), $\gamma_{p,s}$ (Table 7.10) and equivalence ratio (Table 7.11), and by choosing realistic values for nozzle discharge coefficient and stream thrust. Then, the uncertainties of performance parameters were determined for efficiencies based on characteristic velocity (c^*), vacuum specific impulse (i^*_{vac}), temperature rise ($T_{t4} - T_{t2}$), equivalence ratio (ϕ) and combustion chamber pressure loss (p_{t4}/p_{t2}), again by error propagation of appropriate measured and calculated input parameters (Table 7.12).

7.1.4 Influence Coefficients Comparisons

A sensitivity analysis was performed for each input parameter (both measured and calculated) used in the calculation of combustion efficiency. Influence coefficients were established for each input parameter by numerically perturbating the performance equations for a 1% difference

		Type Error		Description of Error Sources
		b	s	
Standards Calibration Hierarchy	.....	0.3°C		b_1- Manufacturer specification of wire or standard lab calibration
Data Acquisition	Calibration System Errors			
	• Level	0.4°C		b_2- Reference temperature level
	• Stability		0.2°C	s_3- Reference temperature stability
	Recording System Errors			
	• Sampling	0.1°C		b_4- Data variations due to facility or engine instabilities
	• Channel	0.1°C		b_5- Signal conditioning, electrical calibrations and digital systems
Data Reduction	Data Processing Errors ..		0.28°C	s_6- Curve fits of calibration data
Other Effects	Installation Effects Errors			
	• Probe Recovery	*		b_7- Probe design caused by radiation, convection, etc.
	• Conduction Error	*		b_8- Heat conduction
	• Temperature Gradients	*		b_9- Temperature gradients along nonhomogeneous thermocouple wire
	Root Sum Square	0.5°C	0.3°C	

* Negligible Error with proper design/installation

Table 7.5: Temperature measurement error sources (Case 1)

in that parameter, while keeping all other parameters constant at their nominal values (using the procedure specified in Appendix A, Section A.2.2). Results are presented in Table 7.12.

		Type Error (%)		Description of Error Sources
		b	s	
Standards Calibration Hierarchy	.....	0.12		b_1- Standard lab calibration, including traceability to national standards
Data Acquisition	Calibration System Errors			
	• Off-Axis Effects	*		b_2- Force measurement on axis different from centerline
	• Tare Correction			
	– Hysteresis		0.1	s_3- Force measurement system hysteresis
	– Non-repeatability		(s_3)	s_4- Sensor non-repeatability from repeat calibrations (combined with s_3)
	– Non-linearity	0.05		b_5- System calibration non-linearity
	Recording System Errors			
	• Sampling		*	s_6- Data variations due to facility or engine instabilities
	• Channel		0.12	s_7- Signal conditioning, electrical calibrations and digital systems
Data Reduction	Data Processing Errors ...	0.1		b_8- Curve fits of calibration data
Other Effects	Installation Effects Errors			
	• Stand Alignment	*		b_9- Misalignment of engine and data load cell force vectors
	• Load Cell	*		b_{10}- Shift in load cell calibration caused by attachments
	Pressure Effects Errors			
	• Load Cell	*		b_{11}- Cell pressure change on load cell
	• Test Cell	*		b_{12}- Cell pressure change on test cell wall ground
	• Service Lines	0.05		b_{13}- Line pressure change on tare forces
	Temperature Effects Errors			
	• Load Cell	*		b_{14}- Temperature change on load cell
	• Service Lines	(b_{16})		b_{15}- Line temperature change on tare forces (combined with b_{16})
	• Thrust Stand	0.1		b_{16}- Thermal growth of stand
	• Vibration Error		*	s_{17}- Vibration of load cell
	• Scrub Drag Error		*	s_{18}- Secondary airflow external drag
	Root Sum Square	0.2	0.15	

* Negligible Error

Table 7.6: Scale force measurement error sources (Case 1)

		Type Error (%)		Description of Error Sources
		b	s	
Standards Calibration Hierarchy	.....	0.002		b_1- Standard lab calibration for measurement instrument, including traceability to national standards
Other Effects	• Diameter Measurement Error	0.04		b_2- Determining cross-sectional area
	• Temperature Compensation Error	0.1		b_3- Difference in measurement and test temperatures, including effect of temperature error
	Root Sum Square	0.11	0	

Table 7.7: Area measurement error sources (Case 1)

		Type Error (%)		Description of Error Sources
		b	s	
Standards Calibration Hierarchy	.....	0.1		b_1- Standard lab calibration, including traceability to national standards
Data Acquisition	Calibration System Errors			
	• Cal Fluid Properties	0.15		b_2- Mismatch between calibration and test fluids
	• Flowmeter Repeatability	0.12		b_3- Non-repeatability from repeat flowmeter calibrations
	Recording System Errors			
	• Sampling		*	s_4- Data variations due to facility or engine instabilities
	• Channel		0.17	s_5- Signal conditioning, electrical calibrations and digital systems
Data Reduction	Data Processing Errors	0.1		b_6- Curve fits of calibration data
Other Effects	Installation Effects Errors			
	• Cavitation	*		b_7- Insufficient static pressure in flowmeter
	• Turbulence	*		b_8- Sharp bends, etc., upstream flowmeter
	• Meter Orientation	*		b_9- Orientation difference from calibration to test
	Environmental Effects Errors			
	• Temperature			
	– Flowmeter	*		b_{10}- Ambient temperature change on flowmeter
	– Viscosity	0.12	0.05	b_{11} & s_{11}- Determination of test fluid viscosity
	– Specific Gravity	0.1	0.05	b_{12} & s_{12}- Determination of test fluid specific gravity
	• Vibration		*	s_{13}- Vibration on flowmeter
	• Pressure	*		b_{14}- Ambient pressure change on flowmeter
	Root Sum Square	0.28	0.18	

* Negligible Error

Table 7.8: Fuel flow measurement error sources (Case 1)

	Basic Measurements			Air Mass Flow Rate ($\dot{m}_{air}$)		
	Input Parameters I	Bias Limits B_i (%)	Precision Index S_i (%)	Influence Coefficients IC (%/%)	Bias Limits $B_k = B_i IC$ (%)	Precision Index $S_k = S_i IC$ (%)
1	p_t	0.2	0.15	1.0	0.2	0.15
2	T_t	0.2	0.15	0.5	0.1	0.07
3	A	0.05	0	1.0	0.05	0
4	c_D	0.4	0	1.0	0.4	0
					$B = 0.46\,\%$	$S = 0.17\,\%$
					$U = 0.8\,\%$	

Table 7.9: Error propagation for air flow rate (Case 1)

	Basic Measurements			Process $\gamma_{p,s}$		
	Input Parameters I	Bias Limits B_i (%)	Precision Index S_i (%)	Influence Coefficients IC (%/%)	Bias Limits $B_k = B_i IC$ (%)	Precision Index $S_k = S_i IC$ (%)
1	T_{t2}	0.20	0.15	0.024	0.0048	0.0036
2	p_{t4}	0.20	0.15	0	0	0
3	ϕ	0.40	0.25	0.096	0.038	0.24
4	A_4/A_5	0.07	0	0.008	0.00056	0
					$B = 0.038\,\%$	$S = 0.24\,\%$
					$U = 0.52\,\%$	

Table 7.10: Error propagation for process $\gamma_{p,s}$ (Case 1)

	Basic Measurements			Equivalence Ratio (ϕ)		
	Input Parameters I	Bias Limits B_i (%)	Precision Index S_i (%)	Influence Coefficients IC (%/%)	Bias Limits $B_k = B_i IC$ (%)	Precision Index $S_k = S_i IC$ (%)
1	$\dot{m}_{air}$	0.29	0.17	1.0	0.29	0.17
2	$\dot{m}_f$	0.28	0.18	1.0	0.28	0.18
					$B = 0.40\,\%$	$S = 0.25\,\%$
					$U = 0.9\,\%$	

Table 7.11: Error propagation for equivalence ratio ϕ (Case 1)

	Influence Coefficients											Errors		
	A_4/A_5	A_5	c_{D5}	f/a	p_4	F_5	p_5	p_{amb}	T_{t2}	$\dot{m}_{air}$	$\gamma_{p,s}$	B [%]	S [%]	U [%]
η_{c^*}														
• p_4, $\gamma_{p,s}$	-0.2	1	1.2	-2.6	1	0	0	0	<-0.1	-1.0	<0.1	0.6	0.3	1.2
• p_4 without γ	-0.2	1	1	-2.6	1	0	0	0	<-0.1	-1.0	0	0.6	0.3	1.2
• F_5, $\gamma_{p,s}$	<0.1	0.1	0	-2.7	0	0.9	0	0.1	<-0.1	-1.0	-0.1	0.5	0.3	1.1
• F_5 without γ	0	0.1	0	-2.9	0	0.9	0	0.1	-0.1	-1.0	0	0.5	0.3	1.1
$\eta_{i^*_{vac}}$														
• p_4, $\gamma_{p,s}$	-0.2	1	0.7	-2.8	1	0	0	0	-0.1	-1.0	0.2	0.5	0.3	1.1
• p_4 without γ	-0.2	1	0.6	-2.8	1	0	0	0	-0.1	-1.0	0.1	0.5	0.3	1.1
• F_5, $\gamma_{p,s}$														
• F_5 without γ	0	0.1	0	-2.9	0	0.9	0	0.1	-0.1	-1.0	0	0.5	0.3	1.1
$\eta_{\Delta T}$														
• p_4, $\gamma_{p,s}$	-0.5	2.9	3.5	-1.0	2.9	0	0	0	-0.4	-3.0	1.2	1.8	0.8	3.4
• p_4 without γ	-0.5	2.9	2.9	-0.9	2.9	0	0	0	-0.3	-3.0	0	1.7	0.8	3.3
• F_5, $\gamma_{p,s}$	<-0.1	0.4	0	-1.0	<-0.1	2.6	0	0.4	-0.4	-3.0	0.7	1.6	1.0	3.6
• F_5 without γ	0	0.4	0	-1.0	<0.1	2.6	0	0.4	-0.4	-3.0	0	1.6	1.0	3.6
η_ϕ														
• p_4, $\gamma_{p,s}$	-0.6	3.4	4.0	-0.9	3.4	0	0	0	-0.4	-3.5	0.2	2.1	0.9	3.9
• p_4 without γ	-0.6	3.4	3.4	-0.9	3.4	0	0	0	-0.4	-3.5	0	2.0	0.9	3.8
• F_5, $\gamma_{p,s}$	<0.1	0.5	0.5	-0.9	0	3.0	0	0.5	-0.4	-3.5	-0.5	1.8	1.2	4.2
• F_5 without γ	0	0.5	0.5	-1.0	0	3.0	0	0.5	-0.4	-3.5	0	1.8	1.2	4.2

Table 7.12: Sensitivity analysis and uncertainty for performance parameters (Case 1)

7.2 LFRJ Performance with Vitiated Air Heater (Case 2)

Sample calculations are provided for a methane-fueled air vitiator with make-up oxygen. The geometrical data and ramjet measured test data are the same as for Case 1 except for air and vitiator flowrates.

7.2.1 Calculation Procedure

7.2.1.1 General Test Information

The vitiated air consists of the following ingredients with their associated composition and heat of formation at $298.15K$.

- Ramjet fuel: $C_{10}H_{20}$ kerosene
- Vitiator fuel: CH_4
- Air: $N_{156.2}O_{41.96}Ar_{0.934}C_{0.0314}$

7.2.1.2 Geometric Data

- Flow areas

$$\begin{aligned} A_2 &= 0.010325\ m^2 \\ A_4 &= 0.022698\ m^2 \end{aligned}$$

- Exhaust nozzle (Fig. 5.1 and C.1)

$$\begin{aligned} A_5 &= 0.012668\ m^2 \\ c_{D5} &= 0.996 \\ A_b &= 0.004304\ m^2 \end{aligned}$$

7.2.1.3 Measured Test Data

- Mass flows

$$\begin{aligned} \dot{m}_{vf} &= 0.047\ kg/s \\ \dot{m}_{O_2} &= 0.262\ kg/s \\ \dot{m}_{air} &= 6.383\ kg/s \\ \dot{m}_f &= 0.311\ kg/s \end{aligned}$$

- Thrust and forces

$$\begin{aligned} F_{LC} &= 13400\ N \\ F_{tare} &= 5000\ N \end{aligned}$$

- Pressures and Temperatures

$$\begin{aligned} p_{amb} &= 101300\ Pa \\ p_2 &= 650200\ Pa \\ p_4 &= 568800\ Pa \\ p_5 &= 341203\ Pa \\ p_b &= 78065\ Pa \\ T_{t2} &= 606\ K \\ T_f &= 298.15\ K \end{aligned}$$

7.2.1.4 Preliminary Calculations

The following preliminary calculations must be made to provide inputs for the efficiency parameter equations in Chapter 6:

- Ramjet fuel enthalpy

$$\begin{aligned} h_f &= \text{book value at measured } T_f \\ h_f &= -2016.60\ kJ/kg = -67607 cal/mole \end{aligned}$$

- Nozzle stream thrust (Eqs. C.26 – C.25)

$$\begin{aligned} F_{meas} &= F_{LC} - F_{tare} \\ &= 13400 - 5000 \\ &= 8400\ N \end{aligned}$$

$$\begin{aligned} F_5 &= F_{meas} - A_b(p_b - p_{amb}) \\ &= 8400 - 0.004304\,(78065 - 101300) \\ &= 8500\ N \end{aligned}$$

- Station 2 conditions

  The properties of the vitiated air are determined using one of the methods of Section 4.4.5.3. Method 3 was used in this example. The aerothermochemical equilibrium code was run to determine the properties of the vitiator products at the measured T_{t2}. In this case, the thermodynamic state of the vitiator products is specified by p_{t2} and T_{t2}, thus, the enthalpies used in the input file are irrelevant. Samples of the code input and output are shown in Appendix D (Fig. D.8).

  - inputs: p_{t2} (assumed equal to the measured p_2), T_{t2}, vitiator mass flows
  - outputs:

$$\begin{aligned} \mathcal{M}_2 &= 28.908\ kg/kmol \\ \gamma_2 &= 1.3687 \\ h_2 &= h_{t2} \\ &= -69.041\ kJ/kg = -477.0\ cal/mole \end{aligned}$$

composition (mole fractions):

$$\begin{aligned} \chi_{N_2} &= 0.74339 \\ \chi_{O_2} &= 0.20946 \\ \chi_{H_2O} &= 0.02531 \\ \chi_{CO_2} &= 0.01295 \\ \chi_{Ar} &= 0.00889 \end{aligned}$$

Vitiated air composition:
$N_{1.4868}O_{0.4701}C_{0.01295}H_{0.05062}Ar_{0.00889}$

$$\begin{aligned} R_2 &= \frac{\mathcal{R}_2}{\mathcal{M}_2} \\ &= \frac{8314.51}{28.908} \\ &= 287.62 \frac{J}{kg\ K} \end{aligned}$$

- Chamber total pressure (p_{t4})
  - run aerothermochemical equilibrium code using p_4 as a first approximation to p_{t4} (Fig. D.9)
    - ⋆ inputs: p_4, $A_4/(A_5\ c_{D5})$, h_2, h_f, $\dot{m}_2$,$\dot{m}_f$, air composition
    - ⋆ outputs:

$$\left(\frac{p_{t4}}{p_4}\right)_{th} = 1.0791$$

  - compute p_{t4} using (Eq. 6.5):

$$\begin{aligned} p_{t4} &= p_4 \left(\frac{p_{t4}}{p_4}\right)_{th} \\ &= 568800 \times 1.0791 \\ &= 613792\ Pa \end{aligned}$$

  - rerun aerothermochemical equilibrium code at $p_{t4} = 613792Pa$ to get more accurate results (Fig. D.10)
    - ⋆ input: p_{t4}, $A_4/(A_5\ c_{D5})$, h_2, h_f, $\dot{m}_2$, $\dot{m}_f$, air composition
      (all unchanged except for p_{t4})
    - ⋆ output:

$$\begin{aligned} \left(\frac{p_{t4}}{p_4}\right)_{th} &= 1.0791 \\ p_{5,th} &= 339950\ Pa \\ T_{t4,th} &= 2044.96\ K \\ T_{5,th} &= 1819.27\ K \\ c^*_{th} &= 1167\ m/s \\ i^*_{vac,th} &= 1457.1\ Ns/kg \\ \mathcal{M}_4 &= 28.855\ kg/kmole \\ \phi &= 0.7201 \end{aligned}$$

  - calculate the stoichiometric fuel/air ratio using Eq. 4.2

$$\begin{aligned} \left(\frac{f}{a}\right)_{exp} &= \frac{\dot{m}_f}{\dot{m}_{vit}} \\ &= \frac{\dot{m}_f}{\dot{m}_{air} + \dot{m}_{vf} + \dot{m}_{O_2}} \\ &= \frac{0.311}{6.383 + 0.047 + 0.262} \\ &= 0.0465 \end{aligned}$$

$$\begin{aligned} \left(\frac{f}{a}\right)_{stoich} &= \frac{(\dot{m}_f/\dot{m}_{air})_{exp}}{\phi} \\ &= \frac{0.0465}{0.7201} \\ &= 0.06457 \end{aligned}$$

- Mass flows

$$\begin{aligned} \dot{m}_2 &= \dot{m}_{air} + \dot{m}_{vf} + \dot{m}_{O_2} \\ &= 6.383 + 0.047 + 0.262 \\ &= 6.692\ kg/s \\ \dot{m}_4 &= \dot{m}_5 = \dot{m}_2 + \dot{m}_f \\ &= 6.692 + 0.311 \\ &= 7.003\ kg/s \end{aligned}$$

7.2.1.5 Performance Calculation

The performance parameters can now be calculated by employing the equations of Chapter 6 as summarized in Table 7.1. Only method 2 is presented. Results are presented in Table 7.13.

1. Efficiency based on characteristic velocity
   From Eq. 6.2

$$\begin{aligned} c^*_{exp} &= \frac{p_{t4} A_5 c_{D5}}{\dot{m}_4} \\ &= \frac{613792 \times 0.012668 \times 0.996}{7.003} \\ &= 1105.87\ m/s \end{aligned}$$

   Using Eq. 6.1

$$\begin{aligned} \eta_{c^*} &= \frac{c^*_{exp}}{c^*_{th}} \\ &= \frac{1105.87}{1167} \\ &= 0.9476 \end{aligned}$$

2. Efficiency based on vacuum specific impulse
   From Eq. 6.12

$$\begin{aligned} i^*_{vac,exp} &= c^*_{exp} \left(\frac{i^*_{vac}}{c^*}\right)_{th} \\ &= 1105.97 \left(\frac{1457.1}{1167}\right) \\ &= 1380.77\ Ns/kg \end{aligned}$$

Method		1	2	3	4
Calculation Procedure		p_4 using γ	p_4 without using γ	F_5 using γ	F_5 without using γ
M_2	-		0.352		
p_{t2}	Pa		706963		
$\gamma_{p,s}$ 1^{st} iter.	-		-		
M_4	-		-		
p_{t4}	Pa		613792		
$R_{4,exp}$	$J/kg/K$		288.2		
c^*_{exp}	m/s		1106		
$T_{t4,exp}$	K		1836		
$\gamma_{p,s}$ 2^{st} iter.	-		-		
$i^*_{vac,exp}$	Ns/kg		1381		
ϕ_b	-		0.573		
$(f/a)_{stoich}$	-		0.0646		
ϕ_{inj}	-		0.720		
η_{c^*}	-		0.948		
η_{i^*}	-		0.948		
$\eta_{\Delta T}$	-		0.855		
η_ϕ	-		0.796		
p_{t4}/p_{t2}	-		0.868		
$(p_{t2}-p_{t4})/p_{t2}$	-		0.132		

Table 7.13: LFRJ performance with vitiated air (Case 2)

From Eq. 6.8

$$\begin{aligned}\eta_{i^*_{vac}} &= \frac{i^*_{vac,exp}}{i^*_{vac,th}} \\ &= \frac{1380.77}{1457.1} \\ &= 0.9476\end{aligned}$$

3. Efficiency based on temperature rise

Using Eq. 6.18 with $R_{4,exp} = R_{4,th}$

$$\begin{aligned}R_{4,th} &= \frac{\mathcal{R}}{\mathcal{M}_4} \\ &= \frac{8314.51}{28.855} \\ &= 288.15\ J/kg/K\end{aligned}$$

$$\begin{aligned}T_{t4,exp} &= \left(\frac{T_{t4}R_4}{c^{*2}}\right)_{th}\frac{c^{*2}_{exp}}{R_{4,exp}} \\ &= \left(\frac{2044.96\times 288.15}{1167^2}\right)\frac{1105.87^2}{288.15} \\ &= 1836.33\ K\end{aligned}$$

Using Eq. 6.15

$$\begin{aligned}\eta_{\Delta T} &= \frac{T_{t4,exp}-T_{t2}}{T_{t4,th}-T_{t2}} \\ &= \frac{1836.33-606}{2044.96-606} \\ &= 0.8550\end{aligned}$$

4. Efficiency based on equivalence ratio

The equivalence ratio (ϕ_b) necessary to theoretically produce the measured $c^*_{exp} = 1105.87\ m/s$ is determined from a plot similar to Figure 7.1, but calculated for vitiated air.

$$\phi_b = 0.5727$$

Using Eq. 6.21.

$$\begin{aligned}\phi_{inj} &= \left(\frac{\dot{m}_f}{\dot{m}_{air}}\right)_{exp}\frac{1}{(f/a)_{stoich}} \\ &= \left(\frac{0.311}{6.692}\right)\frac{1}{0.06457} \\ &= 0.7197\end{aligned}$$

Using Eq. 6.20

$$\begin{aligned}\eta_\phi &= \frac{\phi_b}{\phi_{inj}} \\ &= \frac{0.5727}{0.7197} \\ &= 0.7957\end{aligned}$$

5. Calculation of combustor total pressure loss

- calculate the Mach number at station 2: using Eq. 6.25

$$M_2\sqrt{1+\frac{\gamma_2-1}{2}M_2^2} = \frac{\dot{m}_2}{p_2A_2}\sqrt{\frac{R_2T_{t2}}{\gamma_2}}$$

$$M_2\sqrt{1+\frac{1.3687-1}{2}M_2^2} =$$

$$\frac{6.692}{650200 \times 0.010325} \times \sqrt{\frac{287.62 \times 606}{1.3687}}$$
$$M_2 = 0.3517$$

- calculate the total pressure at station 2 using Eq. 6.24:

$$p_{t2} = p_2 \left(1 + \frac{\gamma_2 - 1}{2} M_2^2\right)^{\frac{\gamma_2}{\gamma_2 - 1}}$$
$$= 650200 \times \left(1 + \frac{1.3687 - 1}{2} 0.3520^2\right)^{\frac{1.3687}{1.3687-1}}$$
$$= 706963\ Pa$$

- calculate the total pressure ratio

$$\frac{p_{t4}}{p_{t2}} = \frac{613792}{706963} = 0.8682$$

- calculate the relative difference of the total pressures

$$\frac{p_{t2} - p_{t4}}{p_{t2}} = \frac{706963 - 613792}{706963} = 0.1318$$

7.3 Ducted Rocket Mass Flow Rate (Case 3)

The fuel mass flow of a ducted rocket can be determined by equation 5.4 for a choked gas generator, a constant injection throat area and a constant c^*:

Fig. 7.2 shows a typical gas generator pressure-time trace (two transducer outputs are shown in the diagram) for an end burning grain. The integration of the gas generator pressure over time is done between the points where the gas generator is choked relative to the ramburner. For the case presented, the integration limits were at 0.3 MPa for the start and at 0.5 MPa for the end. A correction of the pressure integral may be needed to take into account the mass flow injected at unchoked conditions during burnout.

The integral derived from the pressure-time trace of Fig. 7.2 amounts to 69.2994 $MPa \times s$. Together with the used propellant mass (initial propellant mass minus residues retained in the gas generator after burnout) of 5.053 kg and using Eq. 5.4, a mass flow given by Fig. 7.3 is calculated.

It should be mentioned that a period of increasing pressure between ignition and the stationary level (e.g., during the first four seconds of the trace in Fig. 7.2) can be attributed to a rising c^* or temperature. This leads to an error in the mass flow determination by underestimating the mass flow in the phase of rising pressure and overestimating the mass flow in the phase of constant pressure.

Pressure progressivity during or at the end of the stationary burning phase may be attributed to:

- intentional increases of the propellant burning surface area induced by grain geometry
- accidental increases of the propellant burning surface area induced by nonuniform (e.g., conical) burning or voids in the grain
- clogging of the gas generator nozzle throat

The first two phenomena do not affect the accuracy of the mass flow evaluation according to Eq. 5.4 as long as the c^* does not vary within the range of the pressure progressivity. The pressure rise at the end of burning (Fig. 7.2) was caused by voids at the bottom of the end burning grain.

Any significant variation of the gas generator nozzle throat area denies the applicability of Eq. 5.4 for mass flow evaluation. Even when corrections are conceivable to take into account a varying gas generator throat area, the uncertainty of the mass flow evaluated from the pressure integration will be high.

The fuel mass flow can be determined alternatively by Eq. 5.5 for a choked or unchoked gas generator.

In the example the constant burning surface area of the end burning grain is 0.0201 m^2 and the propellant density is 1510 kg/m^3. The burning rate as a function of pressure is given by Fig. 7.4. Thus, the mass flow can be evaluated:

e.g. at 10s

$$p_{t,g} = 4.74 MPa$$
$$r_b = 11.5 mm/s$$
$$\dot{m}_f = 0.349 kg/s$$

For this procedure of mass flow evaluation it is essential that the ballistic data (like given in Fig. 7.4) are valid for the full-scale grain and its geometry. Burn rate data are usually evaluated by firing small motors or by burning strands in a combustion bomb. The applicability of strand burn rate data to full-scale motors is generally poor. Burn rates determined with small ballistic test motors usually show a better comparability to the results from full-scale motors. Nevertheless, the possibilities that differences between model and full-scale grains may affect the burn rate (thermal effects, erosion, etc.) should be carefully considered before applying the above method for mass flow evaluation.

Finally, it has to be mentioned that thermal erosion of the propellant insulation (liner, boot) may contribute to the gas generator mass flow; especially for end burning grains where the effect may be significant. Mass flow from the insulation consumed is included when the mass flow

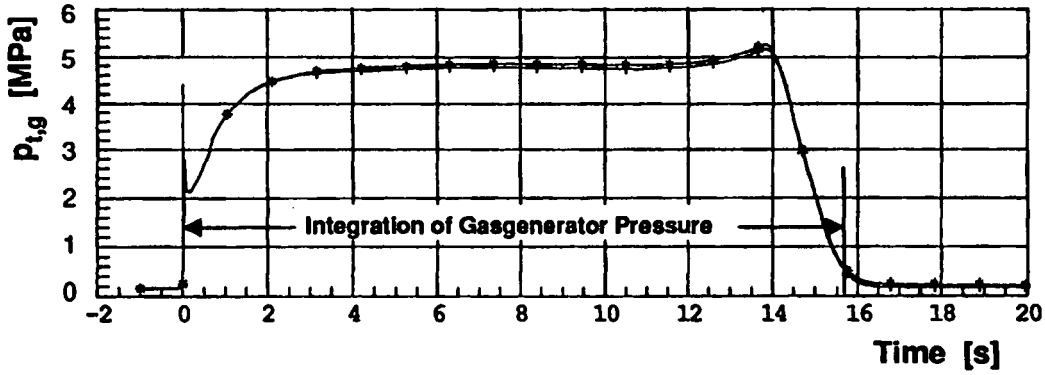

Figure 7.2: Gas generator pressure (Case 3)

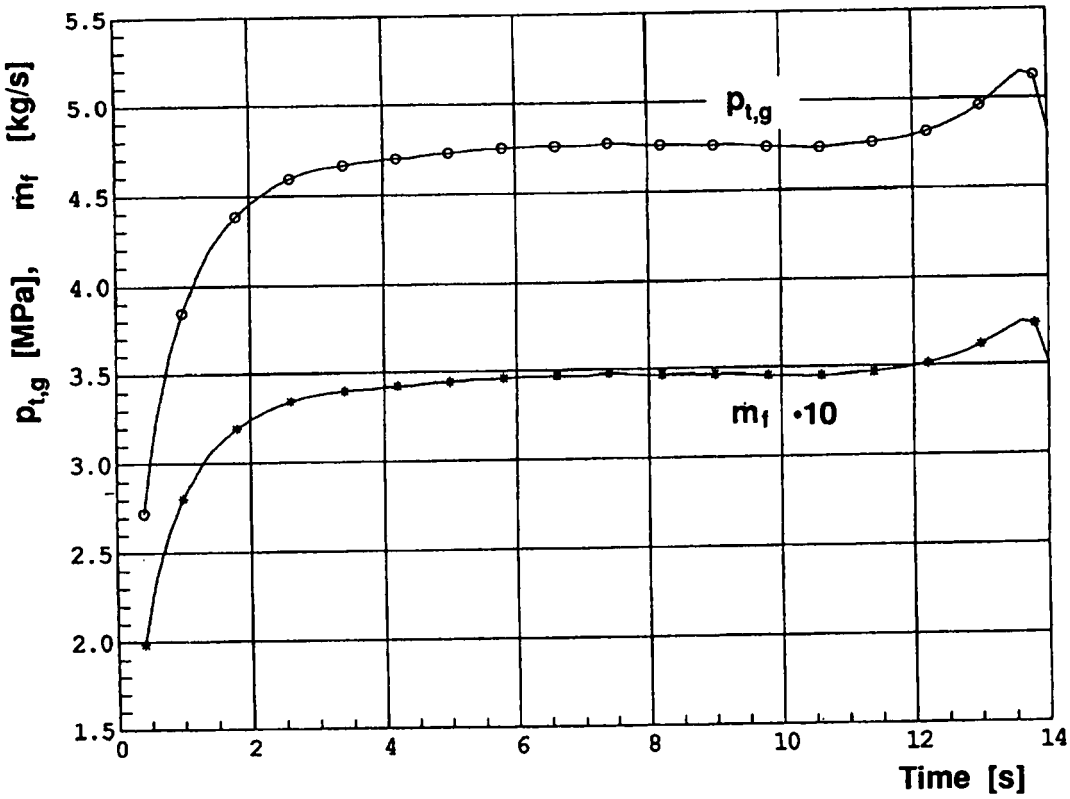

Figure 7.3: Gas generator pressure and calculated fuel mass flow (Case 3)

is determined by the pressure integration method. However, the contribution of insulation to the gas generator mass flow may not be constant during the burn time and the heating value usually differs from that of the propellant. The method for determining the gas generator mass flow based on the ballistic data does not include possible insulation mass flow.

Procedures to correct for the mass flow corresponding to the consumed insulation have to be found, depending on the individual case. It is strongly recommended that the consumption of the grain insulation be checked in order to be aware of the magnitude of the possible errors of the gas generator mass flow evaluation.

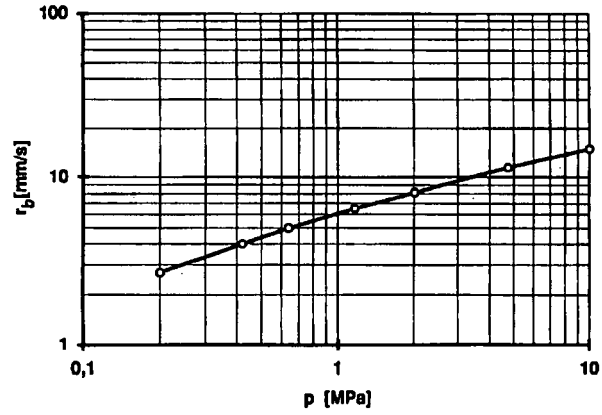

Figure 7.4: Ballistic data of the ducted rocket propellant (Case 3)

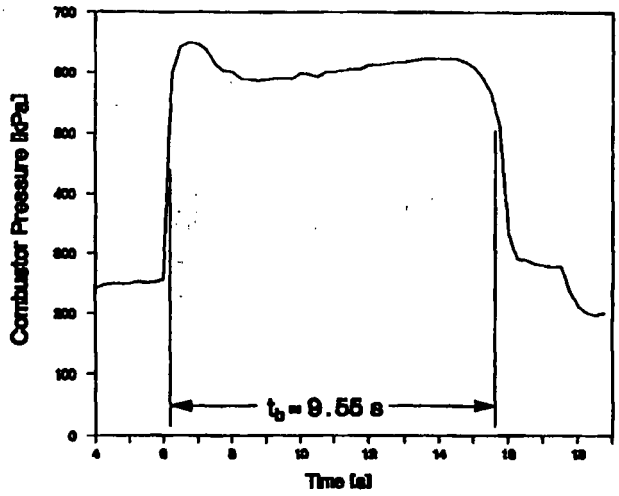

Figure 7.5: SFRJ burn time determination (Case 4)

7.4 Solid Fuel Ramjet Mass Flow Rate (Case 4)

The fuel flow rate for the SFRJ is usually a time averaged value determined from the mass of consumed fuel and combustion burn time according to equation 5.3:

$$\dot{m}_f = \frac{m_{f,i} - m_{f,f}}{t_b}$$

An example is provided for clarity.

$$\begin{aligned} m_{f,i} &= 0.684\ kg \\ m_{f,f} &= 0.305\ kg \\ t_b &= 9.55\ s \end{aligned}$$

determined from Fig. 7.5.

The initial and final fuel masses were determined with a balance or scale. The combustion burn time was determined from a pressure versus time plot as shown in Fig. 7.5. The times at combustor ignition and burnout were determined using 75% of the difference in pressures for combustion and no combustion. This method provides a reasonable alternative to an integral approach and permits quick determination of the burn time. Thus, using equation 5.3, the value for fuel mass flow rate was determined.

$$\begin{aligned} \dot{m}_f &= \frac{0.684\ kg - 0.305\ kg}{9.55\ s} \\ &= 0.0397\ kg/s \end{aligned}$$

8 Air Heaters

Aerodynamic compression through the supersonic inlet of a ramjet causes an increase in the static temperature of the air entering the combustor. Since combustor inlet Mach numbers are quite low, the static temperature is essentially equal to the stagnation temperature. At a flight Mach number of 4, the combustor inlet temperature is approximately $1000K$, at Mach 6 it is near $2000K$, and at Mach 8 the temperatures are in the $3000K$ range. The precise amount of heating required to simulate true flight conditions also varies with altitude. In order to examine combustion performance at realistic flight conditions these combustor inlet temperatures must be reproduced in test facilities, and a method for producing this heated air must be found.

8.1 Real Gas Effects

Since air exhibits non-ideal gas characteristics at elevated temperatures (thermodynamic properties vary with temperature), prediction of air total temperature requirements for a test facility must include consideration of real gas effects. Figure 8.1 shows how combustor inlet total temperature varies with flight Mach number and altitude. Figure 8.2 shows the overprediction of the air temperature that results when assuming constant properties for air as found in standard tables for supersonic flow using a specific heat ratio of 1.4. These tables should not be used to determine the correct total temperature for simulation. The correct values of Figure 8.1 were obtained by calculating enthalpy from the given Mach number and altitude conditions and using an aerothermochemical equilibrium code to solve for the air temperature assuming an isentropic compression. This method takes into account species concentration changes as well as specific heat variations to predict the total temperature required of the test facility air heater.

8.2 Heater Requirements

The ideal heater should deliver air over a wide operational envelope of mass flow, temperature and pressure and be able to support a wide range of test durations. It should also deliver good air flow quality (uniform temperature profile and low turbulence levels) and be free of air contaminants. A heater should be easy, safe and affordable to

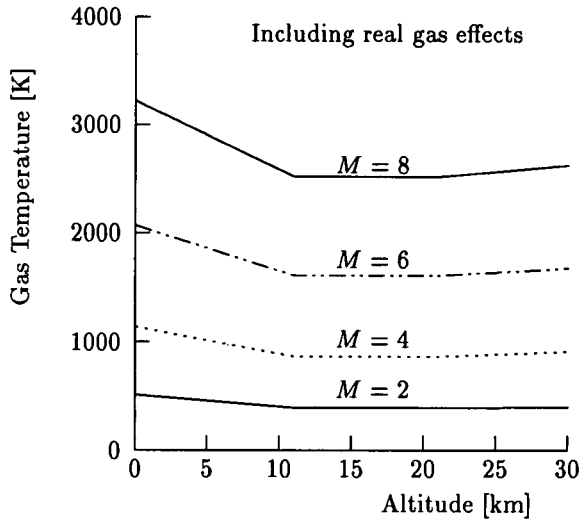

Figure 8.1: Influence of Mach number and altitude on total temperature

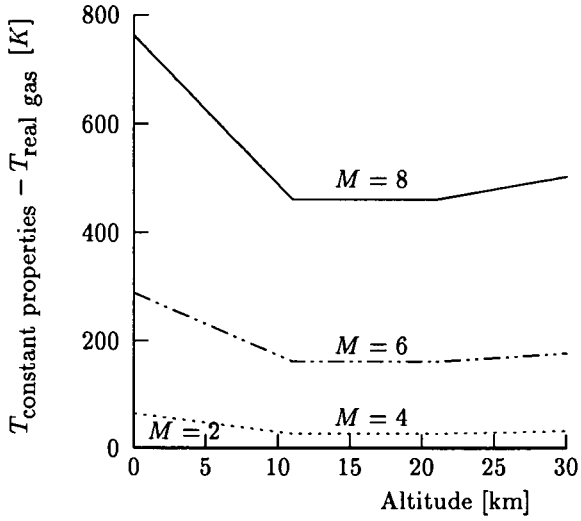

Figure 8.2: Real gas and Mach number effects on air total temperature

use. Ignition and control of the output flow should be simple and dependable and steady state conditions achieved quickly. The heater should be small and have low operation and maintenance costs. The fuel or energy source should also be economical, safe and available.

No heater meets all of these criteria, and each test facility has its own priorities. Therefore, compromises must often be made to match the requirements of a particular facility with the capabilities of available heaters.

8.3 Heater Types

Different air heating methods are used in ramjet testing. They may be grouped into three broad categories: combusting heaters (vitiators), non-combusting heaters (including heat exchangers), and combinations of these heaters.

8.3.1 Combusting Heaters (Vitiators)

Combusting heaters heat air directly with a fuel-oxidizer reaction. Fuel is burned in the air stream, often in a jet engine style combustor. The exhaust gases are used for ramjet testing after the consumed oxygen is replenished.

The main advantages of combusting air heaters are the low cost, because of the low fuel flow required, and their simplicity of operation and maintenance. The disadvantages include the effects of air heater combustion products on subsequent ramjet combustion and the change of air properties like molecular weight.

8.3.2 Non-Combusting Heaters

Non-combusting heaters avoid contamination of the air stream with combustion products and deliver clean air to the ramjet combustor.

In these heaters, air flows through a heat exchanger. The heat source may be electrical resistance or combustion of a separate fuel and oxidizer. The heat exchangers can be quite large and exit temperatures are limited by the material properties of the heat exchanger.

Heat storage devices are heat exchangers of high thermal mass that are gradually heated to operating temperature and during a test run give up stored thermal energy to air passing through them. Commonly, large vessels filled with ceramic or metal pebbles are used, heated by either electrical resistance or hot combustion gases. These storage heaters can heat air to higher temperatures than conventional heat exchangers because the pebbles are more resistant to thermal damage than fragile heat exchanger tubes. Nevertheless, repeated thermal expansion and contraction can rub the pebbles together and introduce dust particles into the air stream. Heater life span is lengthened by reducing the number and magnitude of these thermal cycles. The main challenge in designing heat storage devices is obtaining a constant output temperature for the required run time and range of test conditions. This usually results in large heaters with a high heat capacity so that only a small fraction of the energy is extracted during a run.

Electric arc heaters heat air through the release of energy produced by an electric arc between two electrodes. Arc heaters are capable of producing very high air temperatures. The facility capabilities depend primarily on the limits of the anode and cathode producing the arc. Due to the extremely high temperatures produced by the arc, ionized species are created that react to form NO_x and other undesired constituents that contaminate the air stream. The presence of these contaminants, and the fact that oxygen dissociation begins at approximately $2500K$, sets the upper limits of combustion testing in arc facilities. Above this temperature, care must be taken to account for the chemical effects of the contaminants and dissociated species on combustion. As with any electric heater the high power requirements of arc heaters make them very expensive to operate.

8.3.3 Combination Heaters

Combination heaters use a combination of the previously discussed methods to take advantage of the characteristic strengths of one method to offset the weaknesses of the other. For example, one could use a vitiator to boost the temperature from an electrically powered heat exchanger. This would allow higher temperatures without damaging the heating elements in electric heater, and would deliver lower levels of combustion products when compared to pure combustion heating. In addition this combination allows temperature variation during a run (transient simulations).

8.4 Special Considerations for Vitiators

Since vitiators are so widely used, the following sections address some important issues concerning their operation.

8.4.1 Make-up Oxygen

In heating the air, combustion in a vitiator depletes part of the available oxygen. In order to conduct combustion experiments the oxygen content of the flow must be restored to the proper percentage.

Calculation of make-up oxygen flow rates is often made to yield a mole fraction of oxygen in the vitiator products equal to that in atmospheric air (0.2095 for the first air composition in Table 4.2). To get this mole fraction the stoichiometric chemical reaction for the vitiator fuel and oxidizer combination must be examined. For a hydrogen - air vitiator the reaction is:

$$H_2 + xO_2 + \text{Air} = H_2O + yO_2 + \text{Air}$$

where x is the number of moles of make-up oxygen and y is the number of moles of oxygen in the vitiator products per mole of hydrogen vitiator fuel. Notice that because the air in the reaction already has the correct mole fraction, calculation of the make-up oxygen is only a function of the fuel flow. To get a 0.2095 oxygen mole fraction among the products other than air the following equation must be satisfied:

$$0.2095 = y/(1+y)$$

This gives $y = 0.265$ for the hydrogen-air vitiator.

Using an oxygen balance to define x:

$$2x = 1 + 2y = 1.53$$

thus, $x = 0.7650$.

Converting to a mass ratio:

$$\left(\frac{0.765\ mole\ O_2}{1\ mole\ H_2}\right)\left(\frac{31.9988\ \frac{kg\ O_2}{kmole\ O_2}}{2.016\ \frac{kg\ H_2}{kmole\ H_2}}\right) = 12.142\ \frac{kg\ O_2}{kg\ H_2}$$

Note that this method is not equivalent to adding oxygen to the vitiator exhaust to yield an oxygen mass fraction equivalent to atmospheric air (0.2315). Maintaining the mole fraction of oxygen preserves its partial pressure, and therefore reaction rates which may be important at low combustor pressures or high combustor Mach numbers. If the mass fraction of oxygen is maintained instead, the oxygen available to react in the combustor will be less.

Using the above oxygen balance equation ($2x = 1 + 2y$), and the oxygen mass fraction in atmospheric air (0.2315):

$$0.2315 = \frac{31.9988y}{18.015 + 31.9988y}$$

Hence

$$y = 0.1696$$

Substituting:

$$\begin{aligned} x &= \frac{1+2y}{2} = \frac{1+2\times 0.1696}{2} \\ &= 0.6696\frac{moles\ O_2}{mole\ H_2} \\ &= 0.6696\frac{31.9988}{2.016} \\ &= 10.628 kg\ O_2/kg\ H_2 \end{aligned}$$

This make-up oxygen mass ratio is 12.5% lower than the 12.142 ratio that was computed on a molar basis. The ratio of oxygen in the 'non-air' vitiator products is $0.1696/(1+0.1696) = 0.1450$ instead of 0.2095 as in air. This lowers the partial pressure of oxygen in the entire vitiator products.

The make-up oxygen may be mixed into the flow at any point upstream of the ramburner. However, it is usually helpful to add the oxygen upstream of the vitiator to ensure good mixing and help raise the heater's efficiency and broaden its operating range.

8.4.2 Air Contaminants

The use of vitiated air instead of ideal air to study ramjet combustion in connected-pipe testing will have an effect not only on the experimental performance but also on the theoretical performance prediction.

The most important problem associated with vitiated air tests is the influence of the contaminants on the combustion process. Unreacted vitiator fuel will add energy to the ramjet and species such as CO and H_2O can change ignition, combustion efficiency and flame holding characteristics measured in the combustor.

Concerning the theoretical performance, contaminants complicate the problem of calculating properties such as the molecular weight, specific heat ratio and the enthalpy of the air entering the combustor. However, if the air heater operates efficiently these thermodynamic properties can be calculated with computer codes, assuming the heater products are at equilibrium by the time they enter the combustor.

In the following the effect of vitiated air on both theoretical as well as experimental performances will be discussed in more detail.

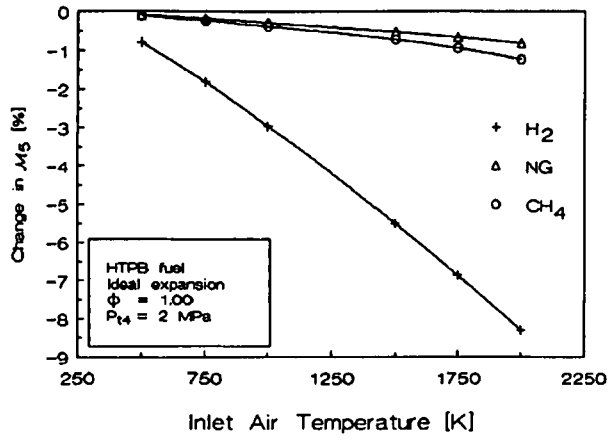

Figure 8.3: Effect of vitiator fuel on $\mathcal{M}_5$ when comparing vitiated air with ideal hot air [34]

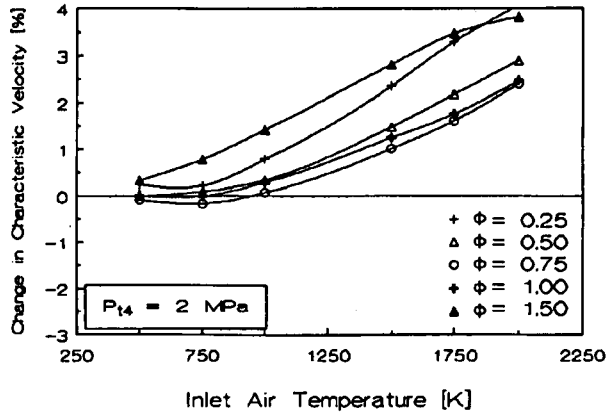

Figure 8.4: Change in SFRJ characteristic velocity when comparing vitiated air for a hydrogen fueled vitiator with ideal hot air[34]

8.4.2.1 Effects of Vitiated Air and Vitiator Fuel Type on Ramjet Theoretical Performance

The effects of vitiated air on ramjet theoretical performance were investigated using the NASA CET89 aerothermochemical equilibrium code. The study ([34]) quantified the effect of vitiated air on solid fuel ramjet performance for hydrogen, methane and natural gas vitiation while maintaining the oxygen mole fraction of 0.2095. The study was performed with an initial air temperature of 298.15 K and the fuel temperature was varied between 50 K and 200 K. The more important results are presented here in Figs. 8.3 to 8.6. It can be observed that variations in ramjet performance increase with increasing combustor inlet temperature. Fig. 8.6 shows that ramjet specific impulse decreases by as much as 10% for natural gas (Groningen) and 3% for methane, but increases up to 14% with hydrogen vitiation. Similar but smaller variations are observed for c^* in Fig. 8.5. Fig. 8.4 shows the variation of c^* with combustor equivalence ratio for hydrogen vitiation. The major reason for the significant effect of hydrogen vitiation on hydrocarbon theoretical performance is the decrease in molecular weight of the vitiated air and subsequently in the ramjet exhaust (Fig. 8.3). These results show that vitiation can significantly alter ramjet performance. These effects must be accounted for when relating the data generated from vitiated air facilities to achievable ramjet performance in atmospheric air.

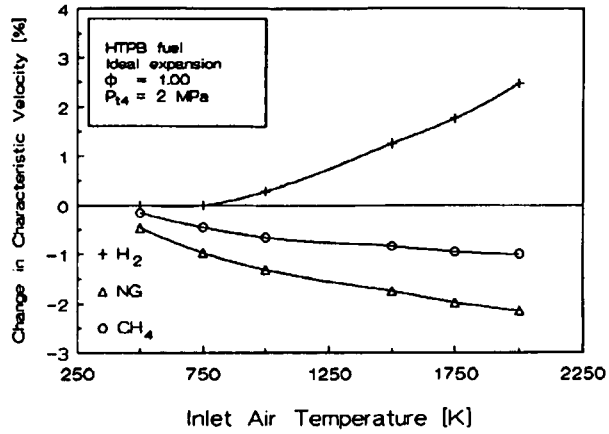

Figure 8.5: Effect of vitiator fuel on SFRJ characteristic velocity when comparing vitiated air with ideal hot air [34]

8.4.2.2 Example Test Results

A comparison was made between the c^* efficiencies obtained from data of some previously conducted test on a ramcombustor fed by vitiated and ideal air. The ramjet fuel was kerosene. Ideal hot air was provided by a

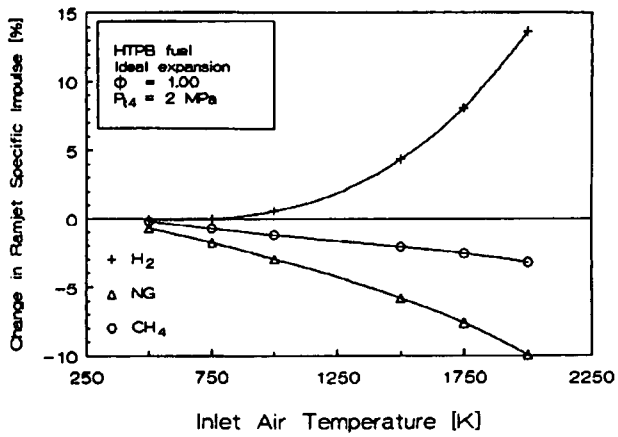

Figure 8.6: Effect of vitiator fuel on SFRJ specific impulse when comparing vitiated air with ideal hot air [34]

heat exchanger. In case of vitiated air tests, vitiator fuel was hydrogen and — contrary to the calculations for the above figures — the mass percentage of oxygen was maintained at 23% in the incoming air of the ramcombustor. The highest simulated temperature was $850K$, which represents a Mach number of about 3.8 at an altitude higher than $11km$.

The theoretical performances were determined using one of the methods of Chapter 4 (method 3 of Section 4.4.5.3). The computations were made for chemical equilibrium at station 2 and 4 with frozen flow in the nozzle. The major results are shown in Figure 8.7.

Tables 8.1 and 8.2 give theoretical and experimental results for the ideal air tests and the vitiated air tests, respectively. Analysis shows:

- an increase in the theoretical c^* with temperature similar to the one shown in Fig. 8.5 for HTPB in which the mole fraction of O_2 was held constant
- up to a total temperature of $800K$ at station 2, no significant difference between the c^* efficiency with ideal or vitiated air
- for a total temperature higher than $800K$ at station 2 the c^* efficiency is higher with ideal air than with vitiated air

These results have been obtained with only one set of experimental data and, of course, it is necessary to make further tests with more measurements and calculations. Nevertheless, this study shows that caution is needed when an experimental combustion efficiency is determined in connected-pipe tests with vitiated air.

8.4.3 Fuel and Oxidizer Choices

The choice of a fuel and oxidizer combination for heating air in a particular test facility is complicated by all the concerns listed in Section 8.2. Fig. 8.8 lists some common fuels and oxidizers together with some of their positive and negative attributes.

8.5 Heater Installation and Use

The performance of a heater is significantly affected by the way it is installed in the facility.

The flow quality of air to the ramjet combustor under test can be modified by means of flow straighteners, screens or plenums to reduce turbulence and spatial variations in flow pressures and temperatures from the heater.

If water cooling is necessary for the heater and the ducting to the combustor, heat loss may induce a temperature gradient in the flow. Insulating the hardware to limit heat loss minimizes this problem.

Acoustic decoupling of the air heater from the fuel and oxidizer feed lines and the ramjet combustor is often necessary to avoid introducing acoustic oscillations unique to the facility installation of the ramjet under test. A basket diffuser having many small holes is often used in the air heater to suppress these pressure oscillations. Sonic orifices between the combustor and heater prevent feed back from the ramburner to the vitiator. This solution, however, requires higher vitiator supply pressures for the air, fuel and make-up oxygen, which necessitates higher pressure supply tanks and/or pumps.

8.6 Heater Performance Determination

The performance of a heater must be measured during its development in order to optimize its ability to properly condition air for ramjet testing. The methodology for heater performance is essentially the method outlined in Chapter 6 for ramjet combustors. During routine testing, simple monitoring for changes in operating performance is usually sufficient to indicate problems that may affect test results.

8.6.1 Performance Parameters

Combustion efficiency is the most important heater performance parameter since unburned heater fuel will affect the results obtained with the ramjet tested. The temperature rise efficiency definition as given in Section 6.2.3 is also appropriate for measuring heater performance, especially as long as the exhaust temperatures are below the limits of direct temperature measurement. An efficiency that compares actual heater fuel flow to the fuel flow theoretically needed for the achieved temperature rise, see Section 6.2.4, also clearly characterizes the heater performance.

Uniform temperature and pressure profiles in the vitiator exhaust are desirable.

The heater should have a smooth combustion behavior with a minimum of pressure oscillations and be free of distinct resonance frequencies.

Heat loss to the heater structure or downstream devices is a performance related parameter since it increases heater fuel flow and subsequently the air contaminants.

The envelope of heater operation should be wide enough to

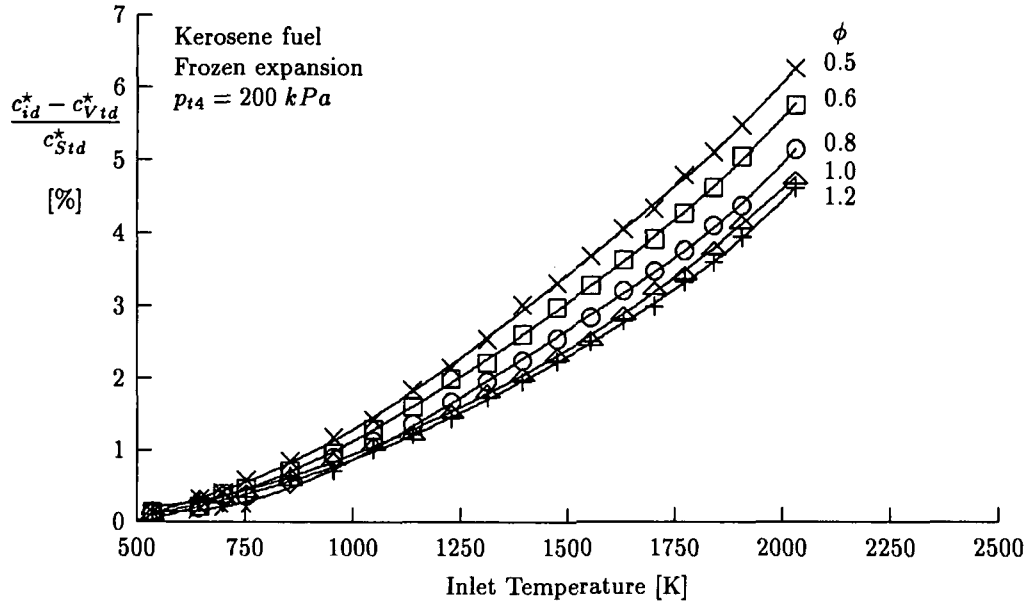

Figure 8.7: Change in LFRJ characteristic velocity when comparing vitiated air with ideal air [35]

Test case	$\dot{m}$ ideal air $[kg/s]$	T_{t2} exp $[K]$	$\dot{m}$ $C_{10}H_{20}$ $[kg/s]$	c^* th $[m/s]$	c^* exp $[m/s]$	η_{c^*}
600K, $\phi \approx 0.60$	1.623	604	0.066	1119	1084	0.969
600K, $\phi \approx 0.70$	1.602	611	0.076	1172	1111	0.948
700K, $\phi \approx 0.60$	1.586	686	0.065	1138	1106	0.972
800K, $\phi \approx 0.50$	1.598	815	0.057	1122	1107	0.987
800K, $\phi \approx 0.60$	1.632	819	0.067	1164	1137	0.973
850K, $\phi \approx 0.60$	1.544	854	0.063	1169	1163	0.995
850K, $\phi \approx 0.80$	1.563	857	0.084	1252	1240	0.990

Table 8.1: Ramcombustor test results with ideal air

Test case	$\dot{m}$ ideal air $[kg/s]$	$\dot{m}$ O_2 $[kg/s]$	$\dot{m}$ H_2 $[kg/s]$	T_{t2} exp $[K]$	$\dot{m}$ $C_{10}H_{20}$ $[kg/s]$	c^* th $[m/s]$	c^* exp $[m/s]$	η_{c^*}
600K, $\phi \approx 0.60$	1.611	52.3×10^{-3}	4.95×10^{-3}	605	0.068	1122	1080	0.962
600K, $\phi \approx 0.70$	1.618	50.96×10^{-3}	4.83×10^{-3}	601	0.080	1174	1109	0.945
700K, $\phi \approx 0.60$	1.510	67.20×10^{-3}	6.32×10^{-3}	703	0.065	1146	1114	0.972
800K, $\phi \approx 0.50$	1.433	88.28×10^{-3}	8.20×10^{-3}	815	0.056	1137	1106	0.973
800K, $\phi \approx 0.60$	1.440	87.23×10^{-3}	8.10×10^{-3}	807	0.063	1168	1129	0.967
850K, $\phi \approx 0.60$	1.384	94.56×10^{-3}	8.77×10^{-3}	846	0.061	1177	1146	0.974
850K, $\phi \approx 0.80$	1.380	94.44×10^{-3}	8.76×10^{-3}	849	0.081	1262	1226	0.972

Table 8.2: Ramcombustor test results with vitiated air

allow for the temperature and mass flow variations needed for flight trajectory simulation.

8.6.2 Experimental Methods

The experimental methods applied to determine the performance of a combusting heater correspond to standard rocket or ramjet development procedures.

The heater can be equipped with a choked exhaust nozzle to provide the desired Mach number in its combustion chamber. Subsequently all combustion efficiencies defined in Chapter 6 can be deduced from measured mass flows and combustor temperature or combustor pressure (or thrust, but this is rare).

Sampling and analysis of the heater exhaust products can also be used as a method to characterize the completeness of heater combustion if the desired heater performance level justifies the expense of this more sophisticated performance evaluation technique. In addition to measuring concentrations of combustion products, this method can also evaluate levels of such species as NO_x that may differ from that of hot atmospheric air.

The uniformity of pressure and temperature of the flow at the heater exit can be measured directly by rakes or grids equipped with pitot or thermocouple probes.

The steadiness of heater combustion can be checked by unsteady pressure measurements.

Specialized non-intrusive measuring techniques may be applied (at considerable expense) if comprehensive characterization of the heater exhaust is desirable or if high temperatures prohibit using probes, as in simulation of hypersonic flight Mach numbers. Laser velocimetry can characterize flow velocity profiles in lieu of measuring pressure profiles. Nevertheless, this technique requires particle seeding which raises the problems of particle injection, velocity relaxation and particle survival depending on the flow environment. Spectroscopic techniques such as Rayleigh scattering, Raman, CARS, LIF, etc., can be applied to characterize temperature profiles and combustion products.

8.6.3 Theoretical Performance Parameters

Experimentally derived performance parameters need to be referenced to theoretical values calculated for complete or equilibrium combustion. The theoretical values most relevant to determining a combusting heater performance are the stagnation temperature and the mole fraction of species at the heater exit (corresponding to a combustor station 4 as defined in Fig. 3.1). Additional parameters as specified in Section 4.1 for stations 4 and 5 are required to determine the stagnation temperature at heater exit indirectly by pressure or thrust measurement (Chapter 6).

- Hydrogen
  - \+ wide flammability and ignition ranges
  - \+ efficient combustion
  - − water vapor and low molecular weight in exhaust
- Hydrocarbon (liquid or gaseous)
  - \+ minimal safety requirements
  - − carbon dioxide and water vapour in exhaust
- MMH and UDMH
  - − toxicity
- NH_3
  - − water vapor in exhaust
  - − toxicity
- N_2O
  - \+ exhaust is similar to air
  - \+ heat release upon decomposition
  - − special handling required
- N_2O_4
  - − toxicity

Figure 8.8: Fuels and oxidizers for combusting heaters

8.6.4 Performance Monitoring

Heater performance monitoring at the test facility is mandatory to ensure the correctness of the simulated operating conditions for the ramjet tested and for test safety. On-line monitoring during the test is desirable, but a heater performance check by post test data reduction may be sufficient if the overall cost of the test and test article is moderate.

Heater monitoring should look at:

- the injected mass flows (heater fuel, make-up oxygen, etc.)
- the exit temperature (most frequently measured by

thermocouples installed through the heater wall, preferably at different circumferential positions).

The mass flow ratio of heater fuel to make-up oxygen must be kept in a narrow tolerance band to maintain the correct oxygen content of the air fed into the ramjet. Combustion efficiency of the heater can be determined on-line from measured data with modern computers. However, on-line performance monitoring can also be done by referencing the measured heater mass flow to a min/max tolerance table as a function of temperature. Depending on the possibility of running heated air before the test to achieve steady state conditions for the heat losses to the structure of the test setup, steady state or transient heat transfer out of the flow must be determined prior to testing and be taken into account for heater performance monitoring.

The uniformity of the (circumferential) heater exit temperature must be monitored within a predetermined tolerance band. The width of the band should take into account the number and locations of the thermocouples and the uncertainty of the measurements.

A possible flameout of the heater may be monitored by using thermocouples to measure the average exhaust temperature or a higher temperature in the combustor zone, or by using optical detectors.

9 Summary, Conclusions and Recommendations

In the initial efforts of AGARD/PEP Working Group 22 it was thought that perhaps a "recommended method" could be established within NATO for the determination of connected-pipe ramjet and ducted rocket performance. It soon became apparent that there was more than one acceptable method. The result was a detailed description of each performance parameter and the interrelationships between them, and an expansion of the Working Group objectives to include detailed examples in order to provide users with a working document.

Agreement was reached (Chpt. 3) on the methods that should be used for reporting test results.

Theoretical performance determination (Chpt. 4) depends upon the parameter chosen to represent performance and the specific aerothermochemical equilibrium code and options which are used. It was found that the various codes (NASA CET89, PEP ...) gave substantially the same results, providing that the latest properties data available were used as input. Specific techniques for handling vitiated air heaters have been recommended and illustrated.

In Chapter 5 the experimental parameters that are required to be measured are given.

Chapter 6 and Appendix C present the fundamental relationships that are needed to calculate experimental performance based on characteristic velocity, vacuum specific impulse, temperature rise, equivalence ratio and pressure losses. Various "isentropic" exponents are often used in performance calculations. An explanation of these are presented in Appendix B, together with recommendations as to which values are most appropriate in the various regions of the combustor and exhaust nozzle.

In Chapter 7 detailed sample calculations are presented, including uncertainty analysis. This chapter presents step-by-step examples for the use of the methods and recommendations.

Since most facilities which experimentally evaluate ramjets and ducted rockets utilize air heaters, some detailed explanations of their operation and recommended techniques for their use have been included in Chapter 8, especially for vitiated air heaters where a variety of techniques have been used throughout the NATO community. It should be emphasized that the influence of air vitiation on ramjet performance is only generally understood, while there is still a lack of detailed investigations to quantify the resulting effects.

A very important result from the experimental determination of performance is the uncertainty of the final reported performance parameter. The extensive work of AGARD/PEP Working Group 15 and AGARD Lecture Series 169 on Comparative Engine Performance Measurements for gas turbines was utilized in the present effort (Appendix A), with specific examples presented for ramjets and ducted rockets.

Special efforts have been made by Working Group 22 to emphasize the working document aspect, in order to facilitate the practical use of the performance determination procedures given in this report.

In conclusion, it is the hope of Working Group 22 that this document will prove to be valuable to both new and experienced investigators in the area of ramjet and ducted rocket performance determination. If the recommended procedures are followed, the document should permit all investigators to be able to communicate their results in a common "performance language" and to readily convert performance values obtained in one facility to those used in other facilities.

No document is without some shortcomings and very few are fortunate to be without a few errors. It is hoped that users of this document will forward their comments and recommendations to AGARD/PEP Standing Committee 02 so that the material can be revised and improved in the future.

A recommended next step is to perform a similar effort for supersonic and dual-mode combustion ramjets.

Bibliography

[1] P.F. Ashwood and J.J. Mitchell (eds), AGARD Advisory Report No. 248, The Uniform Engine Test Programme, February 1990.

[2] J.P.G. Vleghert, AGARDograph No. 307, Measurement Uncertainty Within the Uniform Engine Test Programme, May 1989.

[3] R.B. Abernethy, B.D. Powell, D.L. Colbert, D.G. Sanders and J.W. Thompson, Handbook, Uncertainty in Gas Turbine Measurements, Arnold Engineering Development Center, Arnold Air Force Station, AEDC-TR-73-5, February 1973.

[4] ISO 5168, Measurement of Fluid Flow – Estimation of Uncertainty of a Flow-Rate Measurement, 1978.

[5] ANSI/ASME PTC 19.1, Measurement Uncertainty, 1983.

[6] R.B. Abernethy and J.W. Thompson, Instrument Society of America, Measurement Uncertainty Handbook, ISBN: 0-87664-483-3, Revised 1990.

[7] S. Gordon and B.J. McBride, Computer Program for Calculation of Complex Chemical Equilibrium Compositions, Rocket Performance, Incident and Reflected Shocks, and Chapman-Jouguet Detonations, NASA-SP-273 Interim Revision, March 1976.

[8] B.J. McBride, Computer Program for Calculation of Complex Chemical Equilibrium Compositions, Rocket Performance, Incident and Reflected Shocks, and Chapman Jouguet Detonations, NASA-SP-273, Revision July 15, 1986.

[9] B.J. McBride, CET89 – Chemical Equilibrium with Transport Properties (Cosmic Program LEW-15113), Lewis Research Center, 1989.

[10] D.R. Cruise, Theoretical Computations of Equilibrium Compositions, Thermodynamic Properties, and Performance Characteristics of Propellant Systems, Naval Weapons Center, China Lake, CA, April 1979, NWC-TP-6037.

[11] J.W. Humphrey, Computations of One Dimensional Acoustic Modes as Applied to Ramjet Inlet/Combustors, Naval Weapons Center, China Lake, CA, October 1983, NWC-TM-5164.

[12] J.W. Humphrey, Application of a One Dimensional Acoustic Analysis to Side Dump Ramjet Configurations, Naval Weapons Center, China Lake, CA, November 1983, NWC-TM-5165.

[13] A.A. Amsden, J.D. Ramshaw, P.J. O'Rourke and J.K. Dukowicz, KIVA: A Computer Program for Two and Three Dimensional Fluid Flows with Chemical Reactions and Fuel Sprays, Los Alamos National Laboratory, NM, February 1985, LA-10245-MS.

[14] Terminology and Assessment Methods of Solid Propellant Rocket Exhaust Signatures, AGARD Propulsion and Energetics Panel Working Group 21, AGARD AR 287, February 1993.

[15] S.R. Brinkley, Jr., Calculation of the Equilibrium Composition of Systems of Many Constituents, J. Chem. Phys., Vol. 15 (1947), pp. 107-110.

[16] H.J. Kandiner and S.R. Brinkley, Calculation of Complex Equilibrium Relations, Ind. Eng. Chem., Vol. 42 (1950), pp. 850-855.

[17] V.N. Huff, S. Gordon and V.E. Morrell, General Method and Thermodynamic Tables for Computation of Equilibrium Composition and Temperature of Chemical Reactions, National Advisory Committee on Aeronautics, Washington, D.C., 1951, NACA Report 1037.

[18] H.N. Browne Jr., M.M. Williams and D.R. Cruise, The Theoretical Computation of Equilibrium Compositions, Thermodynamic Properties and Performance Characteristics of Propellant Systems, Naval Ordnance Test Station, China Lake, CA, 1960, NAVWEPS Report 7043, NOTS TP-2434, publication UNCLASSIFIED.

[19] D.S. Villars, A Method of Successive Approximations for Computing Combustion Equilibria on a High Speed Digital Computer, J. Chem. Phys., Vol. 63 (1959), pp. 521-525.

[20] D.S. Villars, Computation of Complicated Combustion Equilibria on a High Speed Digital Computer, in Proceedings of the First Conference on Kinetics, Equilibria and Performance of High Temperature Systems, Ed. by G.S. Bahn and E.E. Zukosky. Butterworths, London, 1960.

[21] B. Bourasseau, Programme de Calcul des Performances des Systèmes Propulsifs, COPPELIA: Description Théorique, ONERA Rapport 5/3589EY, 1986.

[22] W.C. Reynolds, The Element Potential Method for Chemical Equilibrium Analysis: Implementation in

the Interactive Program STANJAN, version 3, Department of Mechanical Engineering, Stanford University, January 1986.

[23] C.A. Powars and R.M. Kendall, User's Manual Aerotherm Chemical Equilibrium (ACE) Computer Program, Aerotherm Corporation, May 1969.

[24] D.R. Stull and H. Prophet, JANAF Thermochemical Tables, Second Edition, NSRDS-NBS-37, US Department of Commerce, June 1971.

[25] M.W. Chase Jr., C.A. Davies, J.R. Downey Jr., D.J. Frurip, R.A. McDonald and A.N. Syverud, JANAF Thermochemical Tables, Third Edition, Part I and Part II, Journal of Physical and Chemical Reference Data, Volume 14, 1985, Supplement No. 1. American Chemical Society and American Institute of Physics for the National Bureau of Standards.

[26] Purdue University, Thermophysical Properties of Matter; The TPRC Data Series, a Comprehensive Compilation of Data, Published in 14 Volumes by IPI/Plenum, New York Washington with Y.S. Touloukian, Series Editor. ISBN (set) 0-306-67020-8.

[27] R.C. Weast, M.J. Astle and W.H. Beyer, Handbook of Chemistry and Physics, CRC Press.

[28] I. Barin and O. Knacke, Thermochemical Properties of Inorganic Substances, Vol. I, Springer Verlag, Berlin, 1973.

[29] I. Barin, O. Knacke and O. Kubaschewski, Thermochemical Properties of Inorganic Substances, Vol. II, Supplement, Springer Verlag, Berlin, 1977.

[30] F. Volk, et al., Thermodynamische Daten von Raketen Treibstoffen etc, ICT., Berghausen/Karlsruhe.

[31] M. Karapet'yants, Thermodynamic Constants of Inorganic and Organic Compounds, Ann Arbor Humphrey Science Publishers, 1970.

[32] J. Keenan, J. Chao and J. Kaye, Gas Tables: Thermodynamic Properties of Air Products of Combustion and Component Gases, Compressible Flow Functions, Including those of A.H. Shapiro and G.M. Edelman, 2nd Edition, Wiley-Interscience, 1980.

[33] L.H. Back and R.F. Cuffel, Flow Coefficients for Supersonic Nozzles with Comparatively Small Radius of Curvature Throats, J. Spacecraft, Vol. 8, No. 2, Feb. 1971, pp. 196-198.

[34] A.E.H.J. Mayer and P.A.O.G. Korting, Effect of Vitiated Air on Ramjet Performance, TNO Prins Maurits Laboratory, PML 1991-66, 1991.

[35] A. Cochet, O. Dessornes, M. Scagnetti et C. Vigot, Détermination de l'Effet de la Viciation de l'Air par un Réchauffeur à Hydrogène sur les Performances d'un Statoréacteur à Kérosène. ONERA Rapport 67/1983 EN, 1993.

[36] R.B. Abernethy and B. Ringhiser, History and Statistical Development of the New Measurement Uncertainty Methodology, ASME/SAE/AIAA/ISO Paper 85-1403, July 1985.

[37] J.D. Anderson Jr., Hypersonic and High Temperature Gas Dynamics, McGraw-Hill, New York, 1989.

A Uncertainty Analysis Methodology

The methodology and terminology used by AGARD-PEP WG 15 in their interfacility comparisons of turbine engine performance ([2]) has been adopted in this report.

A.1 Error Types

It is an acceptable fact that measurements have errors and, therefore, error sources. Elemental error sources are classified as either precision (random errors) or bias (fixed errors). The following sections define precision, bias and uncertainty interval (combined error).

A.1.1 Precision (or Random Error)

Random error is seen in repeated measurements of a single parameter. Measurements do not and are not expected to agree exactly. There are always numerous small effects which cause disagreements. The variations between repeated measurements can be quantified by the precision index (S).

$$S = \sqrt{\frac{\sum_{i=1}^{N}(x_i - \overline{x})^2}{N-1}} \qquad \text{(A.1)}$$

where $\overline{x}$ is the average value of N individual measurements x_i, in the sample.

A.1.2 Bias (or Fixed Error)

The second error component is the systematic error, which is constant for repeated measurements and can only be determined by comparison with the true value of the quantity measured. A true value comparison is normally impossible within a single measurement process, but tests can be arranged to provide some bias information. Examples are:

1. Interlab and interfacility test comparisons on measurement devices, test rigs, and full scale engines.
2. Calibration of the measuring instruments against lab standards during the test, e.g., incorporating a standard in the scanning cycle.
3. Comparisons employing redundant instruments or measuring techniques.

Large differences in measurements can usually be attributed to a mistake, but this progressively gets more difficult as the size of the difference reduces. Hence, one tends to be left with small unexplained differences, which constitute part of the bias limit.

A.1.3 Uncertainty (Combined Error)

For comparison of measurement results, a single value is desirable to express a reasonable error limit or uncertainty interval. This value must be a relevant combination of bias and precision. Precision is a statistic, which lends itself to the calculation of confidence limits, within which the actual measurement can be reasonably expected to lie in the absence of bias error. It is, however, impossible to define a single rigorous statistic for the total error, because bias is an upper limit, which has unknown characteristics, and is to some extent dependent on engineering judgment.

Usually, the bias (B) plus a multiple of the precision index is used to estimate the total error or uncertainty interval (U).

$$U = \pm(B + t_{95}S) \qquad \text{(A.2)}$$

in which t_{95} is the 95th percentile point for the two-sided Student's "t" Distribution ([3]).

A.2 Error Analysis Process

A single measuring chain stretches from the physical phenomenon being measured (e.g. pressure, temperature, thrust), via probe and connecting line, to the transducer, and from there usually via an electric line — sometimes preamplified — to the multiplexer amplifier and signal conditioner and then to the recorder. Afterwards the signal is played back, and instrumental calibration applied, and a number of measurements are combined to determine a value representative of the physical phenomenon being measured, usually by averaging in space and/or time. Such Basic Measurements are then used to calculate Performance Parameters, (e.g., thrust, combustion efficiency,

		Type Error		Description of Error Sources
Standards Calibration Hierarchy	.....	b_1	s_1	Standard lab calibration, including traceability to national standards
Data Acquisition	Calibration System Errors			
	• Reference Source	b_2	s_2	Determination of reference pressure
	• Sensor			
	– Hysteresis	b_3	s_3	Sensor hysteresis
	– Non-linearity	b_4	s_4	Sensor non-linearity
	– Repeatability	b_5	s_5	Sensor repeatability
	Recording System Errors			
	• Sampling	b_6	s_6	Data variations due to facility or engine instabilities
	• Channel	b_7	s_7	Signal conditioning, electrical calibrations and digital systems
Data Reduction	Data Processing Errors	b_8	s_8	Curve fits of calibration data
Other Effects	Installation Effects Errors			
	• Pressure Probe	b_9	s_9	Design/fabrication of probes
	Environmental Effects Errors			
	• Temperature	b_{10}	s_{10}	Temperature change effect on sensor
	• Vibration	b_{11}	s_{11}	Vibration effect on sensor
	Root Sum Square			

Table A.1: Example of pressure measurement error sources

total pressure loss), which constitute the end product of the measurement.

Each step in the above-mentioned measuring chain contributes to the overall data error in its own specific way and is treated in the error analysis process below.

1. Define **Elemental Errors** (bias and precision) for the Basic Measurements: pressure, temperature, force, length and time.
2. Perform **Sensitivity Analysis** to determine Influence Coefficients and the combined effect (attendant bias and precision) for the Performance Parameters.
3. Estimate **Uncertainty Interval** by combining total bias and precision values for each Performance Parameter.

A.2.1 Elemental Error Sources

The first step is to assess and categorize the elemental errors for both bias and precision, in a separate table (e.g., Table A.1 for pressure measurement) for a single point of each Basic Measurement, keeping bias limits B and precision indices S strictly apart. Each elemantal error source may be composed of bias and/or precision error. These elemental errors are combined by Root-Sum-Square (RSS) addition to give the total B and S values for each Basic Measurement. An important condition required to justify RSS combination is that each item must be independent.

The Abernethy/Thompson methodology described in [3] details the evaluation of the elemental errors. The elemental error of a single measuring chain can be categorized into four groups as follows:

1. Calibration Hierarchy
2. Data Acquisition
3. Data Reduction
4. Other Effects, e.g., non-instrument effects, errors of method, sensor system errors, spatial profile sampling, etc.

For the purpose of conducting a detailed assessment of the facility measurement uncertainties, it may be necessary to define error subgroups for each measurement system (e.g. Table A.1 through A.4). The Uniform Engine Test Programme elemental error groups are documented in [2]. The general definitions of the elemental error groups are given below.

		Type Error		Description of Error Sources
Standards Calibration Hierarchy	.....	b_1	s_1	Manufacturer specification of wire or standard lab calibration
Data Acquisition	Calibration System Errors			
	• Level	b_2	s_2	Reference temperature level
	• Stability	b_3	s_3	Reference temperature stability
	Recording System Errors			
	• Sampling	b_4	s_4	Data variations due to facility or engine instabilities
	• Channel	b_5	s_5	Signal conditioning, electrical calibrations and digital systems
Data Reduction	Data Processing Errors ..	b_6	s_6	Curve fits of calibration data
Other Effects	Installation Effects Errors			
	• Probe Recovery	b_7	s_7	Probe design caused by radiation, convection, etc.
	• Conduction Error	b_8	s_8	Heat conduction
	• Temperature Gradients	b_9	s_9	Temperature gradients along nonhomogeneous thermocouple wire
	Root Sum Square			

Table A.2: Example of temperature measurement error sources

1. **Calibration Hierarchy** traces the possible instrument error back to the National Standard, usually in steps via a Working Standard, a Laboratory Standard and a Transfer Standard. In each step the original bias of the instrument is removed by the calibration and replaced by the (smaller) combination of systematic error of the reference instrument and the random error of the comparison. (Additional details are provided in [2]).

2. **Data Acquisition** errors can be caused by slight variations in exciter voltage, outside influences on data transmission and on the transducer, signal conditioning and recording. The first three items cause non-repeatability (precision error). Another factor is sensor hysteresis; this usually depends on the measuring range and could be reduced if the sensor is only calibrated over the minimum range and if the measuring history is known. In this case, hysteresis is classified as bias. Usually this is not a practical proposition; however, with modern instruments hysteresis is small.

3. **Data Reduction** errors consist of resolution error and calibration curve fit errors and can usually be made negligible, compared with the other groups. An error of half the biggest error elsewhere only contributes 10% to the overall error when added RSS; therefore, it is not effective to use extreme resolution in the computational hardware and software. Calibration curve fit errors can be minimized by choosing the appropriate functional relationship, qualified by visual and numerical inspection.

   When a higher than second order curve fit is used it is important that the calibration points are spaced evenly, otherwise the densely populated part may introduce a calibration bias in the sparsely populated part.

4. **Other Effects** are difficult to separate and as such are open to different interpretations. In general they are concerned with the interaction between the medium and the measuring chain. This is the case for design and fabrication of probes and hole patterns, which renders the measured pressure sensitive to flow.

   Internal flow is nearly always non-uniform, both in space and in time, and not necessarily the same in different installations. This nonuniformity can give a bias error even when using the same instrumentation, both for pressure and temperature. Another possible error is constituted by the assumption that static pressure is constant over the flow area of the parallel section of a duct, where total pressure is measured.

   The mechanics of the thrust stand can introduce bias and/or precision errors — notably in the thrust stand zero — which can not be determined exactly, not even

		Type Error		Description of Error Sources
Standards Calibration Hierarchy	.....	b_1	s_1	Standard lab calibration, including traceability to national standards
Data Acquisition	Calibration System Errors			
	• Off-Axis Effects	b_2	s_2	Force measurement on axis different from centerline
	• Tare Correction			
	– Hysteresis	b_3	s_3	Force measurement system hysteresis
	– Non-repeatability	b_4	s_4	Sensor non-repeatability from repeat calibrations
	– Non-linearity	b_5	s_5	System calibration non-linearity
	Recording System Errors			
	• Sampling	b_6	s_6	Data variations due to facility or engine instabilities
	• Channel	b_7	s_7	Signal conditioning, electrical calibrations and digital systems
Data Reduction	Data Processing Errors ...	b_8	s_8	Curve fits of calibration data
Other Effects	Installation Effects Errors			
	• Stand Alignment	b_9	s_9	Misalignment of engine and data load cell force vectors
	• Load Cell	b_{10}	s_{10}	Shift in load cell calibration caused by attachments
	Pressure Effects Errors			
	• Load Cell	b_{11}	s_{11}	Cell pressure change on load cell
	• Test Cell	b_{12}	s_{12}	Cell pressure change on test cell wall ground
	• Service Lines	b_{13}	s_{13}	Line pressure change on tare forces
	Temperature Effects Errors			
	• Load Cell	b_{14}	s_{14}	Temperature change on load cell
	• Test Cell	b_{15}	s_{15}	Line temperature change on tare forces
	• Thrust Stand	b_{16}	s_{16}	Thermal growth of stand
	• Vibration Error	b_{17}	s_{17}	Vibration of load cell
	• Scrub Drag Error	b_{18}	s_{18}	Secondary airflow external drag
	Root Sum Square			

Table A.3: Example of scale force measurement error sources

in an end-to-end calibration (environmental conditions with an operating ramjet are different from the calibration environment). Pre-test and post-test zeroes are different, and it is usually assumed — but without true justification — that the test zero lies in between.

Length and time can generally be measured very accurately, but when determining flow area the metal temperature must be known as well to compensate for growth. Fuel flow depends on time measurement, but can be influenced by pulse shape and by residual swirl with less than 10-20 diameters of pipe straight section upstream and downstream of the flow meter. In-situ fuel flow calibration is preferred but discrepancies still exist. Determination of fuel properties (lower heating value and specific gravity) can introduce errors of 0.3% to 1% because of reproducibility and repeatability of evaluation methods.

Inadequate sampling or averaging is another error which must be considered. The uncertainty of effective pressure or temperature values obviously decreases with the number of probes ([2]).

When comparing the value of a Performance Parameter, which is a dependent variable, it is necessary to read it from curves at a chosen value of an independent variable (e.g., f/a). Any uncertainty in the chosen independent variable translates into an additional bias error in the performance curve (even though it

has no effect on the individual Performance Parameter values.) A procedure for combining the biases to account for the curve shift effect is described in [2].

A.2.2 Sensitivity Analysis

The second step is to propagate B and S separately for each Basic Measurement (or Input Parameter) to the Performance Parameter. This is done by (1) performing a sensitivity analysis to determine Influence Coefficients (IC) for all Input Parameters that appear in the Performance Parameter calculation and (2) multiplying the B and S values by the appropriate Influence Coefficient to determine B and S for each Performance Parameter.

$$B(\text{Perf. Param.}) = \sqrt{\sum_i (IC_i B_i)^2} \qquad \text{(A.3)}$$

$$S(\text{Perf. Param.}) = \sqrt{\sum_i (IC_i S_i)^2} \qquad \text{(A.4)}$$

The standard equations used to calculate Performance Parameters from the Basic Measurements are presented in chapter 6 of this report. The influence of an error in any Basic Measurement on the outcome can be determined either by Taylor series expansion or numerically by perturbing the equation for a difference in that parameter, keeping all other parameters constant at their nominal values. The latter method is preferred when used with data reduction software because it accounts for implicit as well as explicit functional relationships. The resulting Influence Coefficient is usually expressed as a percentage variation of the calculated Performance Parameter (P) for a one percent deviation of a single Input Parameter (I).

$$\text{Influence Coefficient } IC = \frac{\Delta P/P}{\Delta I/I} \qquad \text{(A.5)}$$

If the perturbation is small, non-linearity effects will be insignificant — but of course the value of the Influence Coefficient will vary over the operating range of the Performance Parameter and is, therefore, a function of ramjet operating and test conditions.

Chapter 7 in this report presents results of a sample Sensitivity Analysis.

A.2.3 Estimated Uncertainty

The total uncertainty interval for both Basic Measurements and Performance Parameters is estimated by (A.2):

$$U = \pm(B + t_{95}S)$$

where B is the total bias error, S the total precision error and t_{95} is the 95th percentile point for a two-sided Student's "t" distribution (a function of the number of points used to calculate S) for the respective measurement/parameter. If the predicted S is determined from a large number of points ($N > 30$) the value $t_{95} = 2.0$ can be taken; Monte Carlo simulations have shown that the coverage of U is about 99 percent ([36]). This means that the comparable Performance Parameter results from all test conditions must be within a band of U. If this is not the case, either a data error exists or an important aspect of the uncertainty estimate has been overlooked.

A form to compute estimated uncertainty for a single Performance Parameter at a selected test condition is presented in Table A.5.

A.3 Test Data Assessment

When the pre-test uncertainty analysis allows corrective action to be taken prior to the test to reduce uncertainties which appear too large, the post-test assessment, which is based on the actual test data, is required to refine the final uncertainty intervals. Test data assessment is also used to confirm the pre-test estimates and/or to identify data validity problems. It can also be made to check for consistency if redundant instrumentation or calculation methods have been used in the data collection system.

A.4 Glossary for Uncertainty Analysis Methodology

This glossary was extracted from Ref. [2].

Accuracy — The closeness or agreement between a measured value and a standard or true value; uncertainty as used herein, is the maximum inaccuracy or error that may be expected (see measurement error).

Average Value ($\bar{x}$) — The arithmetic mean of N readings. The average value is calculated as:

$$\bar{x} = \text{average value} = \frac{1}{N}\sum_{i=1}^{N} x_i$$

Bias (B) — The difference between the average of all possible measured values and the true value. The systematic error or fixed error which characterizes every member of a set of measurements (Fig. A.1).

Calibration — The process of comparing and correcting the response of an instrument to agree with a standard instrument over the measurement range.

		Type Error		Description of Error Sources
Standards Calibration Hierarchy	.....	b_1	s_1	Standard lab calibration, including traceability to national standards
	Calibration System Errors			
	• Cal Fluid Properties	b_2	s_2	Mismatch between calibration and test fluids
	• Flowmeter Repeatability .	b_3	s_3	Non-repeatability from repeat flowmeter calibrations
Data Acquisition	Recording System Errors			
	• Sampling	b_4	s_4	Data variations due to facility or engine instabilities
	• Channel	b_5	s_5	Signal conditioning, electrical calibrations and digital systems
Data Reduction	Data Processing Errors	b_6	s_6	Curve fits of calibration data
	Installation Effects Errors			
	• Cavitation	b_7	s_7	Insufficient static pressure in flowmeter
	• Turbulence	b_8	s_8	Sharp bends, etc., upstream flowmeter
	• Meter Orientation	b_9	s_9	Orientation difference from calibration to test
Other Effects	Environmental Effects Errors			
	• Temperature			
	– Flowmeter	b_{10}	s_{10}	Ambient temperature change on flowmeter
	– Viscosity	b_{11}	s_{11}	Determination of test fluid viscosity
	– Specific Gravity	b_{12}	s_{12}	Determination of test fluid specific gravity
	• Vibration	b_{13}	s_{13}	Vibration on flowmeter
	• Pressure	b_{14}	s_{14}	Ambient pressure change on flowmeter
	Root Sum Square			

Table A.4: Example of fuel flow measurement error sources

Calibration Hierarchy — The chain of calibrations which link or trace a measuring instrument to a national bureau of standards.

Coverage — A property of confidence intervals with the connotation of including or containing within the interval with a specified relative frequency. Ninety-five-percent confidence intervals provide 95-percent coverage of the true value. That is, in repeated sampling when a 95-percent confidence interval is constructed for each sample, over the long run the intervals will contain the true value 95-percent of the time.

Cycle — A whole period of any multiplexer.

Data Point — Can be made up from a number of scans, resulting in an average in time and/or place (i.e., number of pick-ups).

Defined Measurement Process (DMP) — encompasses the overall procedure, including calibration, etc., to arrive at a desired test result using a specified installation or installations. This may be a single test point, a least squares curve fit to a number of test points, or a collection of such fits for different test conditions. Any error that propagates to the result as a fixed error is classified as bias, otherwise it is precision. What is bias for a single point of a curve becomes precision overall, with a remnant test bias and — of course — the possibility of an installation bias.

Degree of Freedom (df) — A sample of N values is said to have N degrees of freedom, and a statistic calculated from it is also said to have N degrees of freedom. But if k functions of the sample values are held constant, the number of degrees of freedom is reduced by k. For example, the statistic

$$\sum_{i=1}^{N}(x_i - \overline{x})^2$$

where $\overline{x}$ is the sample mean, is said to have $N - 1$ degrees of freedom. The justification for this is that (a) the sample mean is regarded as fixed or (b) in normal variation the N quantities $(x_i - \overline{x})$

are distributed independently of x and hence may be regarded as $N-1$ independent variates or N variates connected by the linear relation $\sum(x_i - \bar{x}) = 0$.

Dwell — Time during which a transducer is connected to a pick-up; includes settling (line or filter stabilization) and reading.

Elemental Error — The bias and/or precision error associated with a single component or process in a chain of components or processes.

Fossilization — Random (live) errors in a single calibration run give rise to an uncertainty in the value of the calibration constants, which becomes a fixed "fossilized" bias when this calibration is applied to measurement results.

Laboratory (Lab) Standard — An instrument which is calibrated periodically at a national bureau of standards. The laboratory (lab) standard may also be called an interlab standard.

Mathematical Model — A mathematical description of a system. It may be a formula, a computer program, or a statistical model.

Measurement Error — The collective term meaning the difference between the true value and the measured value. Includes both bias and precision error; see accuracy and uncertainty. Accuracy implies small measurement error and small uncertainty.

Multiple Measurement — More than a single concurrent measurement of the same parameter.

Multiplexer — A unit which connects a number of pick-ups sequentially to a transducer, or a number of transducers to a recorder.

Parameter — An unknown quantity which may vary over a certain set of values. In statistics, it occurs in expressions defining frequency distributions (population parameters). Examples: the mean of a normal distribution, the expected value of a Poisson variable.

Precision Error — The random error observed in a set of repeated measurements. This error is the result of a large number of small effects, each of which is negligible alone.

Precision Index (S) — The precision index is defined herein as the computed standard deviation of the measurements.

Usually,

$$S = \sqrt{\frac{\sum_{i=1}^{N-1}(x_i - \bar{x})^2}{N-1}}$$

but sometimes

$$S = \sqrt{\sum_i s_i^2}$$

Random Error Limit of Curve Fit (RELCF) — The limits on both sides of a fitted curve within which the true curve is expected to lie, with 95% probability; apart from a possible bias error of the DMP. It is calculated from observed random statistical data, including the Residual Standard Deviation.

Reading — A number of samples or an averaged value taken during a dwell.

Sample — A single value giving the momentary output of a transducer, possibly via a (low pass) filter.

Sample Size (N) — The number of sampling units which are to be included in the sample.

Scan — A period during which all pick-ups have been read at least once.

Standard Deviation (σ) — The most widely used measure of dispersion of a frequency distribution. It is the precision index and is the square root of the variance, S is an estimate for σ calculated from a sample of data.

Standard Error of Estimate (S_{EE}) — (also known as Residual Standard Deviation (RSD)) The measure of dispersion of the observed dependent variable (Y_{OBS}) about the calculated least-squares line (Y_{CAL}) in curve fitting or regression analysis. It is the precision index of the output for any fixed level of the independent variable input. The formula for calculating this is

$$S_{EE} = \sqrt{\frac{\sum_{i=1}^{N}(Y_{OBS} - Y_{CAL})^2}{N-K}}$$

for a curve of N data points in which K constants are estimated for the curve.

Standard Error of the Mean — An estimate of the scatter in a set of sample means based on a given sample of size N. The sample standard deviation (S) is estimated as

$$S = \sqrt{\frac{(x - \bar{x})^2}{N-1}}$$

Then the standard error of the mean is $S/\sqrt{N}$. In the limit, as N becomes large, the standard error of the mean converges to zero, while the standard deviation converges to a fixed non-zero value.

Statistic — A parameter value based on data. $\bar{x}$ and S are statistics. The bias limit, a judgement, is not a statistic.

Statistical Confidence Interval — An interval estimate of a population parameter based on data. The confidence level establishes the coverage of the interval. That is, a 95-percent confidence interval would cover or include the true value of the parameter 95-percent of the time in repeated sampling.

	Basic Measurements			Performance Parameter		
	Input Parameters I	Bias Limits B_i (%)	Precision Index S_i (%)	Influence Coefficients IC (%/%)	Bias Limits $B_k = B_i IC$ (%)	Precision Index $S_k = S_i IC$ (%)
1						
2						
3						
⋮						
n						
					$B =$ %	$S =$ %
					$U =$ %	

Table A.5: Error propagation procedure for a specific performance parameter at a selected test condition

Student's "t" Distribution (t) — The ratio of the difference between the population mean and the sample mean to a sample standard deviation (multiplied by a constant) in samples from a normal population. It is used to set confidence limits for the population mean.

Traceability — The ability to trace the calibration of a measuring device through a chain of calibrations to a national bureau of standards.

Transducer — A device for converting mechanical or other stimulation into an electrical signal. It is used to measure quantities like pressure, temperature, and force.

Transfer Standard — A laboratory instrument which is used to calibrate working standards and which is periodically calibrated against the laboratory standard.

True Value — The reference value defined by a National Bureau of Standards which is assumed to be the true value of any measured quantity.

Uncertainty (U) — The maximum error reasonably expected for the defined measurement process:

$$U = \pm(B + t_{95}S)$$

Variance (σ^2) — A measure of scatter or spread of a distribution. It is estimated by

$$S^2 = \frac{\sum_{i=1}^{N}(x_i - \overline{x})^2}{N-1}$$

from a sample of data. The variance is the square of the standard deviation.

Working Standard — An instrument which is calibrated in a laboratory against an interlab or transfer standard and is used as a standard in calibrating measuring instruments.

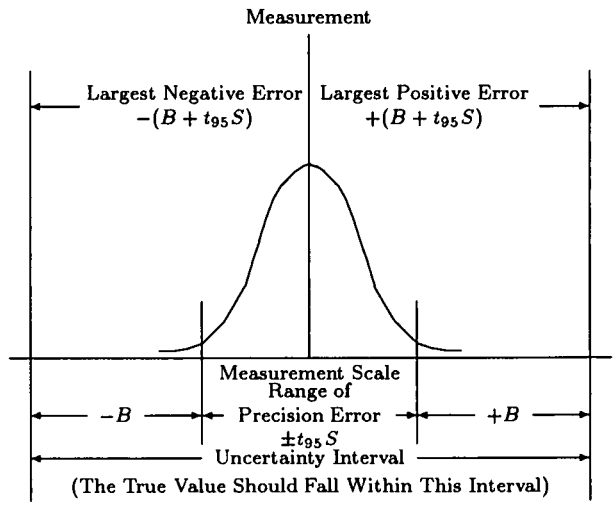

Figure A.1: Sampling systems

B Isentropic Exponents

Simple equations relating static and stagnation properties can be derived for a flowing gas if the following assumptions are made:

- nonreacting, thermally and calorically perfect gas
- adiabatic process

With these assumptions the equations are generally in the form of the static to stagnation ratios for a property (i.e. temperature, pressure, etc.) as a function of Mach number and the isentropic exponent γ (i.e. Poisson relations). The process is easily observed with the help of a temperature-entropy diagram (Fig. B.1). The isentropic exponent derives its name as the exponent from Eq. B.1.

$$pv^{\gamma} = \text{constant} \tag{B.1}$$

$$\gamma = \frac{c_p}{c_v} \tag{B.2}$$

This value of γ does not change for a fixed property flow and, therefore, it is constant when going from static to stagnation conditions.

The difficulty arises when trying to use these relationships for chemically reacting flows such as in the rocket or ramjet

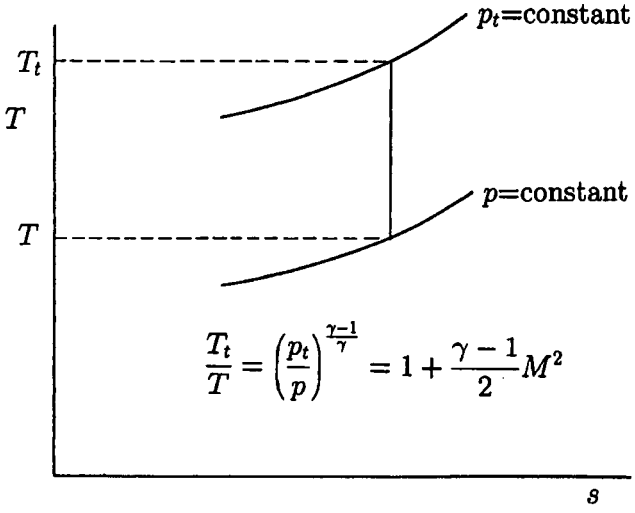

Figure B.1: General temperature-entropy diagram for a $p-T$ process

combustor and exhaust nozzle. Two limiting flow cases are frozen flow and local equilibrium flow. Reaction rates are zero for frozen flow, whereas local equilibrium flow implies infinite chemical and vibrational rates. The specific heats at constant pressure and constant volume are defined for local equilibrium and frozen flows by Eqs. B.3 through B.6 [37].

Specific heats at constant pressure:

$$\bar{c}_{p,s} = \bar{c}_{p,f} + \sum_i \bar{h}_i \left.\frac{\partial \chi_i}{\partial T}\right|_{p,N_j,j\neq i} \tag{B.3}$$

$$\bar{c}_{p,f} = \sum_i \chi_i \bar{c}_{p_i} \tag{B.4}$$

Specific heats at constant volume:

$$\bar{c}_{v,s} = \bar{c}_{v,f} + \sum_i \bar{e}_i \left.\frac{\partial \chi_i}{\partial T}\right|_{v,N_j,j\neq i} \tag{B.5}$$

$$\bar{c}_{v,f} = \sum_i \chi_i \bar{c}_{v,i} \tag{B.6}$$

where - indicates a molar basis.

One can see that for local equilibrium flow there is a contribution to the specific heats from the chemical reaction. This contribution can be large and is affected by a change in species as the temperature changes. Therefore, γ also changes as a function of temperature and strictly speaking, the Poisson relations do not hold any longer in this case. Nevertheless, they conveniently approximate the process. Since the static temperature increases when going from the initial static condition to the stagnation condition (refer to Fig. B.2), γ does not have the same value at the stagnation conditions as it had at the initial static conditions. This creates the problem of which γ to use in the isentropic relations.

The isentropic exponent is calculated in three ways.

Frozen flow:

$$\gamma_f = \frac{c_p(T)}{c_v(T)} \tag{B.7}$$

Local equilibrium flow:

$$\gamma_s = -\left.\frac{\partial \ln p}{\partial \ln v}\right|_s = -\frac{\gamma_f}{\left.\frac{\partial \ln v}{\partial \ln p}\right|_T} \tag{B.8}$$

Process γ_p:

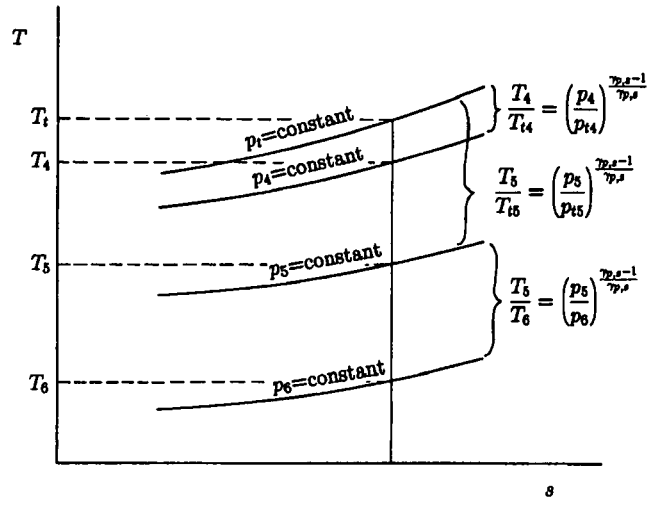

Figure B.2: Temperature-entropy diagram for a p–T process

In general the process isentropic exponent, γ_p, can be defined in terms of pressures and temperatures between any two stations i and j by

$$\gamma_p = \gamma_{p,i-j} = \frac{\ln(p_i/p_j)}{\ln(p_i/p_j) - \ln(T_i/T_j)} \qquad \text{(B.9)}$$

More specifically the pressure and temperature at station i can be either static or stagnation values, leading in the second case to the following form of γ_p as

$$\gamma_p = \gamma_{p,i-j} = \frac{\ln(p_{ti}/p_j)}{\ln(p_{ti}/p_j) - \ln(T_{ti}/T_j)} \qquad \text{(B.10)}$$

For the process between stations 4 and 5 the difference in $\gamma_{p,4-5}$ obtained using the above two definitions has been found to be small since M_4 is small.

An aerothermochemical equilibrium code, such as the NASA CET89 code [7, 8, 9], is used to calculate values for γ_f and γ_s as defined by Eqs. B.7 and B.8, respectively. Values at the combustor, the nozzle throat and the nozzle exit are given by the code. γ_p as defined by Eq. B.10 is not calculated directly by all codes, but it can be determined from the program output.

Both, frozen (γ_f) and local equilibrium (γ_s) isentropic exponents are static point properties of the flow as defined by Eqs. B.7 and B.8, respectively. The combustor γ_f and γ_s are static point properties when a combustor static pressure is entered into the code and stagnation point properties when a combustor stagnation pressure is used. A combustor stagnation pressure must be entered in order for the code to correctly calculate the static point property isentropic exponents for the nozzle throat and nozzle exit.

None of these point property isentropic exponents are the correct ones to use in the isentropic relationships. The isentropic exponent changes for a chemically reacting equilibrium flow that is isentropically expanded from a stagnation condition to a static one. Dissociation or recombination of species as the static temperature changes causes a change in thermochemical properties, such as specific heat and molecular weight. Even for frozen flow the γ_f changes as the static temperature changes. A process isentropic exponent is required that accounts for the change in composition and temperature when going from the static condition to the stagnation condition.

The process isentropic exponent (γ_p), given in Eq. B.10, exactly relates the properties of the specified end states of an isentropic process. It also quite accurately relates the properties of intermediate states to the end states. For these reasons it is the recommended isentropic exponent to be used in equations of Chapter 6.

A ramjet engine has four major station locations where thermochemical properties are needed to determine theoretical and experimental performance. They are the inlet (station 2), the combustor (station 4), the nozzle throat (station 5) and the nozzle exit (station 6). Characteristics of the flows are given below.

1. Flow in the inlet is in chemical equilibrium. In addition, a γ_p can not be easily determined. For low values of M_2 (< 0.5) γ_s or γ_f can be used to relate stagnation to static properties.

2. Flow in the combustor is chemically reacting and is usually in local equilibrium. The Mach number is relatively low (< 0.5) and therefore, the static properties are not very different from the stagnation properties. $\gamma_{s,4}$ relates these states with good accuracy, but it is recommended that the local equilibrium process isentropic exponent, $\gamma_{p,s} = \gamma_{p,4-5}$, be used for compatibility with nozzle throat calculations.

3. Flow in the converging nozzle is generally in local equilibrium. Therefore, it is recommended that the combustor-to-nozzle throat local equilibrium process isentropic exponent, $\gamma_{p,s} = \gamma_{p,4-5}$, be used.

4. Flow in the diverging part of the nozzle generally has fixed composition. Therefore, it is recommended that the nozzle throat-to-nozzle exit frozen flow process isentropic exponent, $\gamma_{p,f} = \gamma_{p,5-6}$, be used.

C Compilation of Equations for Performance Evaluation

The calculation of performance is based on a simplified gasdynamical model of the engine process:

- The flow through the engine is one-dimensional. Over the cross-section of the stream tube, variable values are replaced by average values.
- There is no loss of air or fuel within the engine channel.
- The change of state of the average values follows the aerothermodynamical rules of uniform flow. In particular, the average values of the stagnation flow properties can be derived from the average values of local static flow properties.
- The geometrical cross-sectional areas of the engine channel (e.g. the nozzle throat) are adjusted by flow coefficients in order to obtain conformity between the gasdynamical functions of density and velocity and the law of mass conservation.
- The flow conditions in the convergent part of the nozzle are particularly important for the performance evaluation process. In this nozzle section, isentropic flow is assumed (no change of total temperature or total pressure). Moreover, for the sake of clarity, the assumption of choked nozzle operation is made. This condition exists in the majority of practical tests.

In the following, the equations will be simplified for a thermally and calorically perfect gas ($p = \varrho RT$, $c_p \neq f(T)$). In practice these equations are also applied to real combustion gases, even if there are comprehensive deviations from the idealisation of thermal and calorical perfection, by modifying the coefficients and exponents of the equations.

The geometry used in the following sections is shown in Figure C.1. It should be noted that $c_{D5}A_5$ is commonly called A^* in many textbooks, and is the effective flow area. In addition, the $\star$-location is often used for station 5. The γ used in this Appendix refers to the process γ (γ_p) in Chpt. 6 and Appendix B.

C.1 Stream Thrust

The stream thrust is defined as

$$F_S = \dot{m}c + pA$$

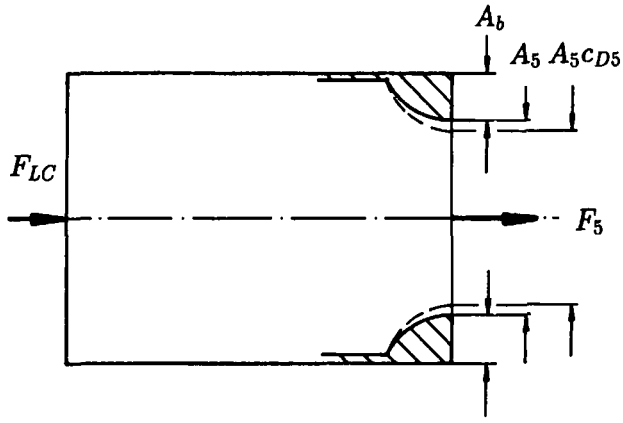

Figure C.1: Definitions for the derivation of the momentum equation

At the throat, this becomes

$$F_{S5} = \dot{m}_5 c_5 + p_5 A_5 \tag{C.1}$$

By introducing the formulas of mass flow

$$\dot{m}_5 = \varrho_5 c_5 A_5 c_{D5} \tag{C.2}$$

and dynamic pressure (with $M_5 = 1.0$)

$$q_5 = \frac{1}{2}\varrho_5 c_5^2 = \frac{\gamma}{2} p_5 M_5^2 = \frac{\gamma}{2} p_5 \tag{C.3}$$

the stream thrust is given by the following equation

$$\begin{aligned} F_{S5} &= \varrho_5 c_5^2 A_5 c_{D5} + p_5 A_5 \\ &= \gamma p_5 A_5 c_{D5} + p_5 A_5 \\ F_{S5} &= p_5 A_5 (1 + \gamma c_{D5}) \end{aligned} \tag{C.4}$$

For some deductions it is more convenient to avoid the pressure term in the equation. This is obtained as follows

$$\begin{aligned} F_{S5} &= \dot{m}_5 c_5 + p_5 A_5 \\ &= \dot{m}_5 c_5 \left(1 + \frac{p_5 A_5}{\dot{m}_5 c_5}\right) \end{aligned} \tag{C.5}$$

By combination of equations C.2 and C.3 a useful relation of the term $\dot{m}_5 c_5$ is derived.

$$\begin{aligned} \dot{m}_5 c_5 &= \varrho_5 c_5^2 A_5 c_{D5} \\ &= \gamma p_5 A_5 c_{D5} \end{aligned} \tag{C.6}$$

Using equation C.6 the second term in the bracket (C.5) reduces to

$$\frac{p_5 A_5}{\dot{m}_5 c_5} = \frac{1}{\gamma c_{D5}} \tag{C.7}$$

With equation C.7 a different formulation of stream thrust is obtained

$$F_{S5} = \frac{1+\gamma c_{D5}}{\gamma c_{D5}} \dot{m}_5 c_5 \tag{C.8}$$

Since $M = 1$ (nozzle throat) equation C.8 specializes to

$$F_{S5} = \frac{\gamma c_{D5}+1}{\gamma c_{D5}} \dot{m}_5 a^\star \tag{C.9}$$

with $a^\star$ being the critical speed of sound.

C.2 Local and Total Parameters

By Bernoulli's equation for compressible flow the local and total parameters are related in the following way:

$$\frac{p_t}{p} = \left(1 + \frac{\gamma-1}{2} M^2\right)^{\frac{\gamma}{\gamma-1}} \tag{C.10}$$

$$M = 1: \quad \frac{p_{t5}}{p^\star} = \frac{p_{t5}}{p_5} = \left(\frac{\gamma+1}{2}\right)^{\frac{\gamma}{\gamma-1}} \tag{C.11}$$

$$\frac{T_t}{T} = 1 + \frac{\gamma-1}{2} M^2 \tag{C.12}$$

$$M = 1: \quad \frac{T_{t5}}{T^\star} = \frac{T_{t5}}{T_5} = \frac{\gamma+1}{2} \tag{C.13}$$

$$\frac{a_t}{a} = \sqrt{\frac{T_t}{T}} = \sqrt{1 + \frac{\gamma-1}{2} M^2} \tag{C.14}$$

$$M = 1: \quad \frac{a_{t5}}{a^\star} = \sqrt{\frac{\gamma+1}{2}} \tag{C.15}$$

C.3 Vacuum Specific Impulse and Characteristic Velocity

$i^\star_{vac}$ is defined as the thrust per unit mass flow of a convergent nozzle discharging into vacuum. This value is identical with the stream thrust per unit mass flow in the sonic throat.

Having in mind this definition and with the help of equation C.4 the following relation can be derived:

$$\begin{aligned} i^\star_{vac} &= \frac{F_{S5}}{\dot{m}_5} \\ &= (\gamma c_{D5}+1)\frac{p_5 A_5}{\dot{m}_5} \\ &= (\gamma c_{D5}+1)\left(\frac{p_5}{p_{t5}}\right)\frac{p_{t5} A_5}{\dot{m}_5} \end{aligned} \tag{C.16}$$

The definition of the characteristic velocity is

$$c^\star = \frac{p_t A^\star}{\dot{m}}$$

In the nomenclature of this report

$$c^\star = \frac{p_{t5} A_5 c_{D5}}{\dot{m}_5}$$

Equation C.16 offers a relation between $i^\star_{vac}$ and $c^\star$, which proceeds to a useful formula by application of equation C.11.

$$\begin{aligned} i^\star_{vac} &= (\gamma c_{D5}+1)\left(\frac{p_5}{p_{t5}}\right)\frac{c^\star}{c_{D5}} \\ &= \left(\frac{2}{\gamma+1}\right)^{\frac{\gamma}{\gamma-1}} c^\star \frac{\gamma c_{D5}+1}{c_{D5}} \end{aligned} \tag{C.17}$$

$$\frac{c^\star}{i^\star_{vac}} = \left(\frac{\gamma+1}{2}\right)^{\frac{\gamma}{\gamma-1}} \frac{c_{D5}}{\gamma c_{D5}+1} \tag{C.18}$$

C.4 Combustion Temperature from $i^\star_{vac}$ or $c^\star$

The combination of equations C.9 and C.15 gives a relation between vacuum specific impulse and sonic speed at total temperature (combustion temperature).

$$\begin{aligned} i^\star_{vac} &= \frac{F_{S5}}{\dot{m}_5} \\ &= \frac{\gamma c_{D5}+1}{\gamma c_{D5}} a^\star \\ &= \frac{\gamma c_{D5}+1}{\gamma c_{D5}}\left(\frac{a^\star}{a_{t5}}\right) a_{t5} \\ &= \frac{\gamma c_{D5}+1}{\gamma c_{D5}} \sqrt{\frac{2}{\gamma+1}}\, a_{t5} \end{aligned} \tag{C.19}$$

With help of the equation for sonic speed

$$a_{t5} = \sqrt{\gamma R_5 T_{t5}}$$

a relation between the total temperature and $i^\star_{vac}$ follows.

$$T_{t5} = \frac{1}{2}\left(\frac{\gamma c_{D5}}{\gamma c_{D5}+1}\right)^2 \frac{\gamma+1}{\gamma} \frac{i^{\star 2}_{vac}}{R_5} \tag{C.20}$$

The combination of equations C.20 and C.18 leads to the relation between total temperature and characteristic velocity.

$$T_{t5} = \gamma \left(\frac{2}{\gamma+1}\right)^{\frac{\gamma+1}{\gamma-1}} \frac{c^{\star 2}}{R_5} \tag{C.21}$$

The practical evaluation always has to deal with the problem of choosing the proper value of γ. It is recommended to take the so called process-γ, which normally is calculated by the aerothermochemical equilibrium code.

The more exact method (which accounts for variable gas properties) is to take directly from the aerothermochemical equilibrium code the ratios between the different parameters, or substitutions, and to use them as proportionality factors. For example, equations C.20 and C.21 turn

over to

$$T_{t5} = \left(\frac{T_{t5}R_5}{i^{*2}_{vac}}\right)_{th} \frac{i^{*2}_{vac}}{R_5} \tag{C.22}$$

or

$$T_{t5} = \left(\frac{T_{t5}R_5}{c^{*2}}\right)_{th} \frac{c^{*2}}{R_5} \tag{C.23}$$

C.5 Determination of the Stream Thrust by Thrust Measurement with a Convergent Nozzle

From the requirement of momentum conservation follows the definition of ramjet nozzle thrust (see Fig. C.1):

$$F_5 = F_{S5} - p_{amb}A_5 \tag{C.24}$$

This can also be written as

$$F_5 = F_{meas} - (p_b - p_{amb})A_b \tag{C.25}$$

where

$$F_{meas} = \text{measured thrust} = F_{LC} - F_{tare} \tag{C.26}$$

F_{LC} load cell force

F_{tare} thrust stand preload

A_5 geometrical cross-sectional area of nozzle throat

p_b pressure on the nozzle base area

In some cases the effects of base pressure are negligible. Then the difference between F_5 and F_{meas} is very small and the usual form of the momentum relationship as seen in textbooks becomes

$$F_{S5} = F_{meas} + p_{amb}A_5 \tag{C.27}$$

C.6 Determination of Total Pressure in the Combustion Chamber from Thrust Measurement (Convergent Nozzle)

From the definition of vacuum specific impulse Eq. 6.9 and Eq. C.24:

$$F_{S5} = \dot{m}_5 i^*_{vac} = F_5 + p_{amb}A_5$$

Division by $A_5 c_{D5}$ gives

$$\frac{\dot{m}_5}{A_5 c_{D5}} i^*_{vac} = \frac{F_5 + p_{amb}A_5}{A_5 c_{D5}}$$

Because of the relation

$$\frac{\dot{m}_5}{A_5 c_{D5}} = \frac{p_{t5}}{c^*}$$

a formula for total pressure is formed.

$$p_{t5} = \left(\frac{c^*}{i^*_{vac}}\right) \frac{F_5 + p_{amb}A_5}{A_5 c_{D5}} \tag{C.28}$$

By introduction of equation C.18 an explicit formulation can be generated.

$$p_{t5} = \left(\frac{\gamma+1}{2}\right)^{\frac{\gamma}{\gamma-1}} \frac{F_5 + p_{amb}A_5}{(1+\gamma c_{D5})A_5} \tag{C.29}$$

Regarding the choice of γ, the same problem exists as mentioned in section C.4. Again the preferable alternative is to use equation C.28, taking the ratio of c^* and i^*_{vac} as the theoretical value from the aerothermochemical equilibrium code.

$$p_{t5} = \left(\frac{c^*}{i^*_{vac}}\right)_{th} \frac{F_5 + p_{amb}A_5}{A_5 c_{D5}} \tag{C.30}$$

D Input and Output Files of Sample Calculations

The following pages contain the input files used with the NASA CET89 aerothermochemical equilibrium code ([9]) to perform the calculations of Chapter 7. All input files are included with the appropriate sections of the output for the Case 1 chamber stagnation conditions and for the Case 2 vitiated air inlet conditions.

For better understanding the spaces or blanks in input files are written as readable characters.

Inputfile:

```
REACTANTS
N␣1.562␣␣O␣.4196␣␣AR.00934␣C␣.000314␣␣␣␣␣␣␣␣␣␣100.00␣␣␣␣␣␣␣␣␣␣G␣␣␣␣␣␣␣␣0

NAMELISTS
␣&INPT2␣KASE=1,TP=T,SIUNIT=T,NSQM=T,T=606.0,P=650200.0␣/
```

Outputfile:

```
                    THERMODYNAMIC EQUILIBRIUM PROPERTIES AT ASSIGNED

                              TEMPERATURE AND PRESSURE

CASE NO.      1

                                                          WT FRACTION    ENERGY   STATE   TEMP
        CHEMICAL FORMULA                                  (SEE NOTE)    KJ/KG-MOL         DEG K
FUEL    N  1.56200   O   .41960   AR  .00934   C   .00031    1.000000         .000   G       .00

            O/F=    .0000    PERCENT FUEL= 100.0000    EQUIVALENCE RATIO=  .0015    PHI=  .0000

THERMODYNAMIC PROPERTIES

P, MPA             .65020
T, DEG K          606.00
RHO, KG/CU M    3.7377 0
H, KJ/KG          310.87
U, KJ/KG          136.91
G, KJ/KG        -3962.01
S, KJ/(KG)(K)     7.0510

M, MOL WT         28.965
(DLV/DLP)T      -1.00000
(DLV/DLT)P        1.0000
CP, KJ/(KG)(K)    1.0525
GAMMA (S)         1.3750
SON VEL,M/SEC      489.1


MOLE FRACTIONS

AR                .00934
CO2               .00031
N2                .78089
O2                .20946
```

Figure D.1: Input and output file 1 (Case 1) for NASA CET89; station 2 conditions

Inputfile:

```
REACTANTS
N␣1.562␣␣0␣.4196␣␣AR.00934␣C␣.000314␣␣␣␣␣␣␣␣␣100.00␣␣␣2152.4␣G␣␣␣␣␣␣␣0
C␣10.␣␣␣␣H␣20.␣␣␣␣␣␣␣␣␣␣␣␣␣␣␣␣␣␣␣␣␣␣␣␣␣␣␣␣␣␣␣100.00␣-67607.0␣L␣␣␣␣␣␣␣F

NAMELISTS
␣&INPT2␣KASE=2,RKT=T,SIUNIT=T,NSQM=T,OF=T,MIX=21.517685,
␣␣P=568800.0␣/
␣&RKTINP␣FROZ=F,SUBAR=1.79895␣/
```

Outputfile:

```
                THEORETICAL ROCKET PERFORMANCE ASSUMING EQUILIBRIUM COMPOSITION DURING EXPANSION

                                FROM INFINITE AREA COMBUSTOR

PINF =    82.5 PSIA
CASE NO.      2

                                                                    WT FRACTION    ENERGY   STATE   TEMP
        CHEMICAL FORMULA                                            (SEE NOTE)    KJ/KG-MOL         DEG K
OXIDANT N  1.56200   O   .41960   AR  .00934   C   .00031           1.000000     9005.642   G        .00
FUEL    C 10.00000   H 20.00000                                     1.000000  -282867.700   L        .00

              O/F= 21.5177    PERCENT FUEL=   4.4410    EQUIVALENCE RATIO=  .6877    PHI=  .6872

                 CHAMBER   THROAT     EXIT
PINF/P             1.0000   1.8082   1.0793
P, MPA              .56880   .31456   .52701
T, DEG K          2065.80  1834.46  2035.14
RHO, KG/CU M    9.5724-1 5.9639-1 9.0035-1
H, KJ/KG           207.51  -124.45   162.50
U, KJ/KG           -386.70  -651.89  -422.84
G, KJ/KG         -17901.3 -16205.3 -17677.5
S, KJ/(KG)(K)      8.7660   8.7660   8.7660

M, MOL WT          28.906   28.918   28.908
(DLV/DLP)T       -1.00022 -1.00006 -1.00019
(DLV/DLT)P         1.0073   1.0021   1.0063
CP, KJ/(KG)(K)     1.4845   1.4041   1.4715
GAMMA (S)          1.2444   1.2588   1.2465
SON VEL,M/SEC       859.9    814.8    854.2
MACH NUMBER          .000    1.000     .351


PERFORMANCE PARAMETERS

AE/AT                       1.0000   1.7989
CSTAR, M/SEC                 1170     1170
CF                            .696     .256
IVAC, M/SEC                 1462.1   2251.0
ISP, M/SEC                   814.8    300.0


MOLE FRACTIONS

AR                  .00891   .00891   .00891
CO                  .00035   .00006   .00029
CO2                 .09147   .09180   .09154
H                   .00001   .00000   .00001
H2                  .00007   .00002   .00006
H2O                 .09079   .09131   .09089
NO                  .00474   .00245   .00438
NO2                 .00001   .00001   .00001
N2                  .74232   .74379   .74257
O                   .00011   .00002   .00009
OH                  .00129   .00046   .00114
O2                  .05993   .06118   .06012
```

Figure D.2: Input and output file 2 (Case 1) for NASA CET89; first run with p_4

Inputfile:

```
REACTANTS
N␣1.562␣␣0␣.4196␣␣AR.00934␣C␣.000314␣␣␣␣␣␣␣␣␣100.00␣␣␣2152.4␣G␣␣␣␣␣␣␣0
C␣10.␣␣␣␣H␣20.␣␣␣␣␣␣␣␣␣␣␣␣␣␣␣␣␣␣␣␣␣␣␣␣␣␣␣␣␣␣␣␣␣100.00␣-67607.0␣L␣␣␣␣␣␣␣F

NAMELISTS
␣&INPT2␣KASE=2,RKT=T,SIUNIT=T,NSQM=T,OF=T,MIX=21.517685,
␣␣P=613838.0
␣&END
␣&RKTINP␣FROZ=F,SUBAR=1.79895
␣&END
```

Outputfile:

```
                    THEORETICAL ROCKET PERFORMANCE ASSUMING EQUILIBRIUM COMPOSITION DURING EXPANSION

                                        FROM INFINITE AREA COMBUSTOR

PINF =    89.0 PSIA
CASE NO.       2
                                                                                WT FRACTION    ENERGY   STATE   TEMP
         CHEMICAL FORMULA                                                       (SEE NOTE)    KJ/KG-MOL         DEG K
OXIDANT N  1.56200   O   .41960   AR  .00934   C   .00031                       1.000000     9005.642   G        .00
FUEL    C 10.00000   H 20.00000                                                 1.000000  -282867.700   L        .00

              O/F= 21.5177    PERCENT FUEL=   4.4410    EQUIVALENCE RATIO=  .6877    PHI=  .6872

                  CHAMBER   THROAT     EXIT
PINF/P              1.0000   1.8083   1.0793
P, MPA               .61384   .33946   .56873
T, DEG K            2066.02  1834.49  2035.32
RHO, KG/CU M    1.0329 0 6.4359-1 9.7155-1
H, KJ/KG            207.51  -124.49   162.49
U, KJ/KG           -386.75  -651.93  -422.89
G, KJ/KG          -17858.0 -16165.4 -17634.5
S, KJ/(KG)(K)       8.7441   8.7441   8.7441

M, MOL WT           28.906   28.918   28.909
(DLV/DLP)T        -1.00022 -1.00005 -1.00018
(DLV/DLT)P          1.0071   1.0020   1.0061
CP, KJ/(KG)(K)      1.4825   1.4035   1.4697
GAMMA (S)           1.2447   1.2589   1.2467
SON VEL,M/SEC        860.0    814.9    854.3
MACH NUMBER           .000    1.000     .351


PERFORMANCE PARAMETERS

AE/AT                      1.0000   1.7989
CSTAR, M/SEC                1170     1170
CF                           .696     .256
IVAC, M/SEC                1462.1   2251.0
ISP, M/SEC                  814.9    300.1


MOLE FRACTIONS

AR                  .00891   .00891   .00891
CO                  .00034   .00006   .00027
CO2                 .09148   .09180   .09155
H                   .00001   .00000   .00001
H2                  .00007   .00001   .00006
H2O                 .09081   .09132   .09090
NO                  .00474   .00245   .00438
NO2                 .00001   .00001   .00001
N2                  .74233   .74379   .74258
O                   .00011   .00002   .00009
OH                  .00127   .00045   .00112
O2                  .05993   .06118   .06012
```

Figure D.3: Input and output file 3 (Case 1) for NASA CET89; p_{t4} for measured p_4 using γ

Inputfile:

```
REACTANTS
N␣1.562␣␣␣0␣.4196␣␣␣AR.00934␣C␣.000314␣␣␣␣␣␣␣␣␣␣100.00␣␣␣␣2152.4␣G␣␣␣␣␣␣␣␣0
C␣10.␣␣␣␣H␣20.␣␣␣␣␣␣␣␣␣␣␣␣␣␣␣␣␣␣␣␣␣␣␣␣␣␣␣␣␣␣␣␣␣␣100.00␣-67607.0␣L␣␣␣␣␣␣␣␣F

NAMELISTS
␣&INPT2␣KASE=2,RKT=T,SIUNIT=T,NSQM=T,OF=T,MIX=21.517685,
␣␣P=613906.0
␣&END
␣&RKTINP␣FROZ=F,SUBAR=1.79895
␣&END
```

Outputfile:

```
                    THEORETICAL ROCKET PERFORMANCE ASSUMING EQUILIBRIUM COMPOSITION DURING EXPANSION

                                        FROM INFINITE AREA COMBUSTOR

PINF =    89.0 PSIA
CASE NO.      2

                                                                          WT FRACTION    ENERGY   STATE   TEMP
        CHEMICAL FORMULA                                                  (SEE NOTE)    KJ/KG-MOL         DEG K
OXIDANT N  1.56200   O   .41960   AR  .00934   C   .00031                  1.000000     9005.642   G        .00
FUEL    C 10.00000   H 20.00000                                           1.000000  -282867.700   L        .00

              O/F= 21.5177    PERCENT FUEL=   4.4410    EQUIVALENCE RATIO=  .6877    PHI=  .6872

                  CHAMBER   THROAT     EXIT
PINF/P             1.0000   1.8083   1.0793
P, MPA              .61391   .33949   .56879
T, DEG K          2066.02  1834.49  2035.32
RHO, KG/CU M    1.0331 0 6.4366-1 9.7166-1
H, KJ/KG           207.51  -124.49   162.49
U, KJ/KG          -386.75  -651.93  -422.89
G, KJ/KG        -17857.9 -16165.4 -17634.5
S, KJ/(KG)(K)      8.7441   8.7441   8.7441

M, MOL WT          28.906   28.918   28.909
(DLV/DLP)T      -1.00022 -1.00005 -1.00018
(DLV/DLT)P         1.0071   1.0020   1.0061
CP, KJ/(KG)(K)     1.4825   1.4035   1.4697
GAMMA (S)          1.2447   1.2589   1.2467
SON VEL,M/SEC       860.0    814.9    854.3
MACH NUMBER          .000    1.000     .351


PERFORMANCE PARAMETERS

AE/AT                      1.0000   1.7989
CSTAR, M/SEC                1170     1170
CF                           .696     .256
IVAC, M/SEC                1462.1   2251.0
ISP, M/SEC                  814.9    300.1



MOLE FRACTIONS

AR                .00891   .00891   .00891
CO                .00034   .00006   .00027
CO2               .09148   .09180   .09155
H                 .00001   .00000   .00001
H2                .00007   .00001   .00006
H2O               .09081   .09132   .09090
NO                .00474   .00245   .00438
NO2               .00001   .00001   .00001
N2                .74233   .74379   .74258
O                 .00011   .00002   .00009
OH                .00127   .00045   .00112
O2                .05993   .06118   .06012
```

Figure D.4: Input and output file 4 (Case 1) for NASA CET89; p_{t4} for measured p_4 without using γ

Inputfile:

```
REACTANTS
O␣1.562␣␣O␣.4196␣␣AR.00934␣C␣.000314␣␣␣␣␣␣␣␣␣␣100.00␣␣␣2152.4␣G␣␣␣␣␣␣␣0
C␣10.␣␣␣␣H␣20.␣␣␣␣␣␣␣␣␣␣␣␣␣␣␣␣␣␣␣␣␣␣␣␣␣␣␣␣␣␣␣␣100.00␣-67607.0␣L␣␣␣␣␣␣␣F

NAMELISTS
␣&INPT2␣KASE=2,RKT=T,SIUNIT=T,NSQM=T,OF=T,MIX=21.517685,
␣␣P=619848.0
␣&END
␣&RKTINP␣FROZ=F,SUBAR=1.79895
␣&END
```

Outputfile:

THEORETICAL ROCKET PERFORMANCE ASSUMING EQUILIBRIUM COMPOSITION DURING EXPANSION

FROM INFINITE AREA COMBUSTOR

PINF = 89.9 PSIA
CASE NO. 2

CHEMICAL FORMULA						WT FRACTION (SEE NOTE)	ENERGY KJ/KG-MOL	STATE	TEMP DEG K
OXIDANT	N 1.56200	O .41960	AR .00934	C .00031		1.000000	9005.642	G	.00
FUEL	C 10.00000	H 20.00000				1.000000	-282867.700	L	.00

O/F= 21.5177 PERCENT FUEL= 4.4410 EQUIVALENCE RATIO= .6877 PHI= .6872

	CHAMBER	THROAT	EXIT
PINF/P	1.0000	1.8083	1.0793
P, MPA	.61985	.34278	.57430
T, DEG K	2066.05	1834.50	2035.35
RHO, KG/CU M	1.0430 0	6.4988-1	9.8106-1
H, KJ/KG	207.51	-124.49	162.49
U, KJ/KG	-386.76	-651.94	-422.89
G, KJ/KG	-17852.4	-16160.4	-17629.0
S, KJ/(KG)(K)	8.7413	8.7413	8.7413
M, MOL WT	28.906	28.918	28.909
(DLV/DLP)T	-1.00021	-1.00005	-1.00018
(DLV/DLT)P	1.0071	1.0020	1.0061
CP, KJ/(KG)(K)	1.4823	1.4034	1.4695
GAMMA (S)	1.2447	1.2589	1.2468
SON VEL,M/SEC	860.1	814.9	854.3
MACH NUMBER	.000	1.000	.351

PERFORMANCE PARAMETERS

AE/AT	1.0000	1.7989
CSTAR, M/SEC	1170	1170
CF	.696	.256
IVAC, M/SEC	1462.1	2251.0
ISP, M/SEC	814.9	300.1

MOLE FRACTIONS

AR	.00891	.00891	.00891
CO	.00034	.00006	.00027
CO2	.09148	.09180	.09155
H	.00001	.00000	.00001
H2	.00007	.00001	.00006
H2O	.09081	.09132	.09090
NO	.00474	.00245	.00438
NO2	.00001	.00001	.00001
N2	.74234	.74379	.74258
O	.00011	.00002	.00009
OH	.00126	.00045	.00112
O2	.05993	.06118	.06012

Figure D.5: Input and output file 5 (Case 1) for NASA CET89; p_{t4} using measured thrust and γ

Inputfile:

```
REACTANTS
N␣1.562␣␣0␣.4196␣␣AR.00934␣C␣.000314␣␣␣␣␣␣␣␣␣␣100.00␣␣␣2152.4␣G␣␣␣␣␣␣␣0
C␣10.␣␣␣␣H␣20.␣␣␣␣␣␣␣␣␣␣␣␣␣␣␣␣␣␣␣␣␣␣␣␣␣␣␣␣␣␣␣␣100.00␣-67607.0␣L␣␣␣␣␣␣␣F

NAMELISTS
␣&INPT2␣KASE=2,RKT=T,SIUNIT=T,NSQM=T,OF=T,MIX=21.517685,
␣␣P=620477.0
␣&END
␣&RKTINP␣FROZ=F,SUBAR=1.79895
␣&END
```

Outputfile:

```
                    THEORETICAL ROCKET PERFORMANCE ASSUMING EQUILIBRIUM COMPOSITION DURING EXPANSION

                                        FROM INFINITE AREA COMBUSTOR

PINF =    90.0 PSIA
CASE NO.      2

                                                                          WT FRACTION    ENERGY   STATE   TEMP
        CHEMICAL FORMULA                                                  (SEE NOTE)    KJ/KG-MOL         DEG K
OXIDANT N  1.56200   O   .41960   AR  .00934   C   .00031                  1.000000     9005.642   G        .00
FUEL    C 10.00000   H 20.00000                                           1.000000  -282867.700   L        .00

              O/F= 21.5177    PERCENT FUEL=   4.4410    EQUIVALENCE RATIO=  .6877    PHI=  .6872

                 CHAMBER   THROAT     EXIT
PINF/P             1.0000   1.8083   1.0793
P, MPA              .62048   .34313   .57488
T, DEG K           2066.05  1834.50  2035.35
RHO, KG/CU M    1.0441 0 6.5054-1 9.8205-1
H, KJ/KG           207.51  -124.49   162.49
U, KJ/KG          -386.76  -651.94  -422.90
G, KJ/KG        -17851.8 -16159.8 -17628.5
S, KJ/(KG)(K)      8.7410   8.7410   8.7410

M, MOL WT          28.906   28.918   28.909
(DLV/DLP)T      -1.00021 -1.00005 -1.00018
(DLV/DLT)P         1.0071   1.0020   1.0061
CP, KJ/(KG)(K)     1.4822   1.4034   1.4695
GAMMA (S)          1.2447   1.2589   1.2468
SON VEL,M/SEC       860.1    814.9    854.3
MACH NUMBER          .000    1.000     .351


PERFORMANCE PARAMETERS

AE/AT                       1.0000   1.7989
CSTAR, M/SEC                  1170     1170
CF                             .696     .256
IVAC, M/SEC                 1462.1   2251.0
ISP, M/SEC                   814.9    300.1


MOLE FRACTIONS

AR                .00891   .00891   .00891
CO                .00034   .00006   .00027
CO2               .09148   .09180   .09155
H                 .00001   .00000   .00001
H2                .00007   .00001   .00006
H2O               .09081   .09132   .09090
NO                .00474   .00245   .00438
NO2               .00001   .00001   .00001
N2                .74234   .74379   .74258
O                 .00011   .00002   .00009
OH                .00126   .00045   .00112
O2                .05993   .06118   .06012
```

Figure D.6: Input and output file 6 (Case 1) for NASA CET89; p_{t4} using measured thrust without γ

Inputfile:

```
REACTANTS
N␣1.562␣␣0␣.4196␣␣AR.00934␣C␣.000314␣␣␣␣␣␣␣␣␣100.00␣␣␣2152.4␣G␣␣␣␣␣␣␣0
C␣10.␣␣␣␣H␣20.␣␣␣␣␣␣␣␣␣␣␣␣␣␣␣␣␣␣␣␣␣␣␣␣␣␣␣␣␣␣␣100.00␣-67607.0␣L␣␣␣␣␣␣␣F

NAMELISTS
␣&INPT2␣KASE=2,RKT=T,SIUNIT=T,NSQM=T,ERATIO=T,MIX=MIX=0.55,0.555,0.56,0.565,0.57,0.575,0.58,0.585,0.59,0.595,0.60,
␣␣P=613906.0
␣&END
␣&RKTINP␣FROZ=F,SUBAR=1.79895
␣&END
```

Outputfile:

```
                    THEORETICAL ROCKET PERFORMANCE ASSUMING EQUILIBRIUM COMPOSITION DURING EXPANSION

                                        FROM INFINITE AREA COMBUSTOR

PINF =    89.0 PSIA
CASE NO.      2

                                                                          WT FRACTION    ENERGY   STATE   TEMP
        CHEMICAL FORMULA                                                  (SEE NOTE)    KJ/KG-MOL          DEG K
OXIDANT N  1.56200   O   .41960   AR  .00934   C   .00031                  1.000000     9005.642   G        .00
FUEL    C 10.00000   H 20.00000                                            1.000000. -282867.700   L        .00

              O/F= 26.9200    PERCENT FUEL=   3.5817    EQUIVALENCE RATIO=  .5500    PHI=  .5493

                  CHAMBER   THROAT     EXIT
PINF/P              1.0000   1.8183   1.0801
P, MPA               .61391   .33763   .56836
T, DEG K            1825.52  1607.73  1796.30
RHO, KG/CU M    1.1700 0 7.3072-1 1.1009 0
H, KJ/KG            227.51  -67.174   187.39
U, KJ/KG           -297.18  -529.23  -328.89
G, KJ/KG          -15356.7 -13792.2 -15147.5
S, KJ/(KG)(K)       8.5369   8.5369   8.5369

M, MOL WT           28.928   28.930   28.928
(DLV/DLP)T       -1.00004 -1.00001 -1.00003
(DLV/DLT)P          1.0014   1.0004   1.0012
CP, KJ/(KG)(K)      1.3785   1.3313   1.3716
GAMMA (S)           1.2643   1.2755   1.2659
SON VEL,M/SEC        814.5    767.7    808.4
MACH NUMBER           .000    1.000     .350


PERFORMANCE PARAMETERS

AE/AT                       1.0000   1.7989
CSTAR, M/SEC                  1094     1094
CF                             .702     .259
IVAC, M/SEC                 1369.6   2105.9
ISP, M/SEC                   767.7    283.3



MOLE FRACTIONS

AR                  .00899   .00899   .00899
CO                  .00003   .00000   .00002
CO2                 .07414   .07417   .07415
H2                  .00001   .00000   .00001
H2O                 .07368   .07382   .07371
NO                  .00288   .00128   .00262
NO2                 .00001   .00001   .00001
N2                  .75052   .75138   .75066
O                   .00002   .00000   .00001
OH                  .00036   .00010   .00031
O2                  .08936   .09024   .08951
```

Figure D.7: Input and output file 7 (Case 1) for NASA CET89; equivalence ratio versus characteristic velocity

Inputfile:

```
REACTANTS
N␣1.562␣␣O␣.4196␣␣AR.00934␣C␣.000314␣␣␣␣␣␣␣␣␣␣6.383␣␣␣␣␣␣␣␣␣␣G␣␣␣␣␣␣␣␣0
C␣1.␣␣␣␣␣H␣4.␣␣␣␣␣␣␣␣␣␣␣␣␣␣␣␣␣␣␣␣␣␣␣␣␣␣␣␣␣␣␣␣␣␣␣␣0.047␣␣␣␣␣␣␣␣␣G␣␣␣␣␣␣␣␣F
O␣2.␣␣␣␣␣␣␣␣␣␣␣␣␣␣␣␣␣␣␣␣␣␣␣␣␣␣␣␣␣␣␣␣␣␣␣␣␣␣␣␣␣␣␣␣␣␣␣␣0.262␣␣␣␣␣␣␣␣␣G␣␣␣␣␣␣␣␣0

NAMELISTS
␣&INPT2␣KASE=3,TP=T,SIUNIT=T,NSQM=T,T=606.0,P=650200.0
␣&END
```

Outputfile:

```
                                THERMODYNAMIC EQUILIBRIUM PROPERTIES AT ASSIGNED

                                TEMPERATURE AND PRESSURE

CASE NO.       3

                                                                    WT FRACTION    ENERGY   STATE   TEMP
         CHEMICAL FORMULA                                           (SEE NOTE)    KJ/KG-MOL         DEG K
OXIDANT N  1.56200   O   .41960   AR  .00934   C   .00031            .960572         .000   G        .00
FUEL    C  1.00000   H  4.00000                                     1.000000         .000   G        .00
OXIDANT O  2.00000                                                  .039428         .000   G        .00

              O/F=141.3830    PERCENT FUEL=    .7023    EQUIVALENCE RATIO=  .1089    PHI=  .1078

THERMODYNAMIC PROPERTIES

P, MPA              .65020
T, DEG K            606.00
RHO, KG/CU M     3.7305 0
H, KJ/KG           -69.041
U, KJ/KG           -243.34
G, KJ/KG          -4389.49
S, KJ/(KG)(K)       7.1294

M, MOL WT           28.908
(DLV/DLP)T        -1.00000
(DLV/DLT)P          1.0000
CP, KJ/(KG)(K)      1.0677
GAMMA (S)           1.3687
SON VEL,M/SEC        488.4


MOLE FRACTIONS

AR                  .00889
CO2                 .01295
H2O                 .02531
N2                  .74339
O2                  .20946
```

Figure D.8: Input and output file 1 (Case 2) for NASA CET89; station 2 conditions

Inputfile:

```
REACTANTS
N␣1.486780␣.47013␣AR.00889␣C␣.01295␣H␣.05062␣␣␣6.692␣␣␣-476.7␣G␣␣␣␣␣␣␣␣0
C␣10.␣␣␣␣H␣20.␣␣␣␣␣␣␣␣␣␣␣␣␣␣␣␣␣␣␣␣␣␣␣␣␣␣␣␣␣␣␣␣␣␣␣␣␣␣␣␣␣␣0.311␣-67607.0␣L␣␣␣␣␣␣␣F

NAMELISTS
␣&INPT2␣KASE=4,RKT=T,SIUNIT=T,NSQM=T,P=568800.0
␣&END
␣&RKTINP␣FROZ=F,SUBAR=1.79895
␣&END
```

Outputfile:

```
                    THEORETICAL ROCKET PERFORMANCE ASSUMING EQUILIBRIUM COMPOSITION DURING EXPANSION

                                        FROM INFINITE AREA COMBUSTOR

PINF =    82.5 PSIA
CASE NO.       4

                                                                                WT FRACTION    ENERGY   STATE   TEMP
         CHEMICAL FORMULA                                                       (SEE NOTE)    KJ/KG-MOL         DEG K
OXIDANT N  1.48678   O   .47013   AR  .00889   C   .01295   H   .05062          1.000000    -1994.513   G        .00
FUEL    C 10.00000   H 20.00000                                                 1.000000. -282867.700   L        .00

              O/F= 21.5177    PERCENT FUEL=   4.4410    EQUIVALENCE RATIO=  .7201    PHI=  .6859

                  CHAMBER   THROAT     EXIT
PINF/P             1.0000   1.8055   1.0791
P, MPA              .56880   .31504    .52711
T, DEG K           2044.75  1819.23  2014.87
RHO, KG/CU M     9.6531-1 6.0118-1 9.0789-1
H, KJ/KG           -155.49  -484.14  -200.02
U, KJ/KG           -744.73 -1008.17  -780.60
G, KJ/KG         -18196.8 -16535.7 -17977.8
S, KJ/(KG)(K)      8.8233   8.8233   8.8233

M, MOL WT          28.853   28.865   28.855
(DLV/DLP)T       -1.00022 -1.00006 -1.00018
(DLV/DLT)P         1.0073   1.0021   1.0063
CP, KJ/(KG)(K)     1.5071   1.4263   1.4940
GAMMA (S)          1.2404   1.2543   1.2424
SON VEL,M/SEC       854.9    810.7    849.3
MACH NUMBER          .000    1.000     .351


PERFORMANCE PARAMETERS

AE/AT                      1.0000   1.7989
CSTAR, M/SEC                1167     1167
CF                           .695     .256
IVAC, M/SEC                1457.1   2243.9
ISP, M/SEC                  810.7    298.4


MOLE FRACTIONS

AR                  .00848   .00848   .00848
CO                  .00033   .00006   .00027
CO2                 .10336   .10368   .10344
H                   .00001   .00000   .00001
H2                  .00008   .00002   .00007
H2O                 .11474   .11528   .11484
NO                  .00439   .00228   .00406
NO2                 .00001   .00001   .00001
N2                  .70680   .70816   .70703
O                   .00010   .00002   .00008
OH                  .00132   .00047   .00117
O2                  .06037   .06154   .06055
```

Figure D.9: Input and output file 2 (Case 2) for NASA CET89; first run with p_4

Inputfile:

```
REACTANTS
N␣1.486780␣.47013␣AR.00889␣C␣.01295␣H␣.05062␣␣␣6.692␣␣␣-476.7␣G␣␣␣␣␣␣␣␣0
C␣10.␣␣␣␣H␣20.␣␣␣␣␣␣␣␣␣␣␣␣␣␣␣␣␣␣␣␣␣␣␣␣␣␣␣␣␣␣␣0.311␣-67607.0␣L␣␣␣␣␣␣␣␣F

NAMELISTS
␣&INPT2␣KASE=4,RKT=T,SIUNIT=T,NSQM=T,P=613792.0
␣&END
␣&RKTINP␣FROZ=F,SUBAR=1.79895
␣&END
```

Outputfile:

```
                    THEORETICAL ROCKET PERFORMANCE ASSUMING EQUILIBRIUM COMPOSITION DURING EXPANSION

                                               FROM INFINITE AREA COMBUSTOR

PINF =     89.0 PSIA
CASE NO.        4
                                                                             WT FRACTION     ENERGY    STATE    TEMP
        CHEMICAL FORMULA                                                      (SEE NOTE)    KJ/KG-MOL          DEG K
OXIDANT N  1.48678   O   .47013   AR  .00889   C    .01295   H    .05062      1.000000     -1994.513   G        .00
FUEL     C 10.00000   H 20.00000                                              1.000000   -282867.700   L        .00

              O/F= 21.5177    PERCENT FUEL=   4.4410    EQUIVALENCE RATIO=  .7201    PHI=  .6859

                  CHAMBER   THROAT    EXIT
PINF/P             1.0000   1.8056   1.0791
P, MPA             .61379   .33995   .56880
T, DEG K          2044.96  1819.27  2015.05
RHO, KG/CU M     1.0416 0 6.4870-1 9.7962-1
H, KJ/KG          -155.49  -484.17  -200.02
U, KJ/KG          -744.78 -1008.21  -780.65
G, KJ/KG         -18153.9 -16496.2 -17935.1
S, KJ/(KG)(K)      8.8013   8.8013   8.8013

M, MOL WT          28.853   28.865   28.855
(DLV/DLP)T       -1.00021 -1.00005 -1.00018
(DLV/DLT)P         1.0071   1.0021   1.0061
CP, KJ/(KG)(K)     1.5051   1.4257   1.4923
GAMMA (S)          1.2406   1.2544   1.2426
SON VEL,M/SEC       855.0    810.8    849.4
MACH NUMBER          .000    1.000     .351


PERFORMANCE PARAMETERS

AE/AT                        1.0000   1.7989
CSTAR, M/SEC                   1167     1167
CF                             .695     .256
IVAC, M/SEC                  1457.1   2243.9
ISP, M/SEC                    810.8    298.4



MOLE FRACTIONS

AR                 .00848   .00848   .00848
CO                 .00032   .00006   .00026
CO2                .10338   .10369   .10345
H                  .00001   .00000   .00001
H2                 .00008   .00002   .00006
H2O                .11476   .11529   .11486
NO                 .00439   .00228   .00406
NO2                .00001   .00001   .00001
N2                 .70681   .70816   .70703
O                  .00009   .00002   .00008
OH                 .00129   .00046   .00115
O2                 .06037   .06154   .06055
```

Figure D.10: Input and output file 3 (Case 2) for NASA CET89; p_{t4} for measured p_4 without using γ

Index

REPORT DOCUMENTATION PAGE

1. Recipient's Reference	2. Originator's Reference	3. Further Reference	4. Security Classification of Document
	AGARD-AR-323	ISBN 92-835-0755-X	UNCLASSIFIED/ UNLIMITED

5. Originator Advisory Group for Aerospace Research and Development
North Atlantic Treaty Organization
7 rue Ancelle, 92200 Neuilly sur Seine, France

6. Title EXPERIMENTAL AND ANALYTICAL METHODS FOR THE DETERMINATION OF CONNECTED-PIPE RAMJET AND DUCTED ROCKET INTERNAL PERFORMANCE

7. Presented on

8. Author(s)/Editor(s)	9. Date
	July 1994
10. Author(s)/Editor's Address	**11. Pages**
	100

12. Distribution Statement There are no restrictions on the distribution of this document. Information about the availability of this and other AGARD unclassified publications is given on the back cover.

13. Keywords/Descriptors

Ramjet engines
Ducted rocket engines
Performance tests
Internal pressure
Error analysis

14. Abstract

Connected-pipe, subsonic combustion ramjet and ducted rocket performance determination procedures used by the NATO countries have been reviewed and evaluated.

A working document has been produced which provides recommended methods for reporting test results and delineates the parameters that are required to be measured.

Explanations and detailed numerical examples are presented covering the determination of both theoretical and experimental performances, the use of air heaters and uncertainty and error analyses.

This Advisory Report was prepared at the request of the Propulsion and Energetics Panel of AGARD.

AGARD Advisory Report 323 Advisory Group for Aerospace Research and Development, NATO EXPERIMENTAL AND ANALYTICAL METHODS FOR THE DETERMINATION OF CONNECTED-PIPE RAMJET AND DUCTED ROCKET INTERNAL PERFORMANCE Published July 1994 100 pages Connected-pipe, subsonic combustion ramjet and ducted rocket performance determination procedures used by the NATO countries have been reviewed and evaluated. A working document has been produced which provides recommended methods for reporting test results and delineates the parameters that are required to be measured. P.T.O.	AGARD-AR-323 Ramjet engines Ducted rocket engines Performance tests Internal pressure Error analysis	AGARD Advisory Report 323 Advisory Group for Aerospace Research and Development, NATO EXPERIMENTAL AND ANALYTICAL METHODS FOR THE DETERMINATION OF CONNECTED-PIPE RAMJET AND DUCTED ROCKET INTERNAL PERFORMANCE Published July 1994 100 pages Connected-pipe, subsonic combustion ramjet and ducted rocket performance determination procedures used by the NATO countries have been reviewed and evaluated. A working document has been produced which provides recommended methods for reporting test results and delineates the parameters that are required to be measured. P.T.O.	AGARD-AR-323 Ramjet engines Ducted rocket engines Performance tests Internal pressure Error analysis
AGARD Advisory Report 323 Advisory Group for Aerospace Research and Development, NATO EXPERIMENTAL AND ANALYTICAL METHODS FOR THE DETERMINATION OF CONNECTED-PIPE RAMJET AND DUCTED ROCKET INTERNAL PERFORMANCE Published July 1994 100 pages Connected-pipe, subsonic combustion ramjet and ducted rocket performance determination procedures used by the NATO countries have been reviewed and evaluated. A working document has been produced which provides recommended methods for reporting test results and delineates the parameters that are required to be measured. P.T.O.	AGARD-AR-323 Ramjet engines Ducted rocket engines Performance tests Internal pressure Error analysis	AGARD Advisory Report 323 Advisory Group for Aerospace Research and Development, NATO EXPERIMENTAL AND ANALYTICAL METHODS FOR THE DETERMINATION OF CONNECTED-PIPE RAMJET AND DUCTED ROCKET INTERNAL PERFORMANCE Published July 1994 100 pages Connected-pipe, subsonic combustion ramjet and ducted rocket performance determination procedures used by the NATO countries have been reviewed and evaluated. A working document has been produced which provides recommended methods for reporting test results and delineates the parameters that are required to be measured. P.T.O.	AGARD-AR-323 Ramjet engines Ducted rocket engines Performance tests Internal pressure Error analysis

Explanations and detailed numerical examples are presented covering the determination of both theoretical and experimental performances, the use of air heaters and uncertainty and error analyses.

This Advisory Report was prepared at the request of the Propulsion and Energetics Panel of AGARD.

ISBN 92-835-0755-X

Explanations and detailed numerical examples are presented covering the determination of both theoretical and experimental performances, the use of air heaters and uncertainty and error analyses.

This Advisory Report was prepared at the request of the Propulsion and Energetics Panel of AGARD.

ISBN 92-835-0755-X

Explanations and detailed numerical examples are presented covering the determination of both theoretical and experimental performances, the use of air heaters and uncertainty and error analyses.

This Advisory Report was prepared at the request of the Propulsion and Energetics Panel of AGARD.

ISBN 92-835-0755-X

Explanations and detailed numerical examples are presented covering the determination of both theoretical and experimental performances, the use of air heaters and uncertainty and error analyses.

This Advisory Report was prepared at the request of the Propulsion and Energetics Panel of AGARD.

ISBN 92-835-0755-X

AGARD

NATO OTAN

7 RUE ANCELLE · 92200 NEUILLY-SUR-SEINE

FRANCE

Télécopie (1)47.38.57.99 · Télex 610 176

DIFFUSION DES PUBLICATIONS
AGARD NON CLASSIFIEES

Aucun stock de publications n'a existé à AGARD. A partir de 1993, AGARD détiendra un stock limité des publications associées aux cycles de conférences et cours spéciaux ainsi que les AGARDographies et les rapports des groupes de travail, organisés et publiés à partir de 1993 inclus. Les demandes de renseignements doivent être adressées à AGARD par lettre ou par fax à l'adresse indiquée ci-dessus. *Veuillez ne pas téléphoner.* La diffusion initiale de toutes les publications de l'AGARD est effectuée auprès des pays membres de l'OTAN par l'intermédiaire des centres de distribution nationaux indiqués ci-dessous. Des exemplaires supplémentaires peuvent parfois être obtenus auprès de ces centres (à l'exception des Etats-Unis). Si vous souhaitez reçevoir toutes les publications de l'AGARD, ou simplement celles qui concernent certains Panels, vous pouvez demander à être inclu sur la liste d'envoi de l'un de ces centres. Les publications de l'AGARD sont en vente auprès des agences indiquées ci-dessous, sous forme de photocopie ou de microfiche.

CENTRES DE DIFFUSION NATIONAUX

ALLEMAGNE
Fachinformationszentrum,
Karlsruhe
D-7514 Eggenstein-Leopoldshafen 2

BELGIQUE
Coordonnateur AGARD-VSL
Etat-Major de la Force Aérienne
Quartier Reine Elisabeth
Rue d'Evere, 1140 Bruxelles

CANADA
Directeur du Service des Renseignements Scientifiques
Ministère de la Défense Nationale
Ottawa, Ontario K1A 0K2

DANEMARK
Danish Defence Research Establishment
Ryvangs Allé 1
P.O. Box 2715
DK-2100 Copenhagen Ø

ESPAGNE
INTA (AGARD Publications)
Pintor Rosales 34
28008 Madrid

ETATS-UNIS
NASA Headquarters
Code JOB-1
Washington, D.C. 20546

FRANCE
O.N.E.R.A. (Direction)
29, Avenue de la Division Leclerc
92322 Châtillon Cedex

GRECE
Hellenic Air Force
Air War College
Scientific and Technical Library
Dekelia Air Force Base
Dekelia, Athens TGA 1010

ISLANDE
Director of Aviation
c/o Flugrad
Reykjavik

ITALIE
Aeronautica Militare
Ufficio del Delegato Nazionale all'AGARD
Aeroporto Pratica di Mare
00040 Pomezia (Roma)

LUXEMBOURG
Voir Belgique

NORVEGE
Norwegian Defence Research Establishment
Attn: Biblioteket
P.O. Box 25
N-2007 Kjeller

PAYS-BAS
Netherlands Delegation to AGARD
National Aerospace Laboratory NLR
P.O. Box 90502
1006 BM Amsterdam

PORTUGAL
Força Aérea Portuguesa
Centro de Documentação e Informação
Alfragide
2700 Amadora

ROYAUME UNI
Defence Research Information Centre
Kentigern House
65 Brown Street
Glasgow G2 8EX

TURQUIE
Millî Savunma Başkanlığı (MSB)
ARGE Daire Başkanlığı (ARGE)
Ankara

Le centre de distribution national des Etats-Unis ne détient PAS de stocks des publications de l'AGARD.
D'éventuelles demandes de photocopies doivent être formulées directement auprès du NASA Center for AeroSpace Information (CASI) à l'adresse ci-dessous. Toute notification de changement d'adresse doit être fait également auprès de CASI.

AGENCES DE VENTE

NASA Center for
AeroSpace Information (CASI)
800 Elkridge Landing Road
Linthicum Heights, MD 21090-2934
United States

ESA/Information Retrieval Service
European Space Agency
10, rue Mario Nikis
75015 Paris
France

The British Library
Document Supply Division
Boston Spa, Wetherby
West Yorkshire LS23 7BQ
Royaume Uni

Les demandes de microfiches ou de photocopies de documents AGARD (y compris les demandes faites auprès du CASI) doivent comporter la dénomination AGARD, ainsi que le numéro de série d'AGARD (par exemple AGARD-AG-315). Des informations analogues, telles que le titre et la date de publication sont souhaitables. Veuiller noter qu'il y a lieu de spécifier AGARD-R-nnn et AGARD-AR-nnn lors de la commande des rapports AGARD et des rapports consultatifs AGARD respectivement. Des références bibliographiques complètes ainsi que des résumés des publications AGARD figurent dans les journaux suivants:

Scientifique and Technical Aerospace Reports (STAR)
publié par la NASA Scientific and Technical
Information Program
NASA Headquarters (JTT)
Washington D.C. 20546
Etats-Unis

Government Reports Announcements and Index (GRA&I)
publié par le National Technical Information Service
Springfield
Virginia 22161
Etats-Unis

(accessible également en mode interactif dans la base de données bibliographiques en ligne du NTIS, et sur CD-ROM)

Imprimé par Specialised Printing Services Limited
40 Chigwell Lane, Loughton, Essex IG10 3TZ

AGARD

NATO OTAN

7 RUE ANCELLE · 92200 NEUILLY-SUR-SEINE

FRANCE

Telefax (1)47.38.57.99 · Telex 610 176

DISTRIBUTION OF UNCLASSIFIED AGARD PUBLICATIONS

AGARD holds limited quantities of the publications that accompanied Lecture Series and Special Courses held in 1993 or later, and of AGARDographs and Working Group reports published from 1993 onward. For details, write or send a telefax to the address given above. *Please do not telephone.*

AGARD does not hold stocks of publications that accompanied earlier Lecture Series or Courses or of any other publications. Initial distribution of all AGARD publications is made to NATO nations through the National Distribution Centres listed below. Further copies are sometimes available from these centres (except in the United States). If you have a need to receive all AGARD publications, or just those relating to one or more specific AGARD Panels, they may be willing to include you (or your organisation) on their distribution list. AGARD publications may be purchased from the Sales Agencies listed below, in photocopy or microfiche form.

NATIONAL DISTRIBUTION CENTRES

BELGIUM
Coordonnateur AGARD — VSL
Etat-Major de la Force Aérienne
Quartier Reine Elisabeth
Rue d'Evere, 1140 Bruxelles

CANADA
Director Scientific Information Services
Dept of National Defence
Ottawa, Ontario K1A 0K2

DENMARK
Danish Defence Research Establishment
Ryvangs Allé 1
P.O. Box 2715
DK-2100 Copenhagen Ø

FRANCE
O.N.E.R.A. (Direction)
29 Avenue de la Division Leclerc
92322 Châtillon Cedex

GERMANY
Fachinformationszentrum
Karlsruhe
D-7514 Eggenstein-Leopoldshafen 2

GREECE
Hellenic Air Force
Air War College
Scientific and Technical Library
Dekelia Air Force Base
Dekelia, Athens TGA 1010

ICELAND
Director of Aviation
c/o Flugrad
Reykjavik

ITALY
Aeronautica Militare
Ufficio del Delegato Nazionale all'AGARD
Aeroporto Pratica di Mare
00040 Pomezia (Roma)

LUXEMBOURG
See Belgium

NETHERLANDS
Netherlands Delegation to AGARD
National Aerospace Laboratory, NLR
P.O. Box 90502
1006 BM Amsterdam

NORWAY
Norwegian Defence Research Establishment
Attn: Biblioteket
P.O. Box 25
N-2007 Kjeller

PORTUGAL
Força Aérea Portuguesa
Centro de Documentação e Informação
Alfragide
2700 Amadora

SPAIN
INTA (AGARD Publications)
Pintor Rosales 34
28008 Madrid

TURKEY
Milli Savunma Başkanlığı (MSB)
ARGE Daire Başkanlığı (ARGE)
Ankara

UNITED KINGDOM
Defence Research Information Centre
Kentigern House
65 Brown Street
Glasgow G2 8EX

UNITED STATES
NASA Headquarters
Code JOB-1
Washington, D.C. 20546

The United States National Distribution Centre does NOT hold stocks of AGARD publications.
Applications for copies should be made direct to the NASA Center for AeroSpace Information (CASI) at the address below.
Change of address requests should also go to CASI.

SALES AGENCIES

NASA Center for
AeroSpace Information (CASI)
800 Elkridge Landing Road
Linthicum Heights, MD 21090-2934
United States

ESA/Information Retrieval Service
European Space Agency
10, rue Mario Nikis
75015 Paris
France

The British Library
Document Supply Centre
Boston Spa, Wetherby
West Yorkshire LS23 7BQ
United Kingdom

Requests for microfiches or photocopies of AGARD documents (including requests to CASI) should include the word 'AGARD' and the AGARD serial number (for example AGARD-AG-315). Collateral information such as title and publication date is desirable. Note that AGARD Reports and Advisory Reports should be specified as AGARD [illegible] AGARD [illegible] phical

Scien
publis
Infor
NASA
Wash
Unite

Printed by Specialised Printing Services Limited
40 Chigwe TZ

ISBN 92-835-0755-X